Free Radical Polymerization of N-Vinylformamide and Novel Comb Structure Polyelectrolytes

By

LEMING GU, B. Eng., M. Eng.

A Thesis

Submitted to the School of Graduate Studies

In Partial Fulfillment of the Requirements

For the Degree of

Doctor of Philosophy

McMaster University

FREE RADICAL POLYMERIZATION OF N-VINYLFORMAMIDE AND NOVEL COMB STRUCTURE POLYELECTROLYTES

DOCTOR OF PHILOSOPHY (2001) McMaster University
(Chemical Engineering) Hamilton, Ontario, Canada

TITLE: Free Radical Polymerization of N-Vinylformamide and Novel Comb-structure Polyelectrolytes

AUTHOR: Leming Gu,
B. Eng (Zhejiang University, P. R. CHINA)
M. Eng (Zhejiang University, P. R. CHINA)

SUPERVISORS: Drs. Shiping Zhu and Andrew N. Hrymak

NUMBER OF PAGES: xvi, 152

ABSTRACT

This thesis summarizes experimental and theoretical studies on N-vinylformamide (NVF) free radical polymerization and the synthesis and evaluation of cationic grafted copolymers for flocculation purpose.

The free radical polymerization of N-vinylformamide was studied in bulk and aqueous solution processes. The molar heat of reaction for NVF polymerization was measured to be 79.4 kJ/mol. The polymerization kinetics, including the conversion versus time, molecular weight and molecular weight distribution, was examined systematically. Significant "gel effect" was observed in bulk and solution polymerization when the monomer concentration was over 40wt% (5.63 mol/L). A semi-empirical model based on the free volume theory was proposed to describe both the bulk and solution polymerizations. It was also confirmed that amide group provided crosslinking points that formed PNVF gel during NVF free radical polymerization. The subsequent acidic and basic hydrolysis to convert PNVF to PVAm was also studied systematically. The effect of temperature, polymer/acid (or base) ratios and polymer concentrations were examined.

Two methods were used to synthesize cationic grafted copolymers for flocculation purposes. In the first method, NVF monomer was copolymerized with two cationic poly dimethylaminoethyl methacrylate (polyDMAEMA) methyl chloride macromonomers to produce a series of comb-grafted copolymers with different cationic contents. One cationic macromonomer had a molecular weight of 14,100 (50 repeating units) and the other had a molecular weight of 28,200 (100 repeating units). The copolymerization reactivity ratio (r_1) of the comonomer pair (NVF(M_1)-macromonomer(M_2)) was determined to be 3.82 and 6.39 for the two macromonomers with 50 and 100 repeating units. The flocculation performance of the graft copolymers was tested on a TiO_2 aqueous dispersion model system. The graft copolymers were found to be more

effective in flocculation than their random linear counterparts. In the second method, poly diallydimethyl ammonium chloride (polyDADMAC) was grafted onto polyacrylamide (PAM) using a mini-mixer in melts with an organic peroxide, Lupersol 130. This process resembled reactive processing usually carried out at a larger scale in extruders to handle highly viscous polymer reactions. The grafting was confirmed and successful. However, severe gelation problem with PAM that occurred during the process hampered the grafting efforts.

Parallel to these studies based on experimental data, a theoretical model was derived to describe the bivariate distribution of molecular weight and branching density for comb-grafted copolymers. This model was based on the random grafting of pre-formed side chains onto backbones (grafting-onto) mechanism. However, it is also applicable to the comb polymers synthesized by grafting-from and grafting-through mechanisms as long as the inclusion of the branching point is a random process.

ACKNOWLEDGEMENTS

After five years of work, this thesis finally comes into being. It is a result of my personal effort as well as the great helps and valuable suggestions I received from my supervisors and supervisory committees, family, colleagues and friends. Without the help and encouragement of these people, I would have never achieved this goal.

First of all, I would like to express my deep and sincere gratefulness to my supervisors, Dr. Shiping Zhu and Dr. Andrew N. Hrymak. They motivate me with valuable advice, continuous guidance and encouragement.

I would also like to thank Dr. Robert Pelton and Dr. Harald Stöver for their valuable insights and comments, and their generous assistance throughout the course of my project.

My special thanks also go to all the members of our research group, in particular Dr. Wenjun Wang, Youqing Shen and Faquan Zeng. I benefit a lot from those discussions with them and day to day experience working together. They are a great pleasure to work with.

I thank Drs. Stephan Drappel and Danielle Boils-Boissier of Xerox Research Center of Canada (XRCC) for the use of GPC instrument. Thank all the staff members and department secretaries for their assistance with technical and administrative issues.

I acknowledge the financial support from the Department of Chemical Engineering, McMaster University, Materials and Manufacturing Ontario, National Science and Engineering Research Council of Canada and Ontario Graduate Scholarship.

Finally, my greatest appreciation goes to my wife, Lan, and my parents, who share all the burdens and hard works with me along the way. I can not possibly repay your support and sacrifice.

TABLE OF CONTENTS

LIST OF FIGURES

LIST OF TABLES

Chapter 1. Introduction

In liquid-solid separations, small, suspended particles or colloids impede rapid gravitational separation. Increasing the effective particle size by flocculation alleviates this difficulty. The process of flocculation is the gathering together or aggregation of small entities, usually in liquid media, into larger masses called flocs therefore allowing. Flocculation is utilized to allow rapid separation of the liquid phase from a liquid-solid suspension. Flocculation, as defined in this research, is the formation of larger aggregates from suspended particles caused by polymeric flocculants. This thesis summarizes experimental and theoretical studies on the synthesis and characterization of cationic grafted copolymers for flocculation purpose.

1.1 Water-soluble polymers as flocculants

Water-soluble polymers have been utilized for water treatment for more than four decades. Their usage has increased rapidly since then. Global sales of water-soluble polymers are projected to be $20 billion by 2003 (Lerner, 2000). Water-soluble polymers are commonly used as flocculants. Generally, water-soluble polymers used as flocculants are divided into two groups: nonionic and ionic polymers (polyelectrolytes). Their water solubility is achieved by ionic and nonionic polar functional groups. Those water-soluble polymers that possess a certain type of charge because of the interaction between polar functional groups and aqueous media are usually called polyelectrolytes. Polyelectrolytes fall into two sub categories, anionic and cationic polymers, depending on their charge types.

Water-soluble polymers can be obtained from natural sources, such as starch and cellulose, or be synthesized, such as polyacrylamide (PAM) and polyethylene oxide (PEO).

Synthetic water-soluble polymers offer the following advantages: product consistency, reliable supply, chemical and biological stability, and the ability to be tailored to a specific application by varying monomers and synthetic methods.

1.1.1 Polymeric flocculants

Employment of polymeric flocculants accomplishes a basic solid-liquid separation that enabled further treatments. Synthetic polymeric flocculants have been developed commercially and studied extensively. Compared with their inorganic counterparts, polymeric flocculants have superior flocculation capacity thus only a small dosage is required to achieve the same level of flocculation and much less sludge is generated (Culp, 1979). Unlike inorganic flocculants, polymeric flocculants usually do not cause an ion concentration increase in solution after the treatment due to the low dosage required (Rose et al, 1990).

There are several molecular factors that affect flocculation: **charge type**, **charge density** and **molecular weight**. Charge types are anionic (negative), cationic (positive) and nonionic. Charge density describes the percentage of monomer units bearing a charged functional group in aqueous media. Cationic charge is obtained in commercial products mainly by quaternizing amine groups. Anionic charge is obtained by incorporating carboxyl or sulfonic acid groups. The molecular weights (MW_w) of polymeric flocculants are between 10^4 and 10^7.

More than half of all polymeric flocculants are based on acrylamide homo- and co-polymers (Rose et al, 1990). They can be easily prepared by free radical polymerization. PAM homopolymer is nonionic. By choosing different types of comonomers, PAM based polymers can be cationic or anionic. PAM resins, especially those with cationic charges, is predicted to hae strong growth in water treatment and paper production (Lerner, 2000). Other important flocculant types are polyamines and quaternary ammonium types. Polydiallyldimethyl ammonium chloride (polyDADMAC) is by far the most popular quaternary ammonium flocculants. The polymer has a repeating unit structure of a five-member ring formed during polymerization (Masterman et al, 1994). Due to the strong charge repulsion between propagating monomeric units and monomers,

polyDADMAC can not reach very high molecular weight, usually less than 5×10^5. A recently developed class of polymers based on poly(N-vinylformamide) (PNVF) (Stinson, 1993) shows a promising prospect as a flocculant. PNVF itself is a non-ionic type polyelectrolyte. After hydrolysis, it becomes polyvinylamine, which is cationic at low pH values.

Polymeric flocculants have been widely used in industries such as sewage plant, water treatment, papermaking, mineral processing and brewing industries (Auhorn et al, 1992; Burkert et al, 1984; Bolto et al, 1996; Gregory, 1983; Monech et al, 1993; Myagchenkov and Kurenkov, 1991; Pfohl et al, 1988, 1989, 1990; Rey and Vasanik, 1986; Theng, 1982; Vorchheimer, 1981), as is discussed in the following sections

Water Treatment: In a water treatment system, a large amount of the suspended colloidal particles must be removed. Settling and separation of the solid phase can not proceed without flocculation. Adding polymeric flocculants increases the efficiency of impurity removal. Polymeric flocculants are also used as sludge conditioners (Culp, 1979; Schwoyer, 1981; Vesilivd, 1979). Sludge collected during sedimentation usually contains up to 95% water by weight and must be dewatered before final disposal. Flocculation yields larger and stronger aggregates to facilitate further filtration or centrifugation to remove water. Sludge conditioning controls the cost of downstream sludge processing and has become an essential unit operation for most industrial and municipal wastewater treatment.

Pulp and paper: Polymeric flocculants are important additives in the pulp and papermaking industry. In paper making, the raw plant materials are milled. The fibers are dispersed into paper slurry. Polymer flocculants can be employed to separate and collect the fibers by means of flocculation. Polymeric flocculants are also used as retention aids to help the sheet-forming process (Gibbs et al, 1997). Titanium dioxide (TiO_2) is added to paper slurry as a white color pigment. When paper slurry is filtered on a screen to form a sheet of paper, the fiber and pigment should be kept in the sheet instead of being washed away. Polymeric retention aids used here are usually cationic or anionic PAM, polyamide and polyamines (Gutcho, 1977). Polymers

are also used as drainage aids in papermaking (Reynold and Wasser, 1981; Scalfarotto and Tarvin, 1984; Springer et al, 1984). Polymeric flocculants are also widely used in the oil, mining process (Kithener, 1977) and food industries as well. This thesis focuses on applications in water treatment.

1.2 Theories of flocculation

The particles that need to be flocculated are mainly in the colloidal range (10^{-9} - 10^{-6} m). Modern colloid and interface theories can well explain colloid dispersion, suspended particle interaction and colloidal particle stabilization-destabilization, which in turn establish the theoretical fundamentals of flocculation.

1.2.1 Colloid stability

A colloidal system can exhibit coagulation, phase separation or re-dispersion, corresponding to the changes of environmental conditions, such as pH value, ion concentration and additives.

Classical colloidal **DLVO** (**D**erjaguin, **L**andan, **V**erwey and **O**verbeek) theory points out that the two most important interactions among colloidal particles are the **Van der Waals force** (attraction) and **electrical repulsion** (Deryaguin and Landau, 1941; Verwey and Overbeek, 1948). The other important force among colloidal particles is the electrical repulsion force. In a stable colloid, colloidal particles bear the same type of surface charge. A layer of counterions is induced around the particle surface. This gives rise to the electrical double layer, which has been modeled by Stern (Stern, 1924 cited in Hunter, 1987). It is the mutual repulsion of these double layers that provides electronic stability for colloidal particles. Graham (Hunter, 1993) improved the Stern double layer to describe a broader diffusive double layer model, in which charges are more sparsely distributed from particle surface to bulk solution by a smaller charge density gradient.

The total interaction between two colloidal particles is the sum of attractive and repulsive forces. At an intermediate range the repulsion is the dominant effect, which leads to an energy

barrier that prevents particles from aggregating, thus the colloid is stable. If particles possess sufficient kinetic energy to overcome the energy barrier or for some reason the barrier is reduced (e.g., by adding flocculants containing counterions), then particles can easily get close enough so that attraction force becomes dominant, and thus flocculation occurred.

1.2.2 Effects of polymers on colloidal stability

When polymers are added to colloid dispersions, they are either adsorbed to particle surfaces or remain free in solution. Polymers can either improve colloidal stability or induce flocculation, depending on the nature of chains, thermodynamic factors and polymer dosage used (Table 1.1).

In steric stabilization, polymer chains form a physical barrier to keep the particles apart. Adsorbed ionic polymer chains are also able to increase the net charge and stabilize the system electrostatically. Both electrostatic and steric stabilization can be factors that contribute to an electrosteric stabilization mechanism.

A recent study showed that charged block copolymers could act as both stabilizers and flocculants depending on the polymer dosage and molecular weight of polymer (Hoogeveen et al, 1996). At high polymer dosage (high surface coverage), high molecular weight copolymers enhanced the colloidal stability. At low polymer dosage (low surface coverage), high molecular weight copolymers usually induced flocculation. For low molecular weight copolymers, charge neutralization (Section1.2.3, polymer flocculation mechanisms) was the dominant mechanism.

1.2.3 Polymer flocculation mechanisms

Polymers play a dual-role in a colloidal system. They can act either as flocculants or stabilizers. In the case of polymers as flocculants, they help to reduce or overcome the repulsive forces and resulting in flocculation. The possible mechanisms are:

1. chain bridging,

2. depletion,

3. charge neutralization, and

4. electrostatic patch.

Chain bridging flocculation is based on the irreversible adsorption of polymer chains onto particle surfaces. In a good solvent (when the polymer-solvent interaction parameter, χ, is less than 0.5), polymer chains have expanded conformations. Polymer chains have attachments to particle surface at multiple points. The unattached chain segments remain extended into the bulk solvent. This kind of adsorption gives a loop chain conformation. Desorption is virtually impossible for polymer chains because of the multiple attachment points (Silberberg, 1962).

Table 1.1 The Effects of polymer on colloidal stability (Hunter, 1987; Jenkins and Snowden, 1996; Li-in-on et al, 1975; Naper, 1983)

Adsorbed			Non-adsorbed
surface coverage by polymers	nonionic polymers	ionic polymers	depletion flocculation or depletion stabilization
Low	Bridging flocculation	electric patch flocculation	
High	Steric stabilization	electrostatic stabilization electrosteric stabilization	

Ruehrwein and Ward (1952) first proposed the concept of a chain bridge flocculation in 1952. If a polymer chain is adsorbed onto more than one particle, the polymer can act as a bridge to bond several particles together resulting in flocculation. The bondage between particle surfaces and polymer chains can be hydrogen bonding, chemical interactions for nonionic polymer chains or electrical attraction if the polymer chains have the opposite type of charges.

When the adsorption of polymer chains is unfavorable, the polymer chains are repelled from the interface, leading to a depletion zone, in which the polymer concentration is lower than that in bulk solution, surrounding the particle surfaces. When particles approach to each other, their depletion zones tend to overlap to reduce the total volume of depletion zones and thus the free energy of the system. Solvent is squeezed out from inter-particle region into bulk solution. This induces **depletion flocculation**. This mechanism is very much affected by the polymer solution and interfacial thermodynamics and is often reversible. Several theoretical models have been proposed (Jenkins and Snowden, 1993; Napper, 1983) to describe this mechanism.

For charged polymers, **charge neutralization** and **electrostatic patch** flocculation mechanisms are important. In charge neutralization, the charges on the particles are neutralized by the addition of counterions. The electrical double layer, that prevents particles from approaching each other, is greatly compressed by counterions. This allows a shorter surface distance between two particles thus short-range attractions become significant. Usually, there is an optimum flocculation dosage for polyelectrolytes for charge neutralization. Previous research proved that optimum flocculation occurred when the electrophoretic mobility of the particle was reduced to nearly zero (Bleier and Goggard, 1980; Sandell and Luner, 1974). The electrophoretic mobility is the moving speed of charged suspension particles in an electric field divided by the electric field strength (Hunter, 1987). However, Black and Vilaret (1969) reported that when a polystyrene suspension was adjusted to zero electrophoretic mobility by adding a low molecular weight but highly charged cationic polymer, the particles were completely stabilized in solution. Optimum

flocculation occurred when mobility was still highly negative (~ -3×10^{-8} m^2 sec^{-1} V^{-1}). They also obtained similar results for clay particles.

Based on Black and Vilaret's (1969) data, Gregory (1973) and Kasper (1971) proposed an electrostatic patch model. Typical suspension particles, such as polystyrene, have relatively low negative surface charge density. When highly charged cationic polymers are adsorbed onto particle surface, positive charges become excessive for neutralization in the attached area. At this time, the net charge of the colloid system is still negative. This results in a mosaic distribution of positive and negative charges on the particle surface. When two particles meet, it is possible that a positively charged area on one particle is able to contact a negatively charged area on the other particle, giving an electronic attraction between particles and triggering flocculation.

1.3 Polyelectrolytes based on poly(N-vinylformamide)

The industrial interest in poly(N-vinylformamide) (PNVF) can be traced back to polyvinylamine (PVAm). Like poly(vinyl alcohol), PVAm is prepared via indirect means. For many years, companies have been trying to find a way to produce PVAm commercially. Recent development of a new low cost monomer technology casts a light onto an easier route to prepare PVAm. This new technology provides a commercially feasible route to N-vinylformamide (NVF). The monomer is stable at room temperature, has low toxicity and is easy to polymerize (Stinson, 1993). The corresponding polymer, poly(N-vinylformamide) (PNVF) can easily be hydrolyzed to PVAm thermally or in acidic or basic solutions. During the past few years, the number of research papers and patents on NVF has been growing rapidly. The most explored applications of PNVF are in flocculation, drainage aids, paper making, oil recovery and flow drag reduction. The basic physical and chemical properties, polymerization, copolymerization and post-production modifications of NVF have been reported. However, the fundamental aspects of

NVF, such as polymerization kinetics, molecular weight (MW) and molecular weight distributions (MWD) has received little attention so far.

Polyvinylamine (PVAm) is a water-soluble polymer with a high density of very polar, Lewis-basic amino groups in its repeating units. The amino groups have many useful reactions which make PVAm very useful in water treatment, papermaking, textile finishes, personal care products, adhesives, coatings and oil field chemicals (Stinson, 1993). However, the simplest precursor to PVAm, vinylamine, is unstable. As a result, PVAm is always synthesized by indirect methods. The first synthesis of a substantially pure PVAm (>90 mol% NH_2) was achieved by hydrolyzing poly(N-vinylphthalimide) with hydrazine (Reynolds and Kenyon, 1947). The developed synthesis routes of PVAm involved modifications of precursor polymers which are readily available, such as polyacrylamide (PAM) (Achari et al, 1993), polyacrylic acid (PAA) (Hughes and Pierre, 1977), polyacrylonitrile (PAN) (Todorov et al, 1996) and poly(N-vinyl *tert*-butylcarbamate) (PTBNVC) (Fischer and Heitz, 1994; Hart, 1959). These methods, always complicated and expensive, usually comprised a series of reactions followed by a final hydrolysis step to PVAm. As a result, a commercial scale production of PVAm was not feasible.

1.3.1 General information about N-vinylformamide

N-vinylformamide is the simplest member of N-vinylamide family. It is developed as a precursor to amide and amine functional polymers. NVF has showed attractive high reactivities in polymerization, copolymerization and hydrolysis. It was first synthesized more than three decades ago (Kurtz and Disselnkoetter, 1965). Different synthetic routes to NVF have since been reported (Pinschmidt and Sagl, 1996). A recently developed production technology used two simple chemicals, acetaldehyde and formamide, to synthesize the precursor of NVF, ethylideneformamide. The latter was then heated to produce NVF with the help of a catalyst. Figure 1.1 shows one of the synthesis routes (Stinson, 1993), as well as the polymerization and hydrolysis steps. This has become the only commercially attractive route now. Air Products and Chemicals (The development has now been discontinued) (1986), BASF (1983) and Mitsubishi

Chemical Corp (1996). all developed similar technologies to produce NVF through cracking of ethylideneformamide.

NVF is a water soluble, colorless liquid, which dissolves in most polar solvents, such as methanol, ethanol, chloroform and THF. N-hexane and n-butane are two of its poor solvents. NVF is stable and can be stored at room temperature for months. The commercial product usually has a light yellow color due to the added inhibitor. Some of NVF's important properties are listed in Table 1.2

PNVF is able to hydrolyze to amine-based polymers in the presence of catalysts. The amino groups are obtained as an acidified amino salt at acidic conditions or free amine groups at basic conditions. Some basic properties of PNVF are listed in Table 1.3.

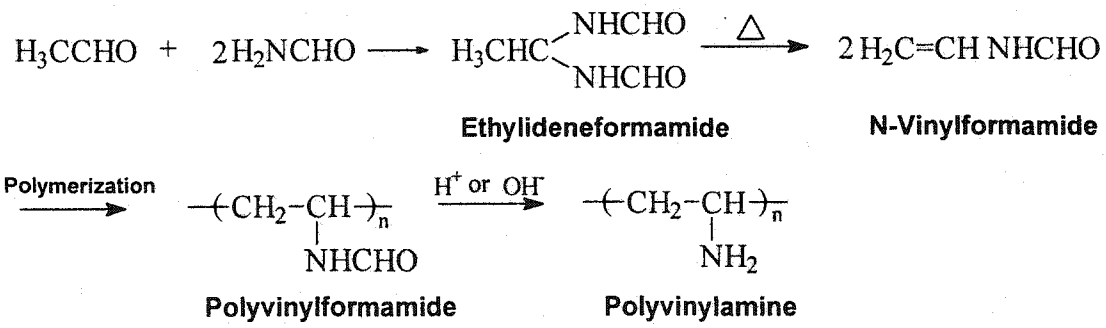

Figure 1.1 Synthesis of NVF, PNVF and PVAm (Stinson, 1993).

Table 1.2 Some basic properties of NVF

Molecular weight	71.02 g/mol
Boiling point	210 °C at 1 atm (Stinson, 1993; Pinschmidt et al, 1997)
	84 °C at 10 mmHg (Stinson, 1993; Pinschmidt et al, 1997)
Specific gravity	1.01 at 25 °C (Pinschmidt et al, 1997; Singley, 1997)
Index of refraction	1.4948 at 20 °C (Mitsubishi, 1998)
Polymerization heat	66.6 kJ/mol aqueous (Mitsubishi, 1998)
	60.0 kJ/mol bulk (Schmidt et al, 1996)
	~80 kJ/mol (Pinschmidt et al, 1997)
Acute oral LD_{50} (rat)	1444 mg/kg (Stinson, 1993; Pinschmidt et al, 1997)

Table 1.3 Some basic properties of PNVF

Glass transition temperature, T_g	126.0 °C, DSC 10 °C/min (Mitsubishi, 1998)
TG analysis	250 °C, side chain decomposition (Mitsubishi, 1998)
	330 °C, main chain breakage (Mitsubishi, 1998)
Mark-Houwink constants	$K=5.43\times10^{-4}$, $\alpha=0.715$, 30 °C (Singley et al, 1997)
	$K=8.31\times10^{-5}$, $\alpha=0.76$, 25 °C (Mitsubishi, 1998)

1.3.2 Homopolymerization of NVF

The free radical route is the most common mechanism of NVF polymerization. Oil or water-soluble azo-compounds, such as AIBN, or organic peroxides are the most suitable free radical initiators. Polymerization is usually carried out in aqueous solution, inverse emulsion, mircroemulsion, dispersion or precipitation polymerization, and more recently supercritical medium (Singley, 1997), such as carbon dioxide. These methods give molecular weights ranging from 5×10^4 to 6×10^6. Emulsion polymerization usually gives higher molecular weight while solution and precipitation polymerizations yields lower molecular weight.

NVF also undergoes cationic oligomerization using protonic or Lewis acids (Pinschmidt et al, 1996, Madl and Spange, 2000). One reported case (Spange and Madl, 1997) used iodine, bis(4-methoxyphenyl)-methyl chloride/silica, triphenylmethyl chloride/silica, and trimthylsilyl triflate as initiators and produced a narrow MWD with moderate yield (20-50wt%). The typical molecular weight range was between 500 and 1000. There is also a patent by Fikenscher and Kroener (1992) on the dimerization and low oligomer synthesis of PNVF with terminal double bonds using anionic polymerization under basic conditions.

The studies of NVF free radical polymerization kinetics have been lagging behind. So far there has been only one paper (Schmidt et al, 1996) that reported a DSC study on NVF bulk free radical polymerization. However, the main purpose of this paper was to compare the accuracy and durability of different calorimeters. Although Schmidt et al (1996) presented the combined rate constant, $k_p/(k_t)^{0.5}$, data at 70 and 80 °C, heat of reaction of polymerization and a simple model, the kinetics has not been adequately explained.

1.3.3 Copolymerization of NVF

According to the well-known Price and Alfrey scheme, the reactivity of radical and monomer Q, and the polarity of the two components e roughly determines the copolymerization ability of a comonomer pair. Usually, the Q and e values of styrene set to 1.0 and –0.8 as

references. Higher Q value indicates higher copolymerization reactivity and higher e value indicates greater electron-withdrawing power (less negative) (Carraler, 1996). The Q and e values of NVF are Q = 0.29 and e = 0.52 (Mitsubishi, 1998). NVF is, therefore, able to copolymerize with a wide range of acrylic and vinyl monomers. Table 1.4 lists the copolymerization reactivity ratios of NVF to other monomers.

When NVF is copolymerized with acrylates, acrylamide, maleates or acrylonitrile, the copolymers are of an alternating type. On the other side, copolymerization with vinyl esters and ethylene yields the random types of copolymers.

1.3.4 Hydrolysis of PNVF

Hydrolysis of NVF polymers and copolymers to amino functional polymers under acidic or basic conditions is relatively faster and requires milder conditions than the other PVAm precursors. PNVF hydrolysis under acidic conditions proceeds to about 60-70mol% conversion because of the charge repulsion effects (Badesso et al, 1992). Stoichiometric basic hydrolysis is usually a better approach with almost 100mol% completion. For example (Badesso et al, 1993; Badesso et al, 1995), at 60-80°C, a 95mol% hydrolysis was achieved in 3 hours. After 6-8 hours, NMR detected no residual amide groups. One problem encountered in hydrolysis is the removal of the hydrolysis byproducts, usually formic acid from acid hydrolysis and sodium formate from base hydrolysis. An alternative approach is to carry out acid hydrolysis reaction in alcohol, such as methanol aqueous solution, so that the decomposed formyl group can form methyl formate that can be stripped as a light component. A recent patent (Ford and Armor, 1996) claimed a thermo-hydrolysis of PNVF to PVAm targeting a low salt concentration in the final products. PNVF homo- or copolymers were heated in aqueous solution under the catalysis of a transition metal compound. The process gave up to 70 mol% hydrolysis conversion.

Table 1.4 Copolymerization reactivity ratios of NVF to other monomers

Monomer 1	Monomer 2	r_1	r_2
NVF	Acrolein	0.18	1.18
(Mitsubishi, 1998)	Acrylamide	0.11	0.51
	Acrylonitrile	0.2	0.26
	Butyl acrylate	0.26	0.32
	Diacetone acrylamide	0.56	1.51
NVF	N, N'-Dimethylacrylamide	0.24	1.77
(Mitsubishi, 1998)	N-Methyl methacrylamide	0.95	1.05
	Ethyl acrylate	0.38	1.52
	Ethylene	16.4	0.06
	2- Ethylhexyl acrylate	0.99	0.44
NVF	Hydroxylethyl acrylate	1.28	0.19
(Mitsubishi, 1998)	Hydroxylethyl methacrylate	2.39	0.25
	Maleic anhydride	0.3	0.002
	Methyl acrylate	0.39	0.74
	Sodium acrylate	0.33	2.56
NVF	Sodium methacrylate	0.3	2.15
(Mitsubishi, 1998)	Styrene	0.34	2.76
	Vinyl acetate	9.54	0.09
	Vinyl ether	11.6	0.05
	N-vinyl pyrrolidone	2.86	0.24
NVF	Acrylamide (Kathmann and McCormick, 1993)	0.046	0.51
(Mitsubishi, 1998)	Butyl acrylate (Kathmann and McCormick, 1993)	0.071	0.55
	Maleic anhydride (Chang and McCormick, 1993)	0.041	0.011
	Sodium acrylate (Kathmann and McCormick, 1993)	0.22	0.52
	Sodium 3-acrylamido-3-methylbutanoate (Kathmann et al, 1996)	0.25	0.29
	Sodium 2-acrylamido-2-methylpropanesulfonate (Kathmann et al, 1996)	0.25	0.24

$r_1 = \frac{k_{p11}}{k_{p12}}, \quad r_2 = \frac{k_{p22}}{k_{p21}}$

* Calculated by Kelen-Tudos method

1.3.5 Applications of PNVF and its derivatives

PNVF based polymers and copolymers have many applications in water treatment, papermaking, flocculation and coatings. Many patents have been issued covering these areas. Table 1.5 lists some of the applications.

1.4 Proposal of new grafted copolymers as a new type of flocculants

The addition of polymers induces flocculation of the colloidal particles from the water phase, thereby either recovering valuable materials or removing unwanted solids. Cationic polymers acting as counterions **neutralize** the surface charges on colloidal particles. Long chain nonionic polymers (e.g. polyacrylamide) rely on irreversible multi-points adsorption of polymer chains onto the surfaces of different colloidal particles. The polymer chains can subsequently bring particles together by **chain bridging**.

In reality, most water-soluble polymeric flocculants incorporate both mechanisms. Cationic charge centers provide firm attraction to particle surfaces while long polymer chains extend from one particle to another. To date, most commercial polymer flocculants are linear copolymers with randomly distributed cationic charges along the polymer chain. Typical examples are modified PAM or copolymers of acrylamide (AM) with cationic comonomers, usually polyquats, polyimines or polyamine (McCormick et al 1988; McDonald and Beaver, 1979; Pelton, 1984).

Table 1.5 Applications of PNVF based polymers and copolymers

Polymers	Applications
Partial hydrolyzed PNVF	increasing dry and wet strength of paper board (Auhorn et al, 1992; Monech et al, 1993; Pfohl et al, 1988, 1989, 1990) flocculating sewage sludge (Burkert et al, 1984) flocculating red mud from Bayer process liquor (Sammese and Mahoney, 1994) dewatering and thickening coal tailing slurries (Sammese and Pillai, 1997) Retention aid (Wang and Tanaka, 2000, 2001)
PNVF copolymers with quaternary ammonium or amine	drainage aids (Monech et al, 1993)
PNVF hydrolyzed with acid or base	oil field recovery (Pinschmidt and Lai, 1990)
PNVF copolymers	radiation and photo curable resins (Comfroth et al, 1994; Pinschmidt and Chen, 1998)

The ionic centers generated by these methods are inevitably distributed randomly along a polymer chain. It is necessary to control the charge density distribution within the chain structure to improve the performance of these flocculants. A graft copolymer model, with a long nonionic backbone and cationic grafts, was proven to be a suitable alternative (Ma, 1996; Subramanian et al, 1999). Figure 1.2 shows the different flocculation situations caused by random and graft copolymers. Graft copolymer makes more efficient use of charge than random copolymer. Instead of having randomly distributed cationic charges along the polymer chain, the graft copolymer has locally concentrated cationic clusters to provide stronger polymer-surface interaction. A high molecular weight backbone enables multi-point adsorption onto particle surface and inter-particle extension. Highly charged commercial polymers are expensive. Such a combination not only reduces the cost of using solely charged homopolymer but also takes the advantage of the high molecular weight backbone polymer.

There are three general synthesis schemes to achieve a graft copolymer. They are **grafting-from**, **grafting-onto** and **grafting-through** (Dreyfuss and Quirk, 1988). **Grafting-from** scheme requires the generation of active sites on a polymer chain, and the subsequent growth of side chains from these sites. As an example, polyDADMAC-*graft*- PAM was synthesized by firstly generating free radicals using ceric ion (Ce^{4+}) on PAM chains and then adding DADMAC monomeric units form polyDADMAC side chains on the PAM chains by free radical polymerization (McLachlan, 1997). **Grafting-onto** scheme usually uses two pre-polymers. A chemical process is initiated to bond the chains into a graft copolymer via functional group reaction or free radical recombination. Since the grafting involves two polymer reactants, reactive processing is usually considered as a good choice for its volume efficiency and the ability of handling highly viscous system (Brown and Orlando, 1990; Lambla, 1993). **Grafting- through** scheme (also referred to as "macromonomer procedure") is divided into two steps. First, a macromonomer with unsaturated end group is synthesized, often by anionic polymerization. Subsequently a second monomer is added to copolymerize with the macromonomer to form a

graft copolymer. It is the only method that controls the size of the side chain (through anionic polymerization) and the charge density in each graft copolymer chain (through semi-batch copolymerization)

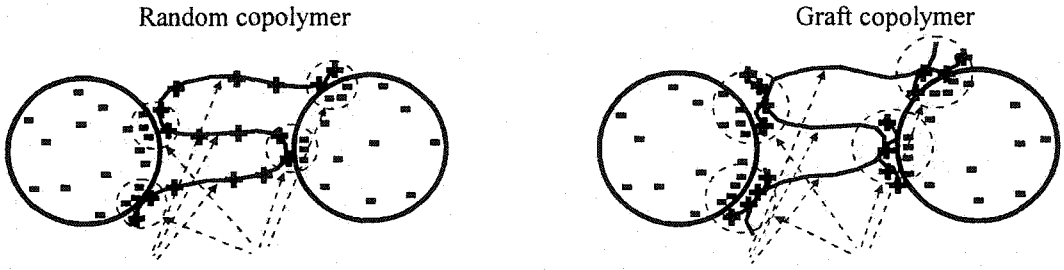

Figure 1.2 Comparison of different molecular design for polymeric flocculants.

1.5 Objectives of current work

With the growing interests in PNVF, PVAm and their derivatives, this work aims at gaining a comprehensive understanding of the polymerization and reactions of NVF monomer. It also intends to explore the impact of graft structure on the flocculation performance of the polymers. In addition, theoretical modeling the grafting process was carried out.

In summary, the thesis objectives are to:

1. study the kinetics of NVF free radical polymerization in bulk and solution,
2. characterize MW and MWD development of the resulting polymers,
3. model the kinetics of NVF free radical polymerization process,
4. study the hydrolysis of PNVF to polyelectrolytes,
5. synthesize graft copolymers with cationic side chains and non-ionic backbones as proposed and test their performance as flocculants, and
6. model grafting processes.

1.6 References

Achari, A. E. Coqueret, X. Lablach-combier, A. and Louchex, C. (1993). "Preparation of Polyvinylamine from Polyacrylamide: A Reinvestigation of the Hofman Reaction". *Makromol. Chem., 194*, 1879.

Auhorn, W. Linhart, F. Lorencak, P. Kroener, M. Sendhoff, N. Denzinger, W. and Hartmann, H. (1992). US. Patent No. 5145559, BASF.

Badesso, R. J. Lai, T. Pinschmidt, R. K. Jr. Sagl, D. J. and Vijayendran, B. R. (1992). "High and Medium Molecular Weight Poly (vinylamine)". *Polymer Preprints, 32*, 110.

Badesso, R. J. Nordquist, A. F. Pinschmidt, R. K. Jr. and Sagl, D. J. (1995). "Synthesis of Amine Functional Homopolymers with N-Ethenylformamide", in *Hydrophilic Polymers: Performance with Environmental Acceptance*, E. Glass ed., American Chemical Society, Washington DC, p. 489.

Badesso, R. J. Pinschmidt, R. K. Jr. and Sagl, D. J. (1993). "Synthesis of Amine Functional Homopolymers with n-Ethenylformamide". *Proc. Amer. Chem. Soc. Div. Polym. Mat. Sci. Eng., 69*, 251,

Black, A. P. and Vilaret, M.R. (1969). "Effect of Particle Size on Turbidity Removal". *J. Amer. Waterworks Ass., 61*, 209.

Bleier, A.and Goggard, E. D. (1980). "Flocculation of Aqueous Silica Suspensions Using Cationic Poly-Electrolytes". *Colloids Surf., 1*, 407.

Bolto, B. Dixon, D. Gray, S. Chee, H. Harbour, P. Ngoc, L. and Ware, A. (1996). "The Use of Soluble Organic Polymers in Waste Treatment". *Water Sci. & Tech., 34(9)*, 117.

Brown, S. and Orlando, C. (1990). "*Reactive Extrusion*", in H. Mark et al, ed., *Encyclopedia of Polymer Science and Engineering*, vol. 14, John Wiley & Sons, New York, 2nd ed., 169.

Brunnmueller; F. Schneider, R. Kroener, M. Mueller, H. and Linhart, F. (1983). US. Patent No. 4421602, BASF.

Burkert, H. Brunnmueller, F. Beyer, K. Kroener, M and Mueller, H. (1984). US Patent No. 4444667, BASF.

Carraler, C. E. Jr., *Polymer Chemistry: An Introduction*, Marcel Dekker Inc., New York, 4th ed., 1996, p. 334.

Chang, Y. and McCormick, C. (1993). "Water-Soluble Copolymers. 47. Copolymerization of Maleic Anhydride and N-Vinylformamide". *Macromol.*, *26*, 4814.

Cornfroth, D. A. Fowler, D. and Renz, W. L. (1994). US Patent No. 5281682, Air Products and Chemicals.

Culp, G. L. (1979). *Handbook of Sludge-Handling Processes*, Garland STPM Press, New York & London.

Dawson, D. and Otteson, K. M. (1986). US. Patent No. 4578515 (1986), Air Products and Chemicals.

Deryaguin, B. V. and Landau, L. D. (1941). " Theory of Stability of Strongly Charged Lyophobic Sols and of the Adhesion of Strongly Charged Particles in Solutions of Electrolytes". *Acta Physicochim, URSS*, Vol 14, p. 633.

Dreyfuss, P. and Quirk, R. P. (1988). "Graft Copolymers", in H. Mark and J. Kroschwitz ed. *Encyclopedia of Polymer Science and Engineering*, 2nd ed., vol. 7, Wiley Interscience, New York, p. 551.

Fikentscher, R. and Kroener, M. (1992). US. Patent No. 5155270 (1992), BASF.

Fischer, T. and Heitz, W. (1994). "Synthesis of Polyvinylamine and Polymer Analogous Reactions". *Macromol. Chem. Phys.*, *195*, 679.

Ford, M. and Armor, J. N. (1996). US. Patent No. 5491199, Air Products and Chemicals.

Gibbs, A. Xiao, H. Deng, Y and Pelton, R. H. (1997). "Flocculants for Precipitated Calcium-Carbonate in Newsprint Pulps". *Tappi J., 80(4)*, 163.

Gregory, J (1983). "Polymeric Flocculants", in C. A. Finch, ed., *Chemistry and Technology of Water-Soluble Polymers*, Plenum Press, New York.

Gregory, J. (1973). "Rates of Flocculation of Latex Particles by Cationic Polymers". *J. Colloid Interface Sci., 42*, 448.

Gutcho, S. (1977). *Waste Treatment with Polyelectrolytes and Other Flocculants*, Noyes Data Corp., New Jersey.

Hart, R. (1959). "Synthese de la Polyvinylamine Hydrolyse du Poly-N-vinylcarbamate de tert.-Butyle". *Makromol. Chem., 32*, 51.

Hoogeveen, N.G. Stuart, C. Martien, A. and Fleer, G. J. (1996). "Can Charged (Block Co-Polymers Act as Stabilisers and Flocculants of Oxides?" *Colloids and Surfaces, 117*, 77.

Hughes, A. R. and Pierre, T. St. *Macromolecules Synthesis*, Vol 6, J. E. Mulvaney Ed., Wiley, New York, 1977, p.6.

Hunter, R. J. (1993). *Introduction to Modern Colloid Science*, Oxford University Press Inc. New York.

Hunter, R.J. (1987). "Polymeric Stabilization and Flocculation", in *Foundations of Colloid Science.* Vol. 1, Chapter 8. Oxford University Press Inc., New York.

Jenkins, P. Snowden, M. (1996). "Depletion Flocculation in Colloidal Dispersions". *Advances in Colloid and Interface Science, 68*, 57.

Kasper, D. R. (1971). Theoretical and experimental investigations of the flocculation of charge particles in aqueous solutions by polyelectrolytes of opposite charge, Thesis (Ph.D.), California Institute of technology, Pasadena, CA.

Kathmann, E. and McCormick, C. (1993). "Water-Soluble Copolymers. 48. Reactivity Ratios of N-vinylformamide with Acrylamide, Sodium Acrylate, and n-Butyl Acrylate". *Macromol.*, *26*, 5249.

Kathmann, E. White, L. and McCormick, C. (1996). "Water-Soluble Copolymers. 67. Polyelectrolytes of N-vinylformamide with Sodium 3-Acrylamido-3-methylbutanoate, Sodium 2-Acrylamido-2-methylpropanesulfonate, and Sodium Acrylate: Synthesis and Characterization". *Macromol.*, *29*, 5268.

Kithener, J. A. (1977). "Flocculation in Mineral Process", in K. J. Ives, ed., *The Scientific Basis of Flocculation*, Sijtjoff & Noordhoff International Publishers, Alpen aan den rijh, The Netherlands, p. 283.

Kurtz, P. and Disselnkoetter, H. (1965). Ger. Offenl. No. 1228246, 1224304, Bayer.

Lambla, M. (1993). *Comprehensive Polymer Science* (first supplement), G. Allen and J.C. Bevingtoon eds., Pergamon Press, New York, p. 619.

Lerner, I. (2000). "New Water Soluble Polymers Association Forms as Market Gears for Growth". *Chemical Market Reporter*, November 13th, 2000. Online: http://www.chemexpo.com/cmronline/stories/11_13_00/12_11_13_00.cfm

Li-in-on, F. K. Vincent, B. and Waite, F.A. (1975). "Stability of Sterically Stabilized Dispersions at High Polymer Concentrations". *ACS Symposium Series*, No 9, p165.

Ma, M. (1996). "Grafting Cationic Polyelectrolytes onto Polyacrylamide for flocculation and sludge dewatering applications", Thesis (Master), McMaster University, Hamilton, Ontario, Canada.

Masterman, T. Dando, N. R. Weaver, D. G. and Seyferth, D. (1994) "Investigation of the Microstructure of Poly(Diallyldimethylammonium Chloride) by Nitrogen-14(15) NMR-Spectroscopy". *J. Polym Sci., Part B: Polymer Phys.*, *32*, 2263.

McCormick, C. Bock, J. and Schulz, D. (1988) "Water-soluble Polymers", in H. Mark and J Kroschwitz ed. *Encyclopedia of Polymer Science and Engineering*, vol 17. Wiley, New York, p 730.

McDonald, C. and Beaver, R. (1979). "The Mannich Reaction of Poly(acrylamide)". *Macromolecules, 12*, 203.

McLachlan, J. (1997). "Synthesis and characterization of graft polyelectrolytes". Thesis (Master). McMaster University, Hamilton, Ontario, Canada.

Mitsubishi Chemical Corp. (1998). *N-vinylformamide*, Product Information Booklet,

Moench, D. Hartmann, H. and Buechner, K. (1993). US. Patent No. 5225088 (1993), BASF.

Monech, D. Hartmann, H. Freudenberg, E. and Stange, A. (1993). US. Patent No. 5262008, BASF.

Myagchenkov, V. A and Kurenkov, V. F. (1991). "Application of Acrylamide Polymers and Copolymers: A Review", *Polym.-Plast. Technol. Eng., 30(2&3)*, 109.

Napper, D. H. (1983). *Polymeric Stabilisation of Colloidal Dispersions*, Academic Press, London.

Pelton, R. H. (1984). "Model Cationic Flocculants From the Mannich Reaction of Polyacrylamide". *J. Polym. Sci. Polym. Chem. Ed., 22*, 3955.

Pfohl, S. Kroener, M. Hartmann, H. and Denzinger, W. (1988). US. Patent No. 4774285, BASF.

Pfohl, S. Kroener, M. Hartmann, H. and Denzinger, W. (1989). US. Patent No. 4880497, BASF.

Pfohl, S. Kroener, M. Hartmann, H. and Denzinger, W. (1990). US. Patent No. 4978427, BASF.

Pinschimdt, R. K. Jr. and Chen, N. (March 1998). "New N-Vinylformamide Derivatives and Their Use in Radiation Cure Coatings". *Polymer Preprints, 39(1)*, 639.

Pinschimdt, R. K. Jr. and Lai, T. (1990). US. Patent No. 4931194.

Pinschmidt, R. Jr., Renz, W. Carroll, E. Yacoub, K. Drescher, J. Nordquist A. and Chen, N. (1997). "N-Vinylformamide – Building Block for Novel Polymer Structures". *J. Macromol. Sci., A34*, 1885.

Pinschmidt, R. K. Jr. and Sagl, D. J. (1996). "Polyvinylamine (Overview)", In J. C. Salamone Ed. *Polymeric Material Encyclopedia.* CRC Press, Boca Raton, p. 7095.

Pinschmidt, R. K. Wasowski, L.A. Orphanides, G.G. and Yacoub, K. (1996). "Amine Functional Polymers Based on N-ethenylformamide". *Proc. 20th Inter. Conf. Orag. Coatings Sci and Technol. 1994. 27*, 209.

Rey, P. A.and Varsanik, R.G. (1986). "Application and Flocculation of Synthetic Polymeric Flocculants in Wastewater Treatment", in J. E. Glass, ed., *Water-Soluble Polymer: Beauty with Performance*, Advances in Chemistry Series 213, American Chemical Society, Washington, D.C.

Reynolds, D. D. and Kenyon, W. O. (1947) "The Preparation of Polyvinylamine, Polyvinylamine Salts and Related Nitrogenous Resins". in *J. Am. Chem. Soc., 69*, 911.

Reynolds, W. J. and Wasser, R. B. (1981). "Dry Strength Resins". in J. P.Casey, ed., *Pulp and Paper Chemistry and Chemical Technology*, 3rd ed., Vol 3, Wiley-Interscience, New York.

Rose, G. and John, M. R. St. (1990). "Flocculation", in H. Mark and J. Kroschwitz ed. *Encyclopedia of Polymer Science and Engineering*, vol 7. Wiley, New York, p 212.

Ruehrwein, R. A. and Ward, D. W. (1952). "Mechanism of Clay Aggregation by Polyelectrolytes". *Soil. Sci., 73*, 485.

Sammese, A. G. and Mahoney, R. P. (1994). US. Patent No. 5346628, Nalco Co.

Sammese, A. G. and Pillai, K. J. (1997). US. Patent No. 5622533, Nalco Co.

Sandell, L. S.and Luner, P. (1974). "Flocculation of Microcrystalline Cellulose with Cationic Ionene Polymers". *J. Appl. Polymer Sci., 18*, 2075.

Sato, S. Mori, Y. and Inoue, T. (1996). US. Patent No. 5527963, Mitsubishi Chemical Corp.

Scalfarotto, R. E. and TARVIN, R. F. (1984). "Efficiency of Polymeric Additives in Drainage and Dewatering". *Tappi J., 67*, 80.

Schmidt, C. Hungenberg, K. and Hubinger, W. (1996). "Vergleich von Kalroimetern fur die Kinetische Untersuchung von Polyreaktionen". *Chem. Ing. Tech., 68*, 953.

Schwoyer, W. L. K. (1981). "Sludge Dewatering". in *Polyelectrolytes for Water and Wastewater Treatment*, CRC Press, Inc., Boca Raton, Fla.

Silberberg, A. (1962). "The Adsorption of Flexible Macromolecules Part I. Isolated Macromolecules at a Plane Interface". *J. Phys. Chem., 66*, 1872.

Singley, E. J. (1997). "Development of Fluoroether Amphiphiles and Their Applications in Heterogeneous Polymerization in Supercritical Carbon Dioxide", Thesis (Ph.D.), University of Pittsburgh, 1997, p.221.

Singley, E. J. Daniel, A. Person, D. and Beckman, E. J. (1997). "Determination of Mark-Houwink Parameters for Poly (N-vinylformamide)". *J. Polym. Sci, Part A, Polym. Chem., 35*, 2533.

Spange, S. Madl, A. Eismann, U. and Utecht, J. (1997). "Cationic Initiation of Oligomerization of Vinylformamide". *Makromol. Rapid Commun., 18*, 1075.

Springer, A. M. Chadrakaran, C. and Wegner, T. H. (1984). "Single Procedure for Measuring Drainage, Retention, and Response to Vacuum of Pulp Slurries". *Tappi J., 67*, 104.

Stern, O. (1924). *Z.Elektrochem. 30*, 508 Cited in R. J. Hunter (1987) Hunter, R.J. (1987). "Electrified Interfaces: The Electrical Double Layer", in *Foundations of Colloid Science*. Vol. 1, Chapter 6. Oxford University Press Inc., New York.

Stinson, S. (1993). "Quest for Commercial Polyvinylamine Advances". *Chem. & Eng. News*, 71*(36)*, 32.

Subramanian, R. Zhu, S. and Pelton, R. H. (1999). "Synthesis and Flocculation Performance of Graft and Random Copolymer Microgels of Acrylamide and Diallyldimethylammonium Chloride". *Colloid. Polym. Sci., 277*, 939.

Theng, B. K. B. (1982). "Clay – Polymer Interactions – Summary and Perspectives". *Clays Clay Miner, 30(1)*, 1.

Todorov, N. G. Valkov, E. N. and Stoyanova, M. G. (1996). "Chemical Modification of Poly(acrylonitrile) with Amines". *J. of Polym. Sci, Part A, Polym. Chem., 34*, 863.

Verwey, E. J. W.and Overbeek, J. Th. G. (1948). *Theory of the Stability of Lyophobic Colloids*, Elsevier, Amsterdam.

Vesilivd, P. A. (1979). *Treatment and Disposal of Wastewater Sludge*, 2nd Ed., Ann Arbor Science Publishers, Inc., Ann Arbor, Mich., Chapter 7.

Vorchheimer, N. (1981). "Synthetic Polyelectrolytes", in *Polyelectrolytes for Water and Wastewater Treatment*, CRC Press, Inc., Boca Raton, Fla.

Wang, F. and Tanaka, H. (2000). "Aminated Poly-N-vinylformamide as a Modern Retention Aid of Alkaline Paper Sizing with Acid Rosin Sizes". *J. of Applied Polym. Sci., 78*, 1805

Wang, F. and Tanaka, H. (2001). "Mechanisms of Neutral-alkaline Paper Sizing with Usual Rosin Size Using Alum-Polymer Dual Retention Aid System". *J. of Pulp and Paper Sci., 27(1)*, 8

Chapter 2. Free Radical Polymerization of N-Vinylformamide

2.1 Introduction

N-vinylformamide (NVF), an isomer of acrylamide, is developed as a precursor for the production of polyvinylamine (PVAm) by the hydrolysis of poly(N-vinylformamide) (PNVF) (Stinson, 1993). NVF monomer has low toxicity and high reactivities for homo and copolymerization. Free radical polymerization is the most convenient method to produce PNVF although other methods include cationic (Spange, et al, 1997) and anionic polymerization. (Fikentscher and Kroener, 1992).

Industrial interests in PNVF and its derivatives (e.g. PVAm) are due to their potential applications in technologies such as wastewater treatment (Burkert et al, 1984) and papermaking (Auhorn et al, 1992; Monech et al, 1993; Pfohl et al, 1988, 1999, 2000) and to their uses as a potential replacement for acrylamide polymers for these applications.

However, a description of the fundamentals of NVF polymerization has not appeared in the literature. The free radical polymerization kinetics has received little attention. Schmidt and co-workers (Schmidt, et. al, 1996) reported a DSC study of NVF bulk polymerization. The combined rate constant $k_p/k_t^{1/2}$ values were estimated to be 1.70 and 2.03 $L/(mol*S)^{0.5}$ at 70 and 80°C respectively. In fact, the study focused more on the evaluation of the thermal measurement techniques than on the polymerization itself. Moreover, the heat of reaction of polymerization (ΔH_p) values also had large discrepancies (See Table 1.2, Chapter 1) to those reported by Pinschmidt et al (1997).

In this chapter, the results of experimental investigations and model simulations for both the bulk and aqueous solution polymerization of NVF are summarized. The heat of reaction NVF

polymerization was determined using a differential scanning calorimeter (DSC). The effects of temperature, and monomer, initiator concentrations on the polymerization kinetics and molecular weight development were examined. A free volume theory was incorporated into the model to describe the kinetic behaviour and molecular weight development throughout the polymerization.

2.2 Experimental

NVF monomer (Aldrich Inc.) was distilled under vacuum at 70 °C and stored at -15 °C before polymerization. The free radical initiator, 2,2'-azoisobutyronitirle (AIBN) and 2,2'-azobis (2-methylpropionamidine) dihydrochloride (AIBA) (Aldrich Inc.) were recrystallized twice before use. Millipore purified water was used for the aqueous solution polymerization.

The heat of reaction of NVF polymerization (ΔH_p) was measured by a Dupont Instruments differential scanning calorimeter, DSC 910 (TA instruments Inc., New Castle DE).

Polymerization kinetics: a given mixture of NVF and AIBN (NVF, AIBA and water in the case of solution polymerization) was charged to a set of glass ampoules, which were subject to 3 freeze-thaw cycles. After degassing, the ampoules were immersed into a circulating water bath maintained at the polymerization temperature. The ampoules were withdrawn at different time intervals and quench-frozen. The reactant mixture was dissolved in water and the polymer precipitated in methanol. All samples were dried under vacuum at room temperature for 48 hours. The polymerization conversion, x, was calculated using:

$$x = \frac{W_P}{M_0} \qquad 2.1$$

where W_p is the mass of polymer and M_0 the initial charge of monomer.

The molecular weight was measured using a Waters aqueous GPC, a 2690 separation module and a 2410 refractive index detector equipped with 3 Waters Ultrahydrogel^{TM} Linear GPC columns (ϕ7.8×300mm). The column temperature was maintained at 30 °C. The mobile phase was 0.05N $NaNO_3$ water solution subject to filtration (0.45μm). Polyacrylamide (PAM) standard

molecular weight samples (broad standards) ranging from 12,000 to 6 million were purchased from Polysciences Inc. A universal calibration was used with K = 0.000543 and $\alpha = 0.715$ for the PNVF samples (Singley, et al, 1997).

Gel fraction: PNVF gel fraction is defined as the weight percentage of dried gel separated from dried polymer by solvent (water) extraction. The gel fraction is defined as

$$\text{Gel}\% = \frac{W_{Gel}}{W_p} \times 100\% \qquad 2.2$$

where W_{Gel} is the mass of the dried gel residual after the extraction, and W_p is the initial mass of the dried polymer containing both sol and gel.

Gel hydrolysis: for gel hydrolysis experiments, reagent grade sodium hydroxide (NaOH) and hydrochloric acid (HCl) were used. A molar ratio of 4 to 1 of acid or base/amide groups was used. The mixture was heated to 80 °C for 24 hours.

2.3 Heat of reaction (ΔH_p) of NVF polymerization

The heat of reaction of NVF polymerization, ΔH_p (kJ/mol), was measured for NVF bulk and aqueous solution polymerization. The measured heats of reaction of isothermal NVF polymerization, in bulk and solution at 65 °C, with a sealed empty DSC cell as the reference are plotted against the solvent weight percentage in Fig 2.1 (dash line). All the measurements were taken after a sufficiently long time (at least 5 hours) until no further heat flux was observed.

Under isothermal conditions, the measured ΔH_p by DSC first increased with the monomer dilution in water and then levelled off. For a bulk polymerization, the system viscosity usually increases with conversion under isothermal conditions. Polymerization stops when the T_g of the polymer-monomer mixture reaches the reaction temperature, i.e. the glassy state. The presence of the solvent reduces the T_g and allows the polymerization to reach a higher conversion. In Figure 2.1, ΔH_p reached a maximum at 60wt% of solvent (40wt% monomer), which the final conversion was at 100% without the glass effect.

A temperature ramp method with linearly rising temperature was then used to complete the polymerization, to avoid the incomplete polymerization caused by the glass effect. Compared to the isothermal method, an extra measure to compensate the heat that was absorbed to raise the sample's temperature was also implemented. A DSC cell sealed with the same weight and composition (for solution polymerization) of PNVF was used as the reference for the ramp method. The ΔH_p results are listed in Table 2.1 and also plotted in Figure 2.1 (solid line). Using the ramp method, polymerization runs at different monomer concentrations gave almost the same ΔH_p results.

The reason for the discrepancy between the isothermal and ramp results at 40wt% monomer (Figure 2.1) is probably due to the interaction between monomeric units and solvent molecules (Joshi, 1962). The ΔH_p results measured for aqueous solution polymerization include the contribution from the difference of the heat of dissolving the monomer and polymer in water.

The average of ΔH_P results listed in Table 2.1 (79.4 kJ/mol) is taken as the molar heat of reaction for NVF polymerization. It is consistent with the result of Pinschmidt et al (1997).

2.4 Bulk polymerization

Figures 2.2 ~ 4 show the bulk polymerization kinetics at 0.006, 0.012 and 0.030 mol/L AIBN concentrations, each at three temperature levels, 50, 60 and 70 °C. All the conversion-time curves displayed an auto-acceleration in the rate ("gel effect" or Tromsdorff effect) from the start of the polymerization. The final conversion increased with increasing polymerization temperature. The glass transition temperature of PNVF was approximately 122 °C measured by DSC at a 10°C/min heating rate. The bulk polymerization yielded a glassy, colourless, transparent monomer-polymer mixture. No visible phase separation was observed throughout the polymerization.

Both the number-average molecular weight ($\overline{M}_n$) (Figures 2.5, 2.6 and 2.7) and weight average molecular weight ($\overline{M}_w$) (Figures 2.8, 2.9 and 2.10) of the NVF bulk polymerization increased with conversion from the start of the polymerization. The $\overline{M}_w$ of the samples ranged from several hundred thousand to approximately 5 million. These values are comparable to the free radical polymerization of acrylamide.

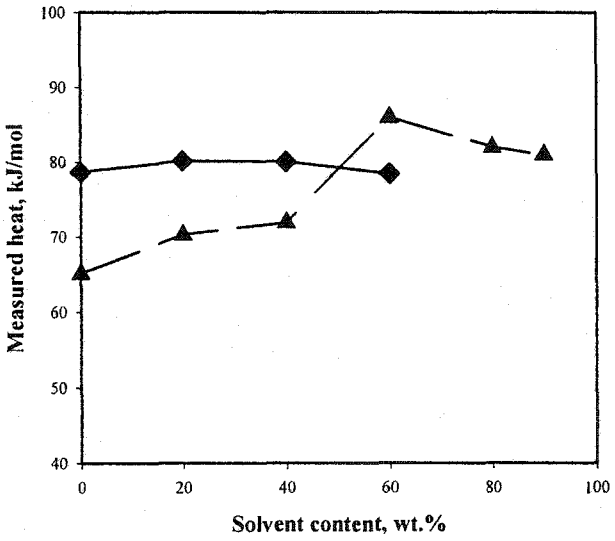

Figure 2.1 Measured ΔH_p of NVF bulk and solution polymerization, ◆ ramp, ▲ isothermal.

Table 2.1 Polymerization heat measured with ramp method

[M], wt%	T, °C	[I], wt%	ΔH_P, kJ/mol
100 (bulk)	40~150	1.0, AIBN	78.7
80	30~95	0.5, AIBA	80.2
60	30~95	0.5, AIBA	80.1
40	30~95	0.5, AIBA	78.5

Under certain experimental conditions, the system gelled. At 50 °C at all 3 initiator concentration levels, and at 60 °C with a concentration of AIBN of 0.006 mol/L, gels were found in the samples at the final stage of polymerization. Gelation was accompanied by a reduction in molecular weight of the sol content as shown in Figures 2.8 ~ 10 (at > 60% conversion). The gelation may be due to chain transfer to polymer followed by radical termination by recombination. For those samples without gel, $\overline{M}_w$ tended to level off at high conversions. All low conversion (less than 5%) samples had a polydispersity index (PDI, $\overline{M}_w / \overline{M}_n$) greater than 2.

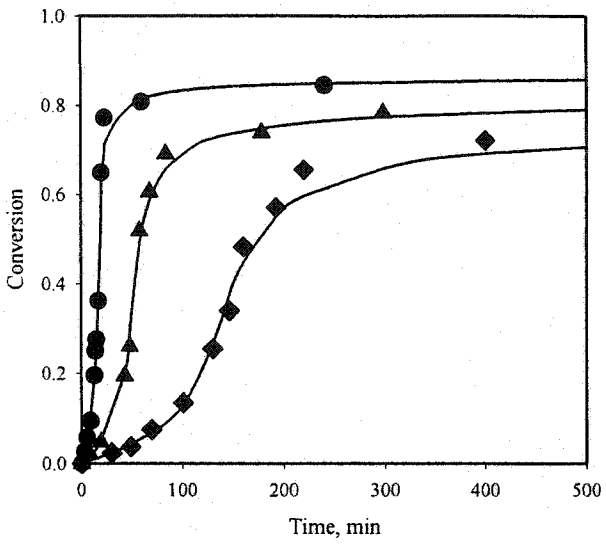

Figure 2.2 Conversion vs. time of NVF bulk polymerization, [I]=0.006mol/L, ◆ 50, ▲ 60, and ● 70 °C, — model.

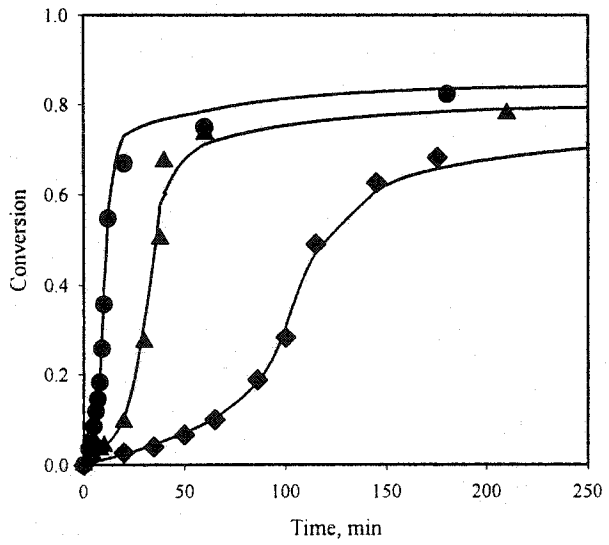

Figure 2.3 Conversion vs. time of NVF bulk polymerization, [I]=0.012mol/L, ◆ 50, ▲ 60, and ● 70 °C, — model.

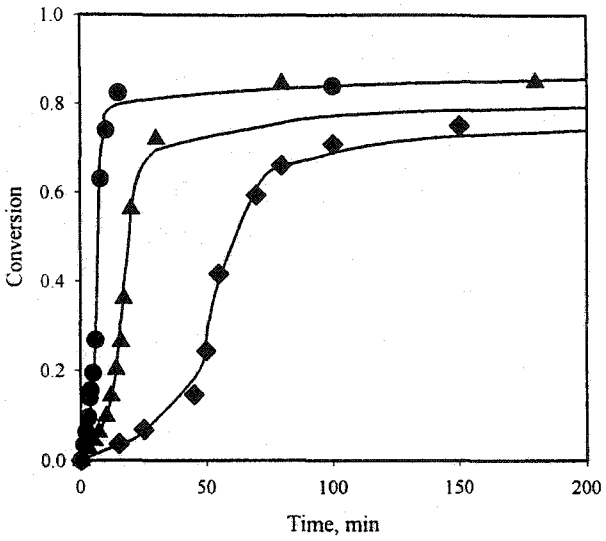

Figure 2.4 Conversion vs. time of NVF bulk polymerization, [I]=0.030mol/L, ◆ 50, ▲ 60, and ● 70 °C, — model.

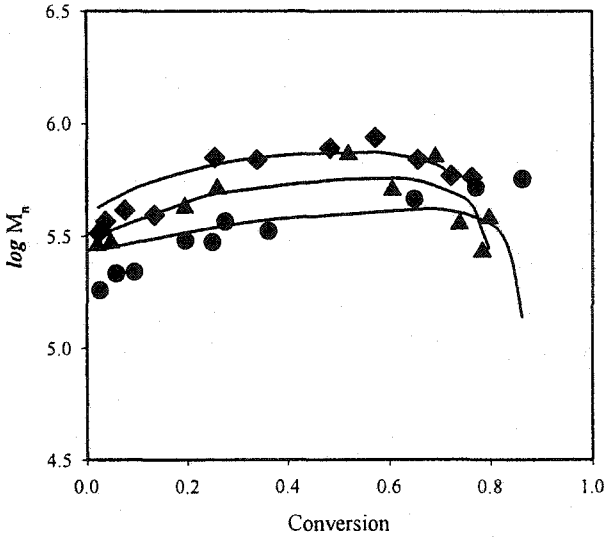

Figure 2.5 Development of $\overline{M}_n$ with conversion in bulk polymerization, [I]=0.006mol/L, ◆ 50, ▲ 60, and ● 70 °C, — model.

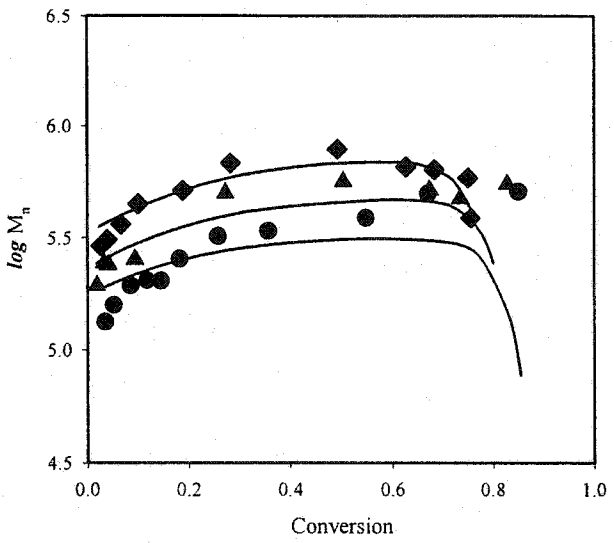

Figure 2.6 Development of $\overline{M}_n$ with conversion in bulk polymerization, [I]=0.012mol/L, ◆ 50, ▲ 60, and ● 70 °C, — model.

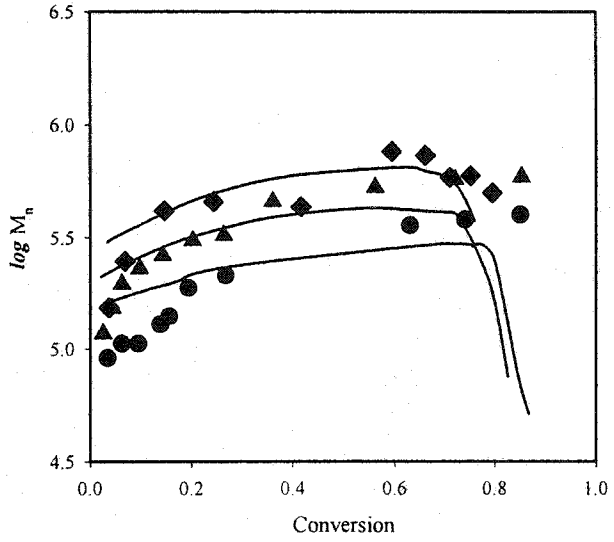

Figure 2.7 Development of $\overline{M}_n$ with conversion in bulk polymerization, [I]=0.030mol/L, ◆ 50, ▲ 60, and ● 70 °C, — model.

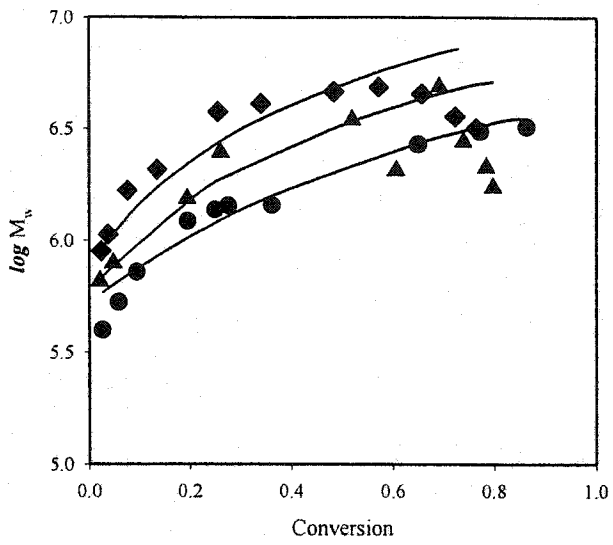

Figure 2.8 Development of $\overline{M}_w$ with conversion in bulk polymerization, [I]=0.006mol/L, ◆ 50, ▲ 60, and ● 70 °C, — model.

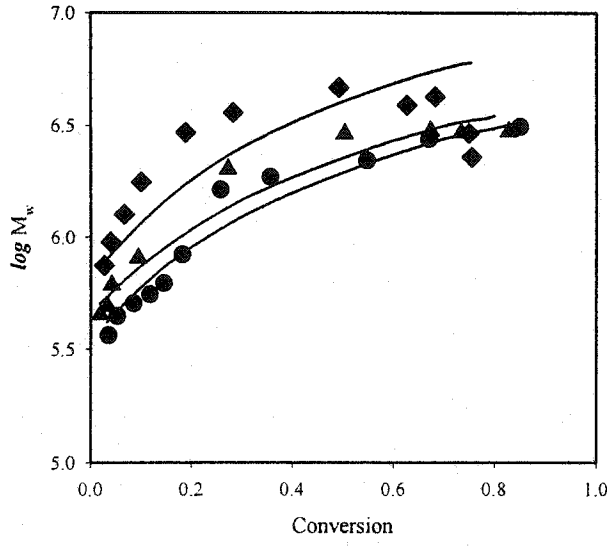

Figure 2.9 Development of $\overline{M}_w$ with conversion in bulk polymerization, [I]=0.012mol/L, ◆ 50, ▲ 60, and ● 70 °C, — model.

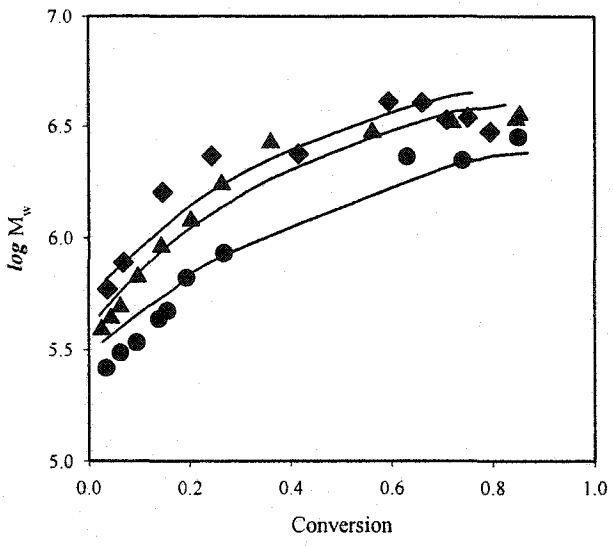

Figure 2.10 Development of $\overline{M}_w$ with conversion in bulk polymerization, [I]=0.030mol/L, ◆ 50, ▲ 60, and ● 70 °C, — model.

2.5 Aqueous solution polymerization

Figure 2.11 shows the solution polymerization kinetics at 50, 60 and 70 °C with a monomer concentration of 40wt% (5.63 mol/L) and an initiator (AIBA) concentration of 1.47×10^{-3} mol/L. Figure 2.12 shows the kinetics at 2.94×10^{-3} mol/L AIBA. These polymerization systems proceed to near completion. Figure 2.13 shows the data at 60 °C with different monomer concentrations, 100wt% (bulk), 40wt% (5.63 mol/L), 20wt% (2.82 mol/L), and 10wt% (1.41 mol/L). The initiator concentration was 2.94×10^{-3} mol/L based on the total (monomer plus solvent) initial reaction volume. The dilution of monomer displayed a trend of increasing final conversion and decreasing of auto-acceleration.

Similar to the bulk system, the high monomer concentration solution polymerization exhibited an increasing trend in $\overline{M}_n$ and $\overline{M}_w$ with conversion from the very beginning of the polymerization (see Figures 2.14-19). At a monomer concentration of 20wt% (2.82 mol/L) and a temperature of 60 °C, $\overline{M}_n$ and $\overline{M}_w$ levelled off after 10% conversion. At a monomer concentration of 10wt% (1.41 mol/L), $\overline{M}_n$ and $\overline{M}_w$ developed a maximum and dropped thereafter (Figures 2.16 and 2.19). These can be attributed to higher radical mobility in lower viscosity solutions. At a monomer concentration of 40wt%, the solution polymerization at 50 °C experienced gelation at about 70% conversion for initiator concentrations of 1.47 and 2.94 mmol/L (Figures 2.14 and 2.17). No gelation was observed when the polymerizations were carried out at 60 and 70 °C. There was also no gelation when monomer concentration was equal to or less than 20wt%.

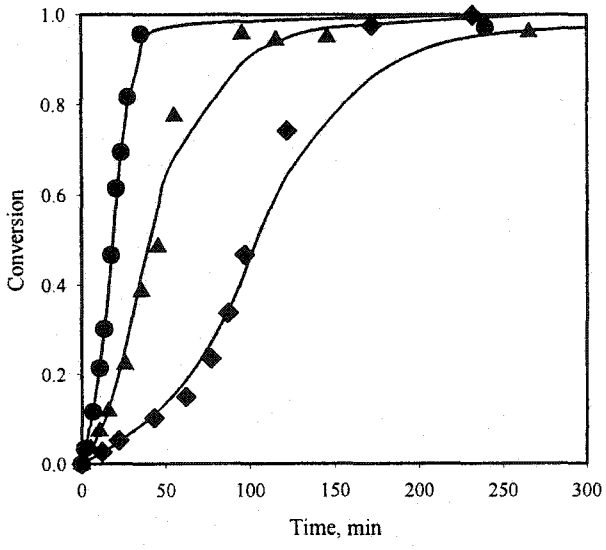

Figure 2.11 Conversion vs. time of NVF aqueous solution polymerization, [I]=1.47×10^{-3} mol/L, [M]=5.63 mol/L, ◆ 50, ▲ 60, and ● 70 °C, — model.

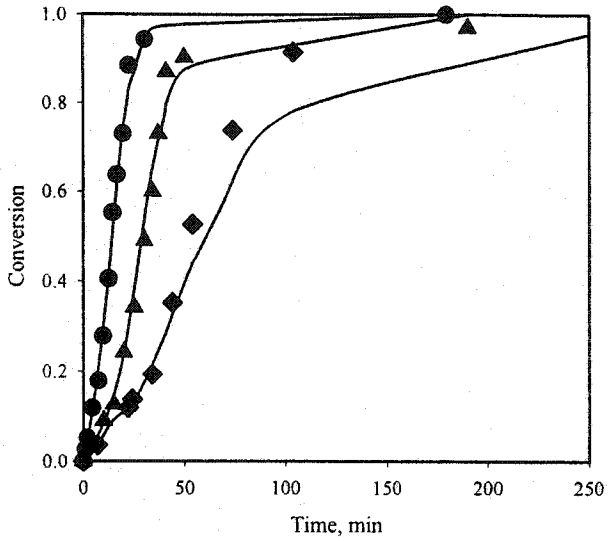

Figure 2.12 Conversion vs. time of NVF aqueous solution polymerization, [I]=2.94×10^{-3} mol/L, [M]=5.63 mol/L, ◆ 50, ▲ 60, and ● 70 °C, — model.

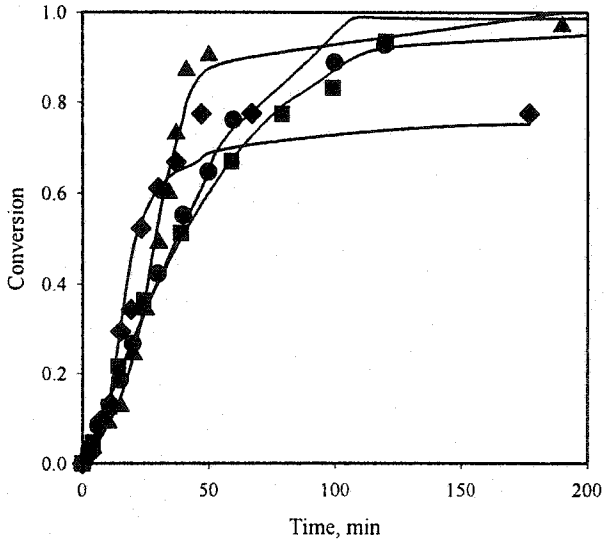

Figure 2.13 Conversion vs. time of NVF aqueous solution polymerization at 60 °C, [I]=2.94×10^{-3} mol/L, ◆ bulk, ▲ 5.63 mol/L, ● 2.82 mol/L, and ■ 1.41 mol/L, — model.

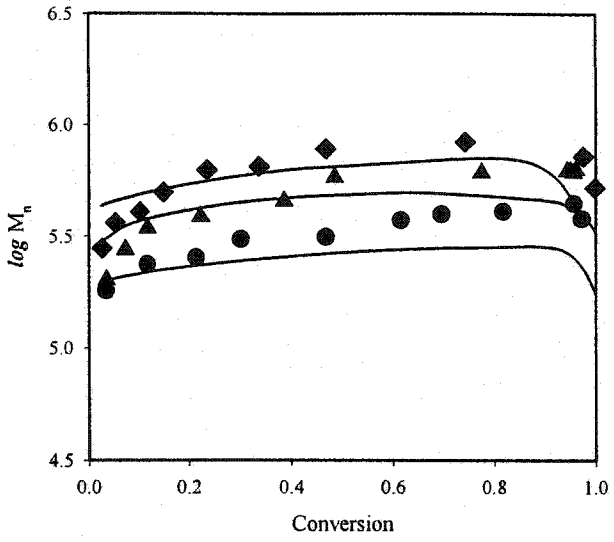

Figure 2.14 Development of $\overline{M}_n$ with conversion in aqueous solution polymerization, [I]= 1.47×10^{-3} mol/L, [M]=5.63 mol/L, ◆ 50, ▲ 60, and ● 70 °C, — model.

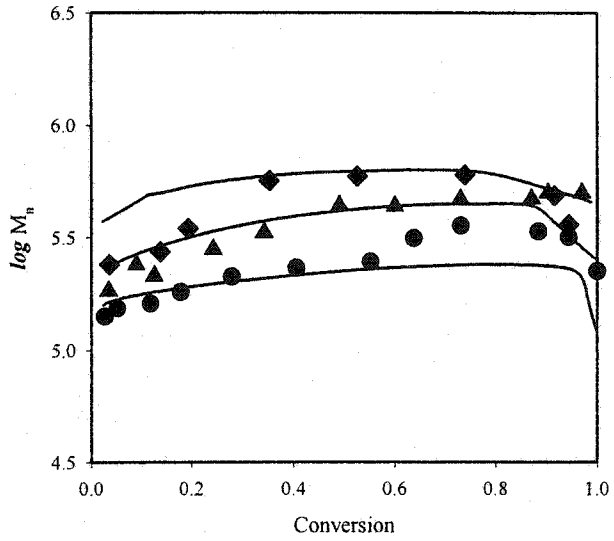

Figure 2.15 Development of $\overline{M}_n$ with conversion in aqueous solution polymerization, [I]= 2.94×10^{-3} mol/L, [M]=5.63 mol/L, ◆ 50, ▲ 60, and ● 70 °C, — model

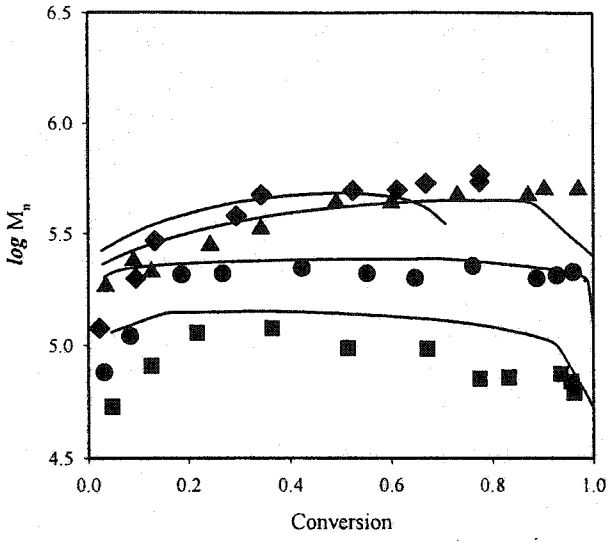

Figure 2.16 Development of $\overline{M}_n$ with conversion in aqueous solution polymerization, 60 °C, [I]=2.94×10^{-3} mol/L, ◆ bulk, ▲ 5.63 mol/L, ● 2.82 mol/L and ■ 1.41 mol/L, — model.

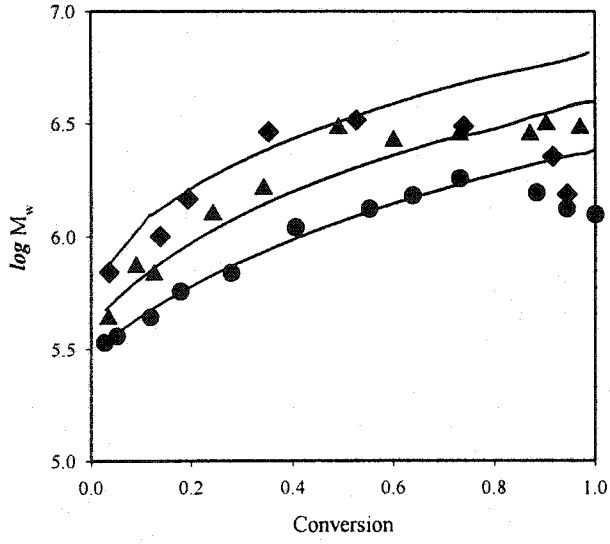

Figure 2.17 Development of $\overline{M}_w$ with conversion in aqueous solution polymerization, [I]= 1.47×10^{-3} mol/L, [M]=5.63 mol/L, ◆ 50, ▲ 60, and ● 70 °C, — model.

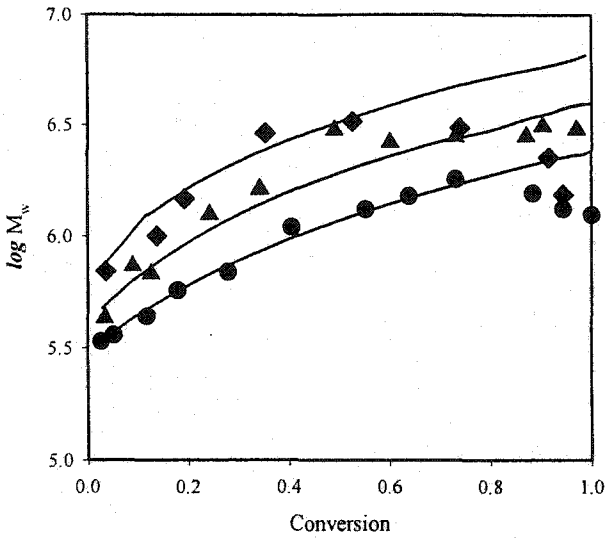

Figure 2.18 Development of $\overline{M}_w$ with conversion in aqueous solution polymerization, [I]= 2.94×10^{-3} mol/L, [M]=5.63 mol/L, ◆ 50, ▲ 60, and ● 70 °C, — model.

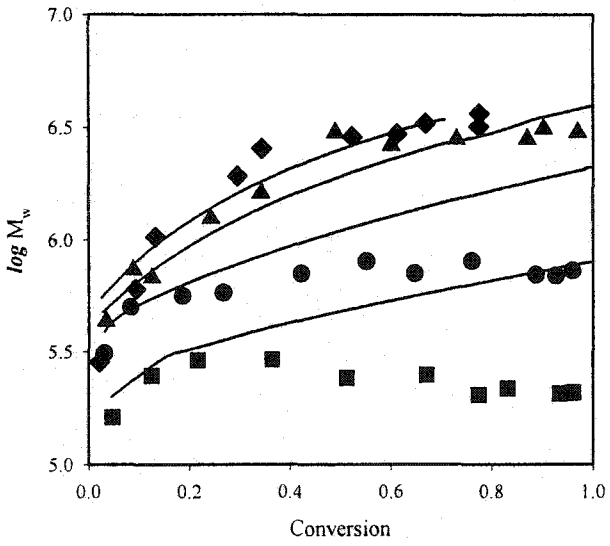

Figure 2.19 Development of $\overline{M}_w$ with conversion in aqueous solution polymerization, 60 °C, [I]=2.94×10^{-3} mol/L, ◆ bulk, ▲ 5.63 mol/L, ● 2.82 mol/L and ■ 1.41 mol/L, — model.

2.6 Model development

2.6.1 Isothermal polymerization kinetics

In free radical polymerization, the formation of NVF polymer chains consists of three kinetic stages: initiation, propagation and termination. The main side reactions are chain transfers to monomer and polymer. Table 2.2 summarizes these elementary reactions and their rate expressions. The chain transfers to monomer and to polymer are two major side reactions.

Generally, polymer chains are long and most monomers are consumed by propagation reactions so that the number of monomers consumed by initiation and chain transfers becomes negligible (long chain hypothesis). The balance equations for both living and dead polymer chains are summarized in Table 2.3 for an isothermal batch polymerization process.

During the polymerization, volume contraction is significant and must be considered. The volume contraction factor is defined as

$$\varepsilon = (d_p - d_m)/d_p \qquad 2.3$$

where d_p and d_m are the densities of polymer and monomer. The volume of reaction mixture at any conversion, x, is therefore

$$V = V_0(1-\varepsilon x)+V_s=V_0(1-\varepsilon x+B) \qquad 2.4$$

where V_0 is the initial monomer volume. V_s is the solvent volume and $B=V_s/V_0$. The method of moments is used to simplify the infinite number of balance equations. The *i*th moments of living and dead polymer chains are defined by

$$\lambda_i = \sum_{n=1}^{\infty} n^i[R_n^\bullet] \qquad 2.5$$

$$\mu_i = \sum_{n=1}^{\infty} n^i[P_n] \qquad 2.6$$

Table 2.2 Kinetics of NVF bulk free radical polymerization

Initiation	$I \rightarrow 2R^{\bullet}$	$R_i = 2fk_d[I]$
Propagation	$R_n^{\bullet} + M \rightarrow R_{n+1}^{\bullet}$	$R_p = k_p[R_n^{\bullet}][M]$
Termination	$R_n^{\bullet} + R_m^{\bullet} \rightarrow P_{n+m}$ (recombination)	$R_{tc} = k_{tc}[R_n^{\bullet}][R_m^{\bullet}]$
	Or $P_n + P_m$ (disproportionation)	$R_{td} = k_{td}[R_n^{\bullet}][R_m^{\bullet}]$
Chain Transfer	$R_n^{\bullet} + M \rightarrow R_1^{\bullet} + P_n$ (to monomer)	$R_{fm} = k_{fm}[M][R_n^{\bullet}]$
	$R_n^{\bullet} + P_m \rightarrow R_m^{\bullet} + P_n$ (to polymer)	$R_{fp} = k_{fp}[P][R_n^{\bullet}]$

Table 2.3 Population balance equations

$$\frac{1}{V}\frac{d([M]V)}{dt} = -k_p[M]\sum_{1}^{\infty}[R_i^{\bullet}]$$

$$\frac{1}{V}\frac{d([I]V)}{dt} = -k_d[I]$$

$$\frac{1}{V}\frac{d([R_1^{\bullet}]V)}{dt} = 2fk_d[I] - k_t[R_1^{\bullet}]\sum_{1}^{\infty}[R_i^{\bullet}] + k_{fm}[M]\lambda_0$$

$$\frac{1}{V}\frac{d([R_n^{\bullet}]V)}{dt} = k_p[M]([R_{n-1}^{\bullet}] - [R_n^{\bullet}]) - k_t[R_n^{\bullet}]\sum_{1}^{\infty}[R_i^{\bullet}] - k_{fm}[M][R_n^{\bullet}] - k_{fp}([R_n^{\bullet}]\sum_{1}^{\infty}i[P_i] - n[P_n]\sum_{1}^{\infty}[R_i^{\bullet}]),$$

$$n > 2$$

$$\frac{1}{V}\frac{d([P_n]V)}{dt} = k_{td}[R_n^{\bullet}]\sum_{1}^{\infty}[R_i^{\bullet}] + k_{fm}[M][R_n^{\bullet}] + k_{fp}([R_n^{\bullet}]\sum_{1}^{\infty}i[P_i] - n[P_n]\sum_{1}^{\infty}[R_i^{\bullet}]), \quad n > 1$$

However, a higher order dead polymer moment μ_3 is involved in calculating λ_2 because of the chain transfer to polymer mechanism. This is solved by applying the quasi-steady state assumption to the radical population, i.e. $\frac{d\lambda_i}{dt} = 0$. The model is further simplified by calculating the sum of the living and dead polymer chain moments, (μ_i + λ_i), instead of each individual entities. The final set of rate equations of the model to be solved is listed in Table 2.4.

The cumulative number-average ($\overline{M}_n$) and weight-average ($\overline{M}_w$) molecular weights are thus calculated by

$$\overline{M}_n = (\lambda_1 + \mu_1)/(\lambda_0 + \mu_0) \qquad 2.7$$

$$\overline{M}_w = (\lambda_2 + \mu_2)/(\lambda_1 + \mu_1) \qquad 2.8$$

2.6.2 Diffusion controlled propagation and termination

Both propagation and termination rates are subject to diffusion control due to the limited mobility of long chain radicals caused by viscosity increase and/or chain entanglement (i.e. the "gel effect"). The onset of the diffusion-controlled termination occurs much earlier than that of propagation because the termination involves diffusion of two long chains.

Various approaches to model the gel effect of free radical polymerizations have been taken. Cardenas and O'Driscoll, (1976, 1977), and Tulig and Tirrell (1981) based their models on the polymer chain entanglements. Chiu et al (1983), Fujita et al (1960), and Marten and Hamielec (1979; 1982) constructed their models using the free volume theory. The latter approach is also used in this study. Modeling diffusion-controlled polymerization process using the free volume theory is a semi-empirical approach by its nature. This method has been applied and tested over the whole range of conversion for various polymerization systems. The Chiu-Carratt-Soong (CCS) model (Chiu et al, 1983) and Marten-Hamielec (MH) model (Marten and Hamielec, 1979; 1982) are two representative models. The MH model suggested that the "gel effect" would not take place until a 'critical' point was reached. This feature leads to a discontinuous feature in the

model and 'artificial onset' free volume fraction values for the diffusion-controlled termination and propagation. In comparison, the CCS model proposed that the effective kinetic constants (both propagation and termination) were the sum of the inverse of diffusion-controlled constant and that of a chemical constant. In this case, both propagation and termination are considered to be diffusion controlled at the beginning of the polymerization.

$$\frac{1}{k_{eff,i}} = \frac{1}{k_{chem,i}} + \frac{1}{k_{diff,i}} \qquad i = \text{propagation or termination} \qquad 2.9$$

Applying Equation 2.9 to propagation and termination yields.

$$\frac{1}{k_p} = \frac{1}{k_{p,c}} + \frac{1}{k_{p,d}} \qquad 2.10$$

$$\frac{1}{k_t} = \frac{1}{k_{t,c}} + \frac{1}{k_{t,d}} \qquad 2.12$$

where the diffusion-controlled constants are defined as

$$k_{p,d} = k_{p,d}^0 \exp(-\frac{a_p}{V_f}) \qquad 2.13$$

$$k_{t,d} = k_{t,d}^0 \exp(-\frac{a_t}{V_f}) \qquad 2.14$$

V_f is the free volume fraction of the reaction mixture. $k_{p,d}^0$ and $k_{t,d}^0$ are two pseudo-kinetic constants related to the diffusion nature in the polymerization system (Soh and Sundberg, 1982). The parameter a_t in Equation 2.13 is further defined as a linear function of the conversion, i.e. $a_t=a_t^0+a_t^1x$. The model equations of the diffusion controlled kinetic constants are summarized in Table 2.5.

2.7 Simulation results

Before the model can be used to simulate the polymerization process, several properties of the initiator, monomer and polymer must be obtained or estimated.

Table 2.4 Model equations

$$\frac{dV}{dt} = -\frac{V_0}{1+B}\varepsilon\frac{dx}{dt}$$

$$\frac{d[I]}{dt} = -k_d[I] - \frac{[I]}{V}\frac{dV}{dt}$$

$$\frac{dx}{dt} = k_p(1-x)\lambda_0$$

$$\frac{d\lambda_0}{dt} = 2fk_d[I] - k_t\lambda_0^2 - \frac{\lambda_0}{V}\frac{dV}{dt}$$

$$\frac{d\lambda_1}{dt} = 2fk_d[I] - k_t\lambda_0\lambda_1 + k_{fm}[M](\lambda_0 - \lambda_1) + k_p[M]\lambda_0 - k_{fp}(\lambda_1\mu_1 - \lambda_0\mu_2) - \frac{\lambda_1}{V}\frac{dV}{dt}$$

$$\frac{d\lambda_2}{dt} = 2fk_d[I] - k_t\lambda_0\lambda_2 + k_{fm}[M](\lambda_0 - \lambda_2) + k_p[M](2\lambda_1 + \lambda_0) - k_{fp}(\lambda_2\mu_1 - \lambda_0\mu_3) - \frac{\lambda_2}{V}\frac{dV}{dt}$$

$$\frac{d(\lambda_0 + \mu_0)}{dt} = \frac{d\mu_0}{dt} = 2fk_d[I] + k_{fm}[M]\lambda_0 - \frac{\mu_0}{V}\frac{dV}{dt}$$

$$\frac{d(\lambda_1 + \mu_1)}{dt} = \frac{d\mu_1}{dt} = 2fk_d[I] + k_{fm}[M]\lambda_0 + k_p[M]\lambda_0 - \frac{\mu_1}{V}\frac{dV}{dt}$$

$$\frac{d(\lambda_2 + \mu_2)}{dt} = \frac{d\mu_2}{dt} = 2fk_d[I] + k_{fm}[M]\lambda_0 + k_p[M](2\lambda_1 + \lambda_0) - \frac{\mu_2}{V}\frac{dV}{dt}$$

Table 2.5 Modeling diffusion-controlled kinetic constants

$$\frac{1}{k_p} = \frac{1}{k_{p,c}} + \frac{1}{k_{p,d}} \qquad \frac{1}{k_t} = \frac{1}{k_{t,c}} + \frac{1}{k_{t,d}}$$

$$k_{p,d} = k_{p,d}^0 \exp(-\frac{a_p}{V_f}) \qquad k_{t,d} = k_{t,d}^0 \exp(-\frac{a_t}{V_f})$$

$$\begin{aligned} V_f &= \phi_m V_{fm} + \phi_p V_{fp} + \phi_s V_{fs} \\ &= \phi_m [0.025 + \alpha_m (T - T_{gm})] + \phi_p [0.025 + \alpha_p (T - T_{gp})] + \phi_s [0.025 + \alpha_s (T - T_{gs})] \end{aligned}$$

$$a_t = a_t^0 + a_t^0 x$$

$$a_p = 0.4, \qquad a_t^0 = 1$$

(1) Initial combined rate constant ($k_{p,c}/k_{t,c}^{0.5}$) and chain transfer to monomer, C_m ($=k_{fm}/k_p$)

According to Equation 2.14, the combined rate constant $k_{p,c}/k_{t,c}^{0.5}$ and chain transfer constant C_m is estimated from the initial polymerization rate and the $\overline{M}_n$ data.

$$\frac{1}{\overline{M}_n} = \frac{k_{t,c}R_p}{(k_{p,c}[M])^2} + C_m \qquad 2.14$$

To obtain the polymerization rate, the data summarized in Table 2.6 are used. The $\Delta x/\Delta t$ values are taken as approximate to dx/dt. Therefore,

$$R_p = [M]\frac{dx}{dt} \approx [M]\frac{\Delta x}{\Delta t} \qquad 2.15$$

The right hand side of Equation 2.14 is plotted against $R_p/[M]^2$ data. The slopes of the least square linear fitting give the inverse of $k_{p,c}/k_{t,c}^{0.5}$ and the intercept, C_m. The data are summarized in Table 2.7. Within the scope of this investigation, $k_{p,c}$ and $k_{t,c}$ can not be estimated separately. To start the calculation of model from zero conversion, the $k_{t,c}$ of acrylamide polymerization was used because of its similarity in structure and water solubility with NVF monomer. When the diffusion effect takes control, $k_{t,c}$ will have little contribution in the overall k_t, the error introduced here is therefore considered small.

(2) Glass transition temperature of the monomer (T_{gm}) and polymer (T_{gp})

The glass transition temperature of NVF monomer is estimated using Fedors' (1979) correlation, T_{gm}= -112 °C. T_{gp} is obtained using DSC, T_{gp} = 122 °C.

(3) Thermal expansion factors of the monomer (α_m) and polymer (α_p)

The thermal expansion factors, α_m and α_p are used in the present model to calculate the free volume fraction during polymerization. The value of α_m (50 °C < T < 110 °C) is calculated from the reported NVF density data (Singley, 1997).

$$\alpha_m = 9.53\times10^{-4} \qquad 2.16$$

A regression method is used to find the α_p. The free volume fraction of the PNVF-NVF mixture at the final conversion is taken to be 0.025 (Bueche, 1962).

Table 2.6 Low conversion $\overline{M}_n$ and $\overline{M}_w$ data and the final conversions (bulk polymerization)

T, °C	[I], mol/L	Time, min	Conversion	$\overline{M}_n$ $\times 10^{-3}$	$\overline{M}_w$ $\times 10^{-3}$	PDI	Final conversion of the run
50	0.006	30	0.024	327	897	2.7	0.77
		49	0.037	367	1063	2.9	
	0.012	20	0.027	291	746	2.6	0.76
		35	0.039	310	951	3.1	
	0.030	15	0.037	154	527	3.4	0.79
60	0.006	8	0.020	287	668	2.4	0.80
		19	0.047	296	799	2.7	
	0.012	5	0.019	194	449	2.3	0.83
		8	0.034	245	629	2.5	
	0.030	3	0.026	117	378	3.2	0.85
70	0.006	3	0.026	182	397	2.2	0.86
		5.5	0.058	215	540	2.5	
	0.012	2.5	0.035	133	358	2.7	0.85
		3.5	0.052	159	441	2.8	
	0.030	1.17	0.034	91.2	265	3.2	0.85

Table 2.7 Combined rate constants, $k_{p,c}/k_{t,c}^{0.5}$ and chain transfer constant, C_m ($=k_{fm}/k_p$)

T, °C	$k_{p,c}/k_{t,c}^{0.5}$, L/(mol*S)$^{0.5}$	$C_m \times 10^4$
50	0.090	7.33
60	0.143	9.37
70	0.245	18.0

Table 2.8 Rate constants and physical properties

Property	Value	Reference
f	0.6	Bamford (1988)
k_d	$2.88\times10^{15}\exp(-15686/T)$ (S^{-1}) AIBN	Xie (1990)
	$9.42\times10^{14}\exp(-14860/T)$ (S^{-1}), AIBA	Brandrup and Immergut (1975)
$k_{t,c}^{0.5}$	$9.19\times10^{4}\exp(-741/T)$ (L/mol/min), acrylamide	Hunkler (1990)
d_m	1.01~0.98 (g/cm^3)	Singley (1997)
d_p	1.25 (g/cm^3)	Estimated, this research
T_{gm}	-114 (°C)	Calculated from Fedors (1979)
T_{gp}	122 (°C)	Measured, this research
T_{gs}	-136 (°C)	Fedors (1979)
Molecular weight	71, monomer 164, AIBN 271, AIBA	
α_m	9.53×10^{-4} (°C^{-1})	Calculated from Singley (1997)
α_P	7.32×10^{-4} (°C^{-1})	Calculated, this research
α_s	5.54×10^{-4} (°C^{-1})	Calculated from Perry et al (1975)

$$V_f = \phi_m[0.025 + \alpha_m(T - T_{gm})] + \phi_p[0.025 + \alpha_p(T - T_{gp})] \qquad 2.17$$

Given the temperature, the corresponding final conversion (bulk polymerization, Table 2.6) and α_m, α_P is obtained by a least square fit

$$\alpha_p = 7.32\times10^{-4} \qquad 2.18$$

For comparison purposes, the suggested "universal" values (Bueche, 1962; Stickler et al, 1984) are 10.0×10^{-4} and 4.8×10^{-4} for α_m and α_p, respectively.

The model calculation and parameter regression are implemented with the Matlab 5.0 software package. The ordinary differential equation solver is a second order Runge-Kutta method (ODE23S) and the optimizer (FMINS) used a Nelder-Mead type simplex search method. The minimization objective function for fitting the model is defined as

$$\text{obj} = \sum_i \frac{(x_{exp,i} - x_{mod,i})^2}{(x_{exp,i})^2} + \sum_i \frac{(M_{w\,exp,i} - M_{w\,mod,i})^2}{(M_{w\,exp,i})^2} \qquad 2.19$$

The experimental number-average molecular weight data, $\overline{M}_n$, are not used in fitting. Instead, the model uses the estimated kinetic parameters obtained from the regression to calculate theoretical $\overline{M}_n$ values for comparison purpose.

In the event of gelation, only the conversion data of the samples are included in the objective function. The molecular weights of the sol samples are not included. In the calculation, data for $k_{t,d}$ of acrylamide (Hunkeler, 1990) is used. The parameters to be estimated are therofore $k^0_{p,d}$, $k^0_{t,d}$, C_{fp} ($=k_{fp}/k_p$) and a_t^1. The parameter a_p is set to 0.4 and a_t^0 to 1.0 for all the polymerization temperatures and initiator concentrations (Fujita et al, 1960; Fujita and Kishimoto, 1961).

The rate constants and physical properties used in the model calculation are summarized in Table 2.8. The regressed parameters are listed in Tables 2.9 and 2.10 for bulk and solution polymerization, respectively. The regressed conversion, $\overline{M}_w$ and calculated $\overline{M}_n$ results from the model are plotted as solid lines along with the experimental data points in Figures 2.2 to 2.19.

In the bulk polymerization, the model gives a better fit of the time-conversion data than the conversion-$\overline{M}_w$ data. It over-predicts $\overline{M}_n$ at the start of the polymerization and shows a slower increase than the experimental $\overline{M}_n$. The regressed $k^0_{p,d}$ values increases with initiator concentration at each temperature level. The $k^0_{t,d}$ values also increases with initiator concentration with the exception at 60 °C, 0.012 mol/L [I] (see Table 2.9). The values of a_t^1 presented in Table 2.9 do not show a clear pattern over the range of experimental conditions. The C_{fp} values at different initiator levels are similar, but increase with polymerization temperature.

In the solution polymerization, the average values of C_{fp} obtained in the regression of the bulk polymerization at 50, 60 and 70°C are used as known constants. The parameters to be fit are thus reduced to $k^0_{p,d}$, $k^0_{t,d}$ and a_t^1 and the results are summarized in Table 2.10.

The model, which does not consider gelation, over-estimates $\overline{M}_w$ at the final stage of polymerization at 50 °C where there is gelation at >70% conversion. The model gives good agreement for conversion, $\overline{M}_w$ and $\overline{M}_n$ data at monomer concentrations greater than 40%. However, the model fails to fit the molecular weight data when the monomer concentrations are 10 and 20 wt% (Figure 2.19), in which the experimental $\overline{M}_w$ levels off or decreases at an early stage (~20% conversion). In order to fit the time-conversion data, the constraint over the $\overline{M}_w$ data is released in the objective function (Equation 2.19). The $\overline{M}_w$ and $\overline{M}_n$ data calculated by the model are plotted in Figures 2.16 and 2.19 instead. The model gives continuously increasing $\overline{M}_w$ results with conversion. The calculated $\overline{M}_n$ results are higher than the experimental values although the increasing trend is as predicted. This suggests that other factors need to be considered in a dilute aqueous solution polymerization.

The trend of a_t^1 change is more obvious in solution than in bulk as shown in Table 2.10. At a monomer concentration of 40wt%, the value of a_t^1 decreases as the polymerization temperature increases from 50 to 70 °C. The value of a_t^1 also decreases with increasing monomer dilution from bulk to 10wt% at 60 °C. A long chain radical has a higher diffusion rate in solution

than in bulk polymerization. In addition, the free volume fraction loss due to monomer conversion is partially offset by the free volume contribution from solvent. This allows a slower decay in the diffusion controlled termination constant, $k_{t,d}$, which is represented by the change in a_t^1.

Finally, it should be pointed out that current model took on a rather empirical approach due to the lack of basic polymerization properties, such as k_t, k_p and diffusion coefficients. There is a possibility that the estimated coefficients are correlated to some degree. This can be improved with the availability of more physical properties.

Table 2.9 Simulation results of bulk polymerization

T, °C	[I], mol/L	$k^0_{p,d}\times10^{-3}$, L/mol*S	$k^0_{t,d}\times10^{-7}$, L/mol*S	$C_{fp}\times10^3$	a_t^1
50	0.006	0.106	0.255	1.11	3.40
	0.012	0.365	4.05	1.29	3.12
	0.030	0.866	14.4	0.99	3.16
60	0.006	0.389	2.23	1.36	3.39
	0.012	0.966	10.5	1.20	3.51
	0.030	0.987	7.63	1.58	3.53
70	0.006	0.847	2.78	2.51	2.90
	0.012	1.081	4.72	2.60	3.79
	0.030	10.39	134	2.25	2.38

Table 2.10 Simulation results of aqueous solution polymerization

T, °C	[M],wt%	$C_{fp}\times10^{3}$	[I], mol/L	$k^{0}_{p,d}\times10^{-3}$, L/mol*S	$k^{0}_{t,d}\times10^{-7}<$ L/mol*S	a_t^{I}
50	40	1.13	0.00147	1.27	11.7	2.07
			0.0294	0.225	0.357	2.74
60	40	1.38	0.00147	1.98	15.7	2.13
			0.00294	3.80	44.2	1.78
70	40	2.45	0.00147	6.24	47.7	1.40
			0.00294	1.87	6.01	1.42
60	100	1.38	0.00294	1.73	9.65	1.83
	40			3.80	44.2	1.78
	20			0.369	0.141	0.49
	10			0.270	0.051	0.03

2.8 The nature of the crosslinking during the polymerization

As the experimental investigations revealed in the previous sections, gelation occurs during the bulk or solution free radical polymerizations of NVF. Under most circumstances, gel is not a desirable product. Gelation is often unwanted in a commercial production process especially if it is not controlled. The presence of gel also limits the scope of end uses as a flocculant.

The mechanism of gel formation during the free radical polymerization of NVF may be due to the combination of chain transfer reaction to polymer and radical termination by recombination. Figure 2.20 gives the structure of PNVF polymer chain and the two most probable sites for chain transfer: (a) hydrogen on the carbonyl group and (b) α-hydrogen on backbone. The objective of this section is to elucidate the nature of the crosslinking unit that is responsible for the gel formation. There is an effective method to identify the actual crosslinking point. If the gel is formed through the amide group (via route (a) in Figure 2.20), the crosslinkage should be severed by hydrolyzing the amide group. A series of acidic and basic hydrolysis reactions of the PNVF gels were conducted to verify this assumption.

Tables 2.11 and 2.12 summarize the final conversion and gel fraction under various polymerization conditions. In bulk polymerization, the gel fraction decreased with increasing initiator concentration, and with increasing temperature. At 70 °C, no gel was found. This is because high initiator concentration and high polymerization temperature produces short polymer chains and, as a result, reduces the gel fraction. In solution polymerization, no gel was formed when the monomer concentration was equal to or less than 20wt%. Gel fraction reached a maximum of 92wt% of dried polymer for the aqueous solution polymerization at a monomer concentration of 60wt% and decreased to 48wt% of dried polymer for the bulk polymerization.

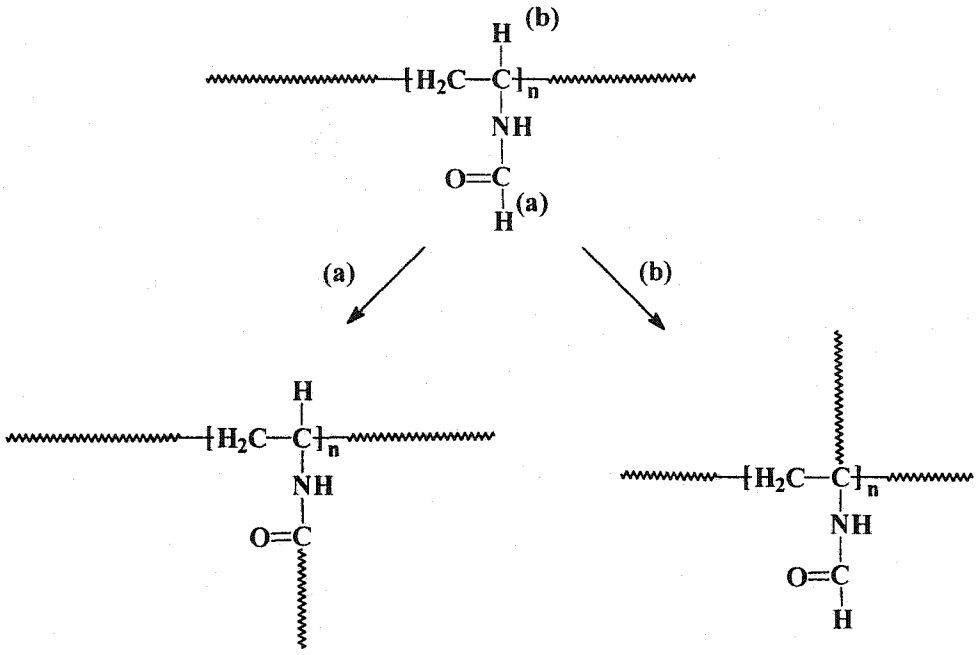

Figure 2.20 Two possible crosslinking mechanisms of PNVF gels.

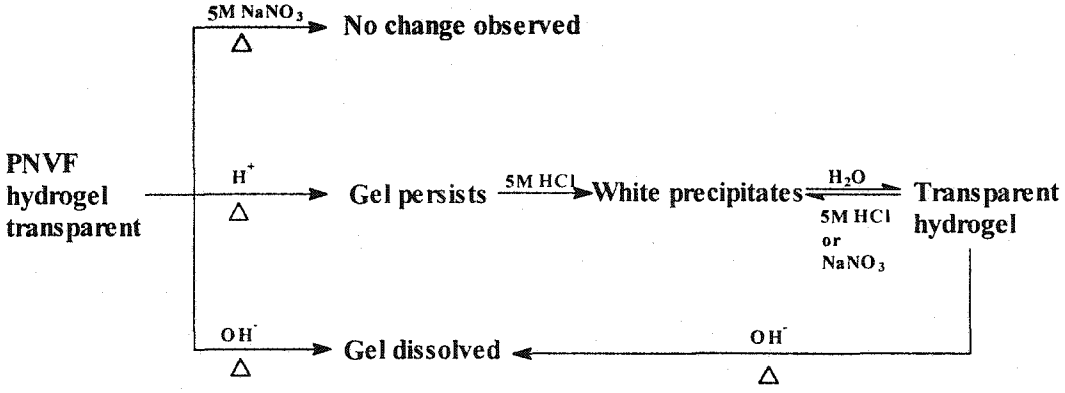

Figure 2.21 Experiments designed to determine the nature of crosslinking in PNVF gels.

Table 2.11 Gel fraction in NVF bulk polymerization

No.	T, °C	[AIBN], $\times 10^{-3}$ mol/L	Conversion	Gel fraction, wt%
1	50	3	0.79	99
2	50	6	0.82	71
3	50	12	0.76	64
4	50	30	0.81	78
5	60	3	0.85	86
6	70	3	0.87	0

Table 2.12 Gel Fraction in NVF solution polymerization, 50 °C, 0.74×10^{-3} mol/L [AIBA]

No.	[M], wt%	Conversion	Gel fraction, wt%
7	10	0.91	0
8	20	0.95	0
9	40	0.98	18
10	60	0.97	92
11	80	0.87	83
12	100	0.73	47

When swollen, all the hydrogels were hard gels with definitive shape and boundaries except for the gels from Samples 9 and 12 (Table 2.12), which were soft gels. The difference in the appearance of the gels from different samples is due to the different crosslinking densities. A high crosslinking density yields a hard gel.

Basic Hydrolysis: All gel samples subject to the basic hydrolysis became soluble linear polymers. The basic hydrolysis of PNVF produced uncharged free amine polymer and proceeded to 100% with excess amount of NaOH. The amide groups on the main chain as well as the crosslinking points were completely hydrolyzed

Acidic Hydrolysis: The acidic hydrolysis of PNVF produced positively charged NH_3^+ groups on the polymer chains. Acidic hydrolysis did not proceed to 100% completion presumably due to electrostatic effects (Badesso et al, 1995; Pinschmidt et al, 1997)

In the acidic hydrolysis, those gel samples having low crosslinking densities (soft gel, Samples 9 and 12 in Table 2.12) became soluble after the experiments. However, the gel samples having high crosslink densities (Samples 1~5 in Table 2.11, and, 10 and 11 in Table 2.12) survived the acidic hydrolysis because some of the crosslinked amide units were intact due to the incomplete hydrolysis. When the surviving gel samples were placed in concentrated HCl or $NaNO_3$ solutions, the samples turned into white precipitates. Adding fresh deionized water subsequently diluted the acid (or salt) concentration and the precipitates changed to transparent gels again. This confirmed a partially hydrolyzed gel network with pendent NH_3^+ groups, which were products of acidic hydrolysis of amide groups.

A swelling experiment of the acid-hydrolyzed gels was also performed. The swelling ratios of the gel samples (Samples 10 and 11 in Table 2.12) in pure water increased from 44.6 and 63.4 to 538.2 and 589.2, respectively, after the hydrolysis. This also indicates a reduction in crosslinking density in the gels, reflecting the partial acidic hydrolysis. Here the swelling ratio of the gel is defined in Equation 2.20, being the weight ratio before and after the gel is swollen by pure water.

$$\text{Swelling ratio} = \frac{W_{Gel,swollen}}{W_{Gel}} \qquad 2.20$$

When gels partially hydrolyzed in acid were subject to basic hydrolysis, they dissolved completely after the hydrolysis. The remaining amide crosslinkages were completely severed. No charge repulsion effect was observed in the basic hydrolysis because the basic hydrolysis of amide groups gave uncharged (NH_2). PNVF was completely hydrolyzed to polyvinylamine. Therefore, the basic hydrolysis proceeded to 100% conversion and dissolved the gel.

These experimental results support the crosslinking mechanism via the amide group (route (a)) as shown in Figure 2.20. The experimental designs and results are also summarized in Figure 2.21.

2.9 Conclusions

In this chapter, the free radical polymerization of N-vinylformamide was examined both in bulk and in aqueous solution processes. The molar heat of reaction for NVF polymerization was measured to be 79.4 kJ/mol. The bulk polymerization showed a severe "gel effect" from the start of polymerization. Both number-average molecular weight, $\overline{M}_n$, and weight-average molecular weight, $\overline{M}_w$, increased continuously from a very low conversion and then levelled off at the final stage of polymerization. The $k_{p,c}/k_{t,c}^{0.5}$ and C_m values at 50, 60 and 70 °C were estimated using the initial conversion and $\overline{M}_n$ data of the bulk polymerization. For the solution polymerization, the "gel effect" was still pronounced at monomer concentrations equal to or greater than 40wt% (2.31 mol/L). $\overline{M}_n$ and $\overline{M}_w$ displayed the same increasing trend as that in the bulk polymerization. Further dilution of the monomer with solvent effectively eased the "gel effect". No auto-acceleration in time-conversion curves was observed at 10 and 20wt% monomer concentrations. A semi-empirical model based on the free volume theory was constructed to describe both bulk and solution polymerizations. The model adequately fit the time-conversion data and conversion- $\overline{M}_w$ data.

Under certain polymerization conditions, in bulk and solution polymerizations, PNVF gels were found during polymerization. Hydrolysis experiments conducted on the gel samples confirmed that the amide group provided crosslinking points to form PNVF gel (as shown in route (a) of Figure 2.20)

2.10 References

Auhorn, W. Linhart, F. Lorencak, P. Kroener, M. Sendhoff, N. Denzinger, W. and Hartmann, H. (1992). US. Patent No. 5145559, BASF.

Badesso, R. J. Nordquist, A. F. Pinschmidt, R. K. Jr. and Sagl, D. J. (1995). "Synthesis of Amine Functional Homopolymers with N-Ethenylformamide", in *Hydrophilic Polymers: Performance with Environmental Acceptance*, E. Glass ed., American Chemical Society, Washington DC, p. 489.

Bamford, C. H. (1988). "*Radical Polymerization*", in H. Mark et al, ed., *Encyclopedia of Polymer Science and Engineering*, vol. 13, John Wiley & Sons, New York, 2nd ed., 789.

Brandrup, J. and Immergut, E. H. ed. (1975). "Polymer Handbook", 2nd Ed., John Wiley & Sons, New York.

Bueche, F. (1962). "Physical Properties of Polymers", Interscience, New York.

Burkert, H. Brunnmueller, F. Beyer, K. Kroener, M and Mueller, H. (1984). US Patent No. 4444667, BASF.

Cardenas, J. and O'Driscoll, K. F. (1976). "High-Conversion Polymerization. I. Theory and Application to Methyl Methacrylate". *J Polym Sci, Polym Chem Ed., 14,* 883.

Cardenas, J. and O'Driscoll, K. F. (1977). "High-Conversion Polymerization. II. Influence of Chain Transfer on the Gel Effect". *J Polym Sci, Polym Chem Ed., 15*, 1883.

Chiu, W. Y. Carratt, G. M. and Soong, D. S. (1983). "A Computer Model for the Gel Effect in Free-Radical Polymerization". *Macromolecules, 16*, 348.

Fedors, R. F. (1979). "A Universal Reduced Glass Transition Temperature for Liquids". *J Polym Sci: Polym Let Ed., 17*, 719.

Fikentscher, R. and Kroener, M. (1992). US. Patent No. 5155270 (1992), BASF.

Fujita, H. and Kishimoto, A. (1961). "Interpretation of Viscosity Data for Concentrated Polymer Solutions". *J Chem Phys, 34*, 393.

Fujita, H. Kishimoto, A. and Matsumoto, K. (1960). "Concentration and Temperature Dependence of Diffusion Coefficients for Systems Polymethyl Acrylate and n-Alkyl Acetates". *Trans Faraday Soc, 56*, 424.

Hunkeler, D. J. (1990). "Acrylic Water Soluble Polymers", Thesis (Ph.D.), McMaster University, Hamilton, Ontario, Canada.

Joshi, R. M. (1962). "Heats of Polymeric Reactions. Part I. Construction of the Calorimeter and Measurement on Some New Monomers". *J. of Polym. Sci.*, Vol. 56, 313-338.

Marten, F. L. and Hamielec, A. E. (1979).). "High-Conversion Diffusion-Controlled Polymerization". *ACS Symp Ser., 104*, 43.

Marten, F. L. and Hamielec, A. E. (1982). "High-Conversion Diffusion-Controlled Polymerization of Styrene". *J Applied Polym Sci, 27*, 489.

Monech, D. Hartmann, H. Freudenberg, E. and Stange, A. (1993). US. Patent No. 5262008, BASF.

Perry, R. H. Chilton, C. H. and Perry, J. H. ed. (1975) "Chemical Engineer's Handbook", McGraw-Hill, New York.

Pfohl, S. Kroener, M. Hartmann, H. and Denzinger, W. (1988). US. Patent No. 4774285, BASF.

Pfohl, S. Kroener, M. Hartmann, H. and Denzinger, W. (1989). US. Patent No. 4880497, BASF.

Pfohl, S. Kroener, M. Hartmann, H. and Denzinger, W. (1990). US. Patent No. 4978427, BASF.

Pinschmidt, R. K. Rentz, W. L. Carrol, W. E. Yacoub, K. Drescher, J. Nordquist, A. F. and Chen, N. (1997). "N-Vinylformamide – Building Block for Novel Polymer Structures". *J. Macromol. Sci., Pure Appl. Chem., A34(10)*, 1885.

Schmidt, C. Hungenberg, K. and Hubinger, W. (1996). "Vergleich von Kalroimetern fur die Kinetische Untersuchung von Polyreaktionen". *Chem. Ing. Tech.*, *68*, 953.

Singley, E. J. (1997). "Development of Fluoroether Amphiphiles and Their Applications in Heterogeneous Polymerization in Supercritical Carbon Dioxide", Thesis (Ph.D.), University of Pittsburgh, 1997, p.221.

Singley, E. J. Daniel, A. Person, D. and Beckman, E. J. (1997). "Determination of Mark-Houwink Parameters for Poly (N-vinylformamide)". *J. Polym. Sci, Part A, Polym. Chem.*, *35*, 2533.

Soh, S. K. and Sundberg, D. C. (1982). "Diffusion-Controlled Vinyl Polymerization. III. Free Volume Parameters and Diffusion-Controlled Propagation". *J Polym Sci, Polym Chem Ed.*, *20*, 1331.

Spange, S. Madl, A. Eismann, U. and Utecht, J. (1997). "Cationic Initiation of Oligomerization of Vinylformamide". *Makromol.Rapid Commun.*, *18*, 1075.

Stickler, M. Panke, D. and Hamielec, A. E. (1984). "Polymerization of Methyl Methacrylate Up to High Degree of Conversion: Experimental Investigation of the Diffusion-Controlled Polymerization". *J Polym Sci, Polym Chem Ed.*, *22*, 2243.

Stinson, S. (1993). "Quest for Commercial Polyvinylamine Advances". *Chem. and Eng. News*, *71(36)*, 32.

Tulig, T. J. and Tirrell, M. "Toward a Molecular Theory of the Trommsdorff Effect". (1981). *Macromolecules*, *14*, 1501.

Xie, T. (1990). "Vinyl Chloride Polymerization", Thesis (Ph.D.), McMaster University, Hamilton, Ontario, Canada.

Chapter 3. Acid and Base Catalyzed PNVF Hydrolysis

3.1 Introduction

N-vinylformamide (NVF) is a precursor for simple and economical production for Polyvinylamine (PVAm) (Stinson, 1993). PVAm is a water-soluble polymer with a high density of reactive amino groups in its chain. However, PVAm can not be synthesized directly from a monomer. The common synthesis routes of PVAm involved modifications of other polymers which are readily available, such as polyacrylamide (PAM) (Achari et al, 1993), polyacrylic acid (PAA) (Hughes and Pierre, 1977), polyacrylonitrile (PAN) (Todorov et al, 1996) and poly(N-vinyl *tert*-butylcarbamate) (Hart, 1959; Fischer and Heitz, 1994) (PTBNVC). These modifications, always complicated and costly, usually consist of a series of reactions followed by a final hydrolysis step to PVAm.

In contrast, NVF can be quite easily converted to poly (N-vinylformamide) (PNVF) by various polymerization methods. PNVF is then converted to PVAm by hydrolysis in either acidic or basic aqueous solution. Acid hydrolysis of PNVF produces cationic polymers while base hydrolysis yields polymers with free amine functional groups. Base hydrolysis is usually a more effective approach with almost 100% conversion (Badesso et al, 1993; Badesso et al, 1995). The electrostatic repulsion arising among the cationic amine groups ($-NH_3^+$) prevents the acidic hydrolysis from a 100% conversion. The byproduct from NaOH hydrolysis, sodium formate salt, can be removed by dialysis or precipitation at great expense. Acidic hydrolysis conducted in a mixture of methanol and aqueous solvent produces methylformate, which can be easily stripped as a volatile component. An alternative approach is catalyzed thermal hydrolysis developed recently by Ford and Armor (1996). The synthesis routes of PVAm via the basic or acidic PNVF

hydrolysis are shown in Figure 3.1. PVAm and partially hydrolyzed PNVF have various applications such as water treatment, papermaking, textile finishes, personal care products, adhesives, coatings and oil field chemicals (Auhorn et al, 1992; Burkert and Brunnmuller, 1984; Monech et al, 1993; Pfohl et al, 1988, 1989 and 1990; Pinschmidt and Lai, 1990; Stinson, 1993)

In this chapter, an experimental investigation of the hydrolysis of PNVF in acidic and basic aqueous solutions was conducted. The effects of temperature, polymer concentration and acid or base concentrations on the hydrolysis kinetics and hydrolysis equilibrium were systematically examined.

3.2 Experimental

NVF monomer (Aldrich Inc.) was used to synthesize PNVF for the hydrolysis study. NVF was distilled under vacuum at <70 °C and stored at -15 °C before polymerization.

Two batches of PNVF samples with different molecular weights were synthesized. The low molecular weight PNVF was produced by a precipitation polymerization in toluene. The weight-average molecular weight, $\overline{M}_w$ was 579,000 with a polydispersity index of 5.84 by GPC as described in Chapter 2, section 2.2. The high molecular weight PNVF was synthesized by an inverse emulsion polymerization. The molecular weight was determined by a viscosity measurement and was found to be about 2 million (Singley, 1997). Both samples were dried under a vacuum for 48 hours and recovered as fine powder. Sodium hydroxide, NaOH (ACP Chemicals Inc.) and hydrochloric acid, HCl (Fisher Scientific) were used as received. Millipore treated water was used for the experiments.

The hydrolysis kinetic experiments were conducted in nitrogen sealed glass vials. All the samples were immersed in a circulating water bath set at a desired temperature. One vial was taken out at each pre-set time and cooled down immediately. The hydrolyzed polymer samples from basic hydrolysis were acidified with a concentrated HCl solution for about 5 minutes prior to precipitation by methanol. Acid hydrolyzed polymer samples were precipitated directly from

water with mixture of methanol and concentrated HCl solution. All samples were dried in a vacuum oven at room temperature for 48 hours.

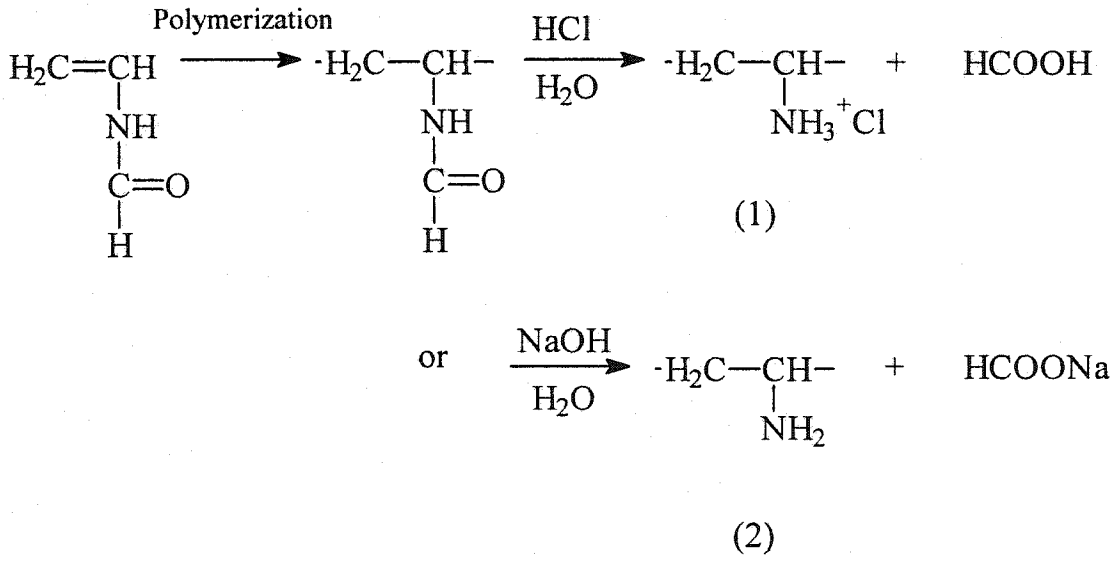

Figure 3.1 Synthesis route of polyvinylamine (PVAm) via (1) acidic and (2) basic hydrolysis of poly (N-vinylformamide) (PNVF).

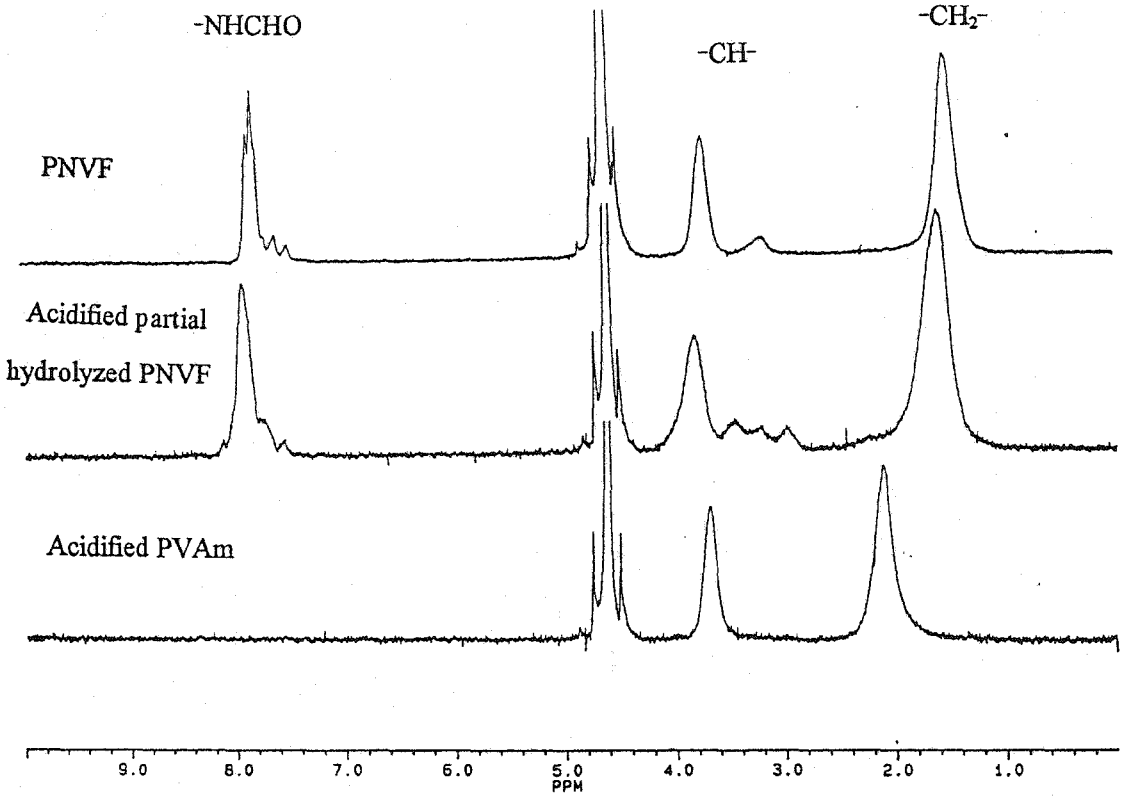

Figure 3.2 H-NMR spectrum of PNVF, acidified partial hydrolyzed PNVF and acidified PVAm, it shows the diminishing of amide group peak along with hydrolysis.

For the equilibrium hydrolysis, three polymer concentrations were tested: 2, 5 and 10 wt% (or 0.28, 0.70 and 1.41 mol/L amide group). The acid or base/amide group molar ratios investigated were 0.1, 0.3, 0.5, 0.8, 1.0, 1.2, 1.5, and 2.0. The equilibrium hydrolysis was carried out over a 48 hour period at pre-set reaction temperatures with the exception that the time for acidic equilibrium hydrolysis at 60 °C and 2 wt% polymer concentration was 7 days. The polymer samples were recovered by precipitation and dried, as per the procedure described previously.

The amide molar conversion of a hydrolyzed sample was determined by H-NMR. Figure 3.2 shows the NMR spectra of pure PNVF and acidified partially hydrolyzed PNVF in D_2O. The chemical shift of amide group is at 7.4 ~ 8.2 ppm. The chemical shift of the backbone $-CH_2-$ group is at 1.2 ~ 2.4 ppm. The area of the amide group peak diminishes with increasing degree of hydrolysis. The molar conversion of hydrolysis was calculated by monitoring the change in the amide group peak area. Equation 3.1 gives the calculation of hydrolysis conversion:

$$\text{Amide conversion} = 1 - \frac{2 \times \text{amide group peak area}}{-CH_2\text{- peak area}} \qquad 3.1$$

3.3 Results and discussion

3.3.1 Hydrolysis kinetics

Acidic hydrolysis kinetics

Figure 3.3 shows the effect of temperature on the acidic hydrolysis kinetics. The amide group concentration was 0.70 mol/L with a 1:1 acid/amide group molar ratio. An higher increase in temperature produced a larger initial rate of hydrolysis.

Acidic hydrolysis was also conducted at 70 °C, with 3 different acid/amide group molar ratio, 0.5, 1.0 and 2.0. The amide group concentration was 0.70 mol/L (5 wt% PNVF in water). Figure 3.4 shows initial hydrolysis rate increases with increasing acid concentration.

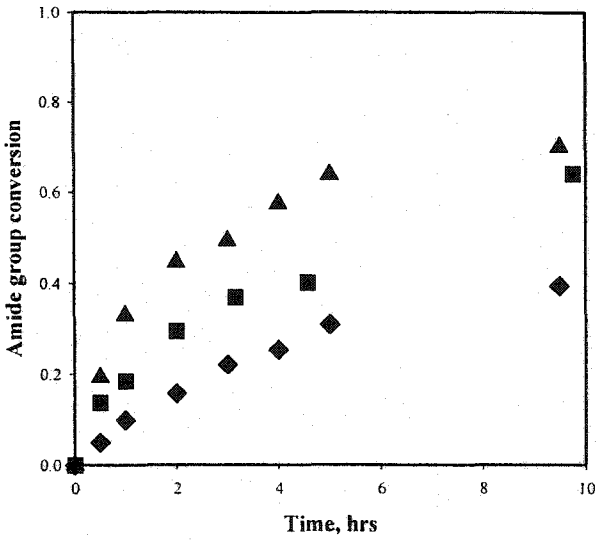

Figure 3.3 Acidic hydrolysis kinetics at different temperatures with 0.70 mol/L amide group and 1:1 acid/amide molar ratio (0.70 mol/L HCl), ◆ 60, ■ 70, ▲ 80 °C.

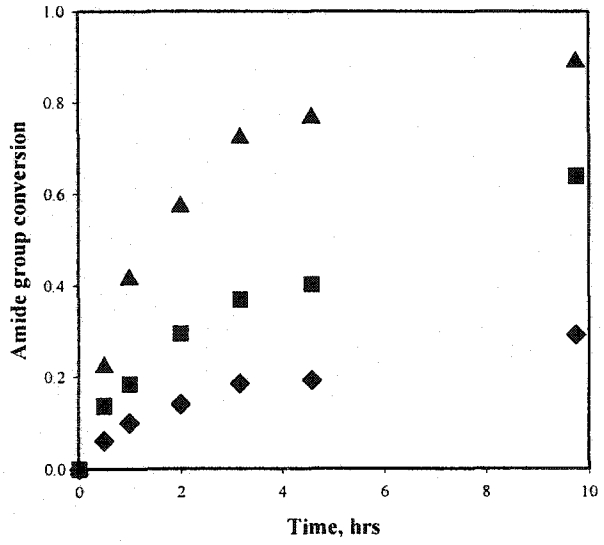

Figure 3.4 Effect of acid/amide molar ratio on hydrolysis kinetics at 70 °C and 0.70 mol/L amide group, ◆ 0.35 mol/L, ■ 0.70 mol/L, ▲ 1.41 mol/L HCl.

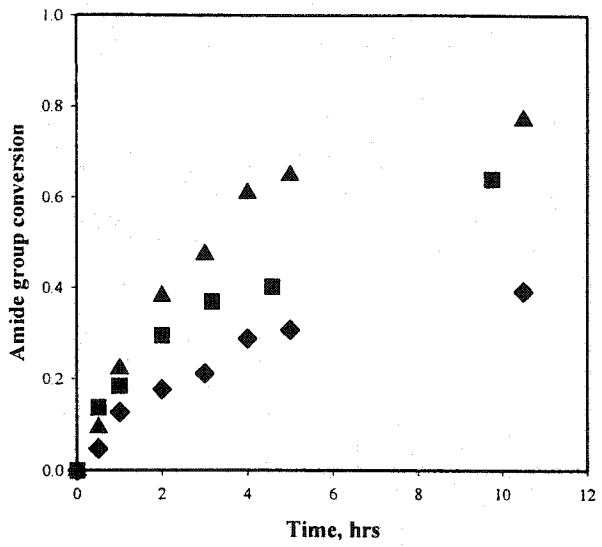

Figure 3.5 Effect of PNVF concentration on acidic hydrolysis at 70 °C and 1:1 acid/amide molar ratio, ▲ 1.41 mol/L PNVF, ■ 0.70 mol/L PNVF, ◆ 0.28 mol/L PNVF.

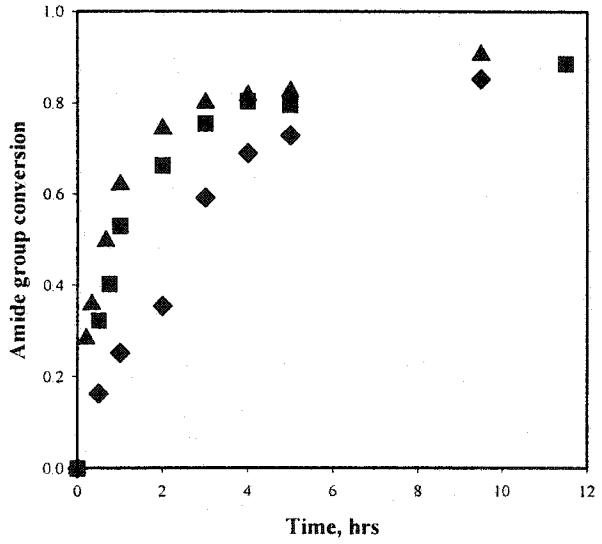

Figure 3.6 Basic hydrolysis kinetics at different temperatures with 0.70 mol/L amide group and 1:1 base/amide molar ratio (0.70 mol/L NaOH), ◆ 60, ■ 70, ▲ 80 °C.

Figure 3.5 shows the effect of the polymer concentration on the acidic hydrolysis kinetics. The polymer and acid concentration were set at 0.28, 0.70 and 1.41 mol/L. When the molar ratio of acid/amide group was set to 1:1, the initial rate increased with the increasing the reactant concentrations.

The acidic hydrolysis reactions did not reach the equilibrium conversion in the 10-hour period for the kinetic experiments (please refer to Section 3.3.2 Equilibrium Hydrolysis). The hydrolysis reaction slowed down dramatically after 8 hours due to the electronic repulsion among cationic groups generated during hydrolysis (Badesso et al, 1992) and the depletion of the reactants.

Basic Hydrolysis Kinetics

Figure 3.6 shows the hydrolysis kinetics at 60, 70 and 80 °C. The polymer concentration was 0.70 mol/L with a 1:1 base/amide group molar ratio. Higher temperatures gave higher initial conversion rates. However, the final hydrolysis conversions reached almost the same value at different temperatures. At the same polymer concentration, the degree of hydrolysis was determined only by the base/amide ratio.

Figure 3.7 shows the effects of the base concentration on the hydrolysis kinetics. The base/amide ratios were 0.5, 1.0 and 2.0 with an amide concentration of 0.70 mol/L. Higher base concentration not only yielded faster initial rates but also gave higher final hydrolysis degrees. At the highest base concentration, the hydrolysis reaction was completed within 5 hours.

Figure 3.8 shows the effect of the polymer concentration on the hydrolysis kinetics. The polymer concentrations were 0.28, 0.70 and 1.41 mol/L. The base concentrations were set at two different levels: 0.28 and 1.41 mol/L. The initial hydrolysis rate at the high base concentration level was higher than that at the low base concentration. However, changing the polymer concentration made almost no difference in the initial rate when the base concentration was 1.41

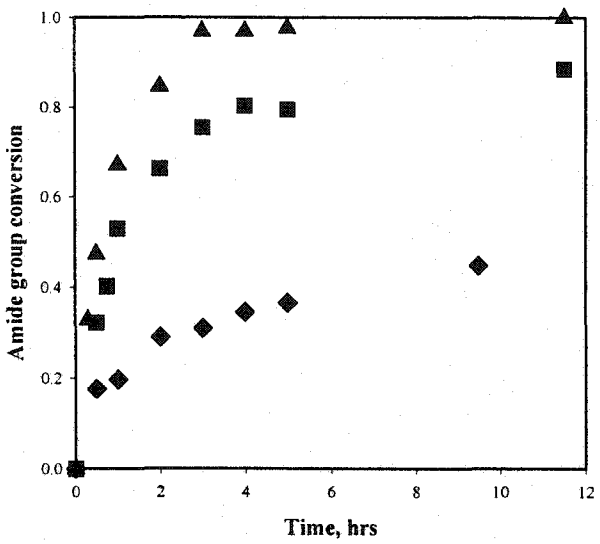

Figure 3.7 Effect of base/amide molar ratio on hydrolysis kinetics at 70 °C and 0.70 mol/L amide group, ◆ 0.35 mol/L, ■ 0.70 mol/L, ▲ 1.41 mol/L NaOH.

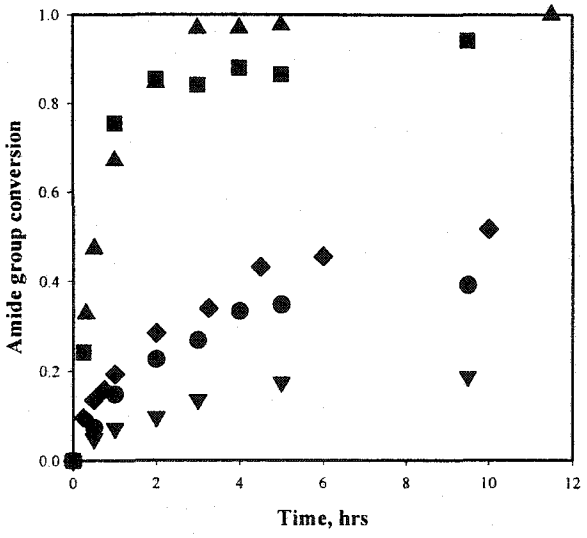

Figure 3.8 Effect of PNVF concentration on basic hydrolysis at 70 °C, ▲ 0.70 mol/L PNVF, 1.41 mol/L NaOH, ■ 1.41 mol/L PNVF, 1.41 mol/L NaOH, ◆ 0.28 mol/L PNVF , 0.28 mol/L NaOH, ● 0.70 mol/L PNVF, 0.28 mol/L NaOH, ▼ 1.41 mol/L PNVF, 0.28 mol/L NaOH.

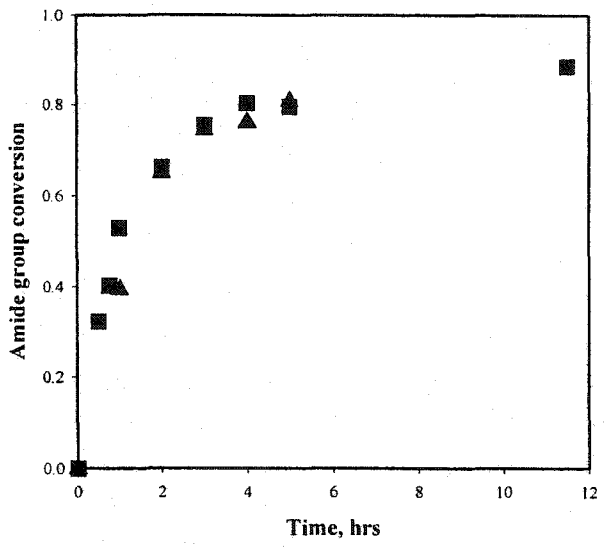

Figure 3.9 Effect of PNVF molecular weight on basic hydrolysis kinetics at 70 °C, 0.70 mol/L amide group and 1:1 base/amide molar ratio, $\overline{M}_w$: ■ 0.58×10^6, ▲ 2×10^6.

mol/L. At a base concentration of 0.28 mol/L, the initial rate decreased with increasing the polymer concentration from 0.28 to 1.41 mol/L.

Compared to the acidic hydrolysis, the basic hydrolysis kinetics displayed higher initial hydrolysis rate and higher equilibrium conversion of amide group at the same reactant concentrations, temperature and time span.

The results presented in Figures 3.3-3.8 were obtained from the low molecular weight ($\overline{M}_w$=579,000) PNVF sample. Figure 3.9 compares the basic hydrolysis kinetics of the low molecular weight PNVF to the high molecular weight sample at 70 °C. The polymer and base concentrations were the same: 0.70 mol/L. The lower molecular weight sample gave a slightly higher initial rate up to about 70% conversion. However, the discrepancy was not significant and disappeared at the final stage of the reaction. A possible explanation is that the high molecular weight sample has an initially higher viscosity and thus the result may suggest a weak viscosity effect on the hydrolysis kinetics at the early stage.

3.3.2 Equilibrium hydrolysis

Figures 3.10 to 15 show the equilibrium conversions of the PNVF hydrolysis at different temperatures, polymer concentrations and acid or base/amide group molar ratios. The data can be divided into two groups. Figures 3.10, 11 and 12 are the results of acidic equilibrium hydrolysis at 60, 70 and 80 °C respectively. Figures 3.13, 14 and 15 are the results of basic equilibrium hydrolysis. The equilibrium hydrolysis conversions are plotted against the initial acid or base/amide group molar ratios. In each figure, a 45-degree equimolar line is also plotted.

Generally, the results show that the final equilibrium hydrolysis conversion increased with increasing acid or base/amide group molar ratios. There was no sign of hydrolysis in parallel blank samples after being heated to the same temperature and held for the same amount of time. This excludes the possibility of thermal hydrolysis. The experimental results suggest that the final

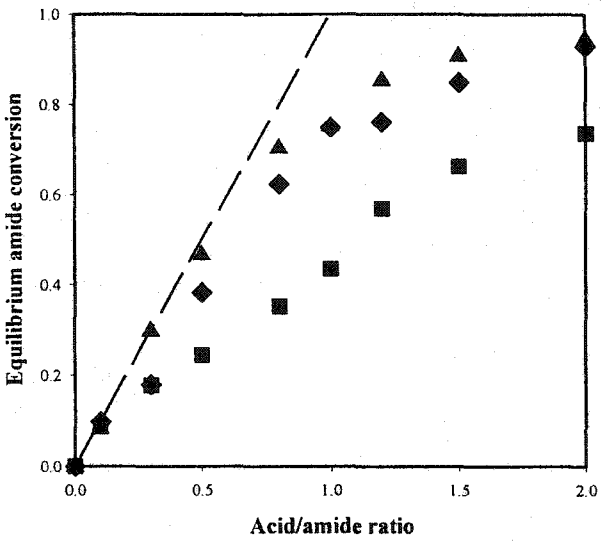

Figure 3.10 Equilibrium amide conversion at different acid/amide molar ratio at 60 °C, ■ 0.28 mol/L, ◆ 0.70 mol/L, ▲ 1.41 mol/L amide group.

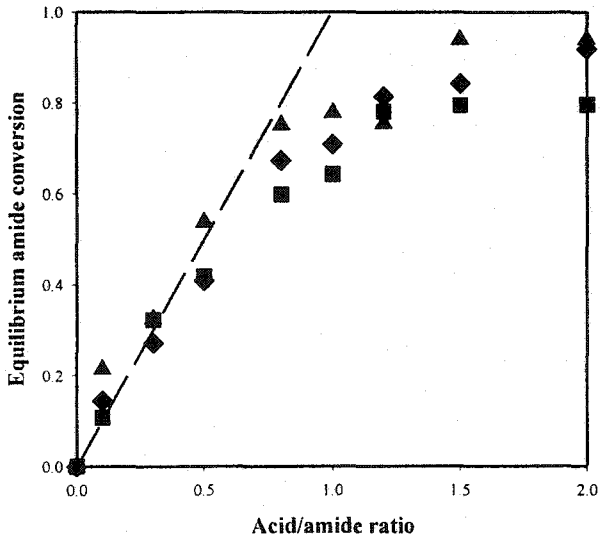

Figure 3.11 Equilibrium amide conversion at different acid/amide molar ratio at 70 °C, ■ 0.28 mol/L, ◆ 0.70 mol/L, ▲ 1.41 mol/L amide group.

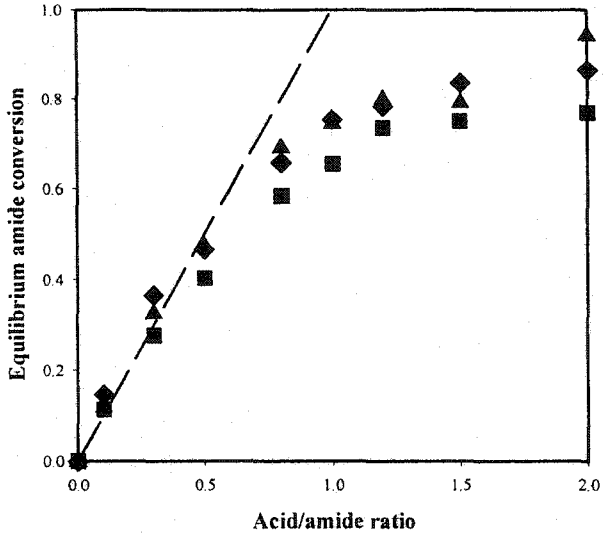

Figure 3.12 Equilibrium amide conversion at different acid/amide molar ratio at 80 °C, ■ 0.28 mol/L, ◆ 0.70 mol/L, ▲ 1.41 mol/L amide group.

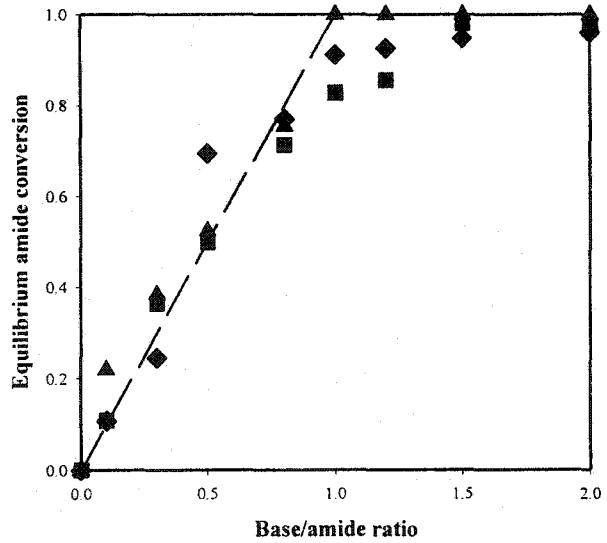

Figure 3.13 Equilibrium amide conversion at different base/amide molar ratio at 60 °C, ■ 0.28 mol/L, ◆ 0.70 mol/L, ▲ 1.41 mol/L amide group.

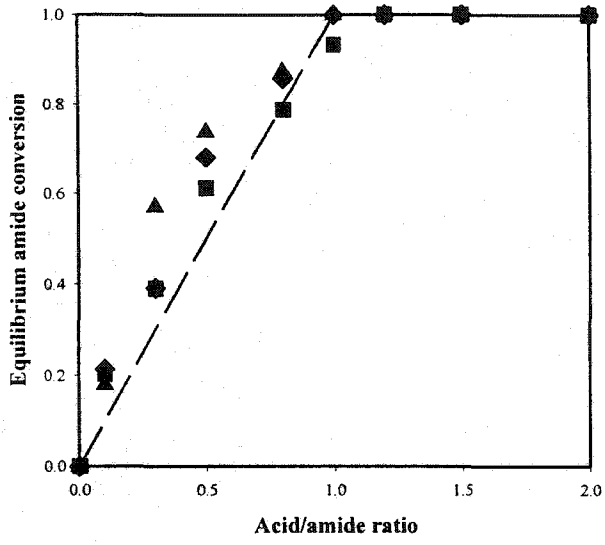

Figure 3.14 Equilibrium amide conversion at different base/amide molar ratio at 70 °C, ■ 0.28 mol/L, ◆ 0.70 mol/L, ▲ 1.41 mol/L amide group.

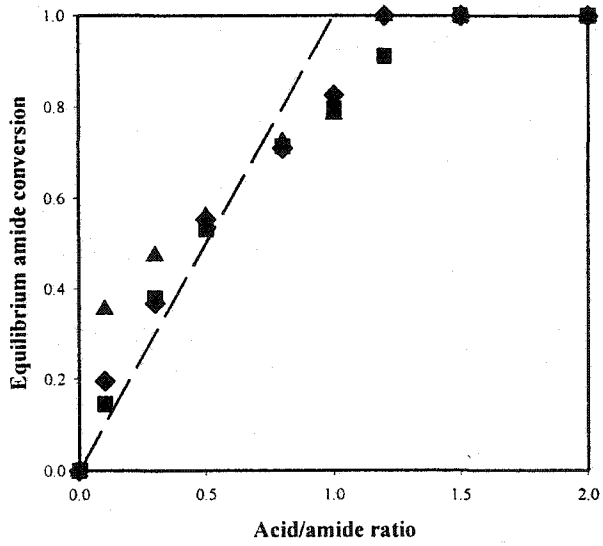

Figure 3.15 Equilibrium amide conversion at different base/amide molar ratio at 80 °C, ■ 0.28 mol/L, ◆ 0.70 mol/L, ▲ 1.41 mol/L amide group.

equilibrium conversions of hydrolysis were determined only by the acid or base/amide group molar ratios.

The equilibrium conversions of acidic hydrolysis are generally lower than those of base hydrolysis at the same temperature, polymer concentration and acid or base/amide group molar ratios.

Acidic hydrolysis runs did not proceed to 100% conversion under current experimental conditions as shown in Figures 3.10 ~12. This can be explained by the fact that acidic hydrolysis introduces cationic charge onto polymer chain (Figure 3.16). When the neighbouring amide groups were hydrolyzed and became cationic amino groups, the remaining amide groups were shielded by these cationic charged amino groups. The electrostatic repulsion between these cationic amino groups and the attacking H_3^+O species prevented a 100% conversion of hydrolysis. It was also observed that under most experimental conditions, the final equilibrium conversion of acid hydrolysis did not exceed the equimolar line in the figures. (The experimental points are always on or below the 45-degree line.)

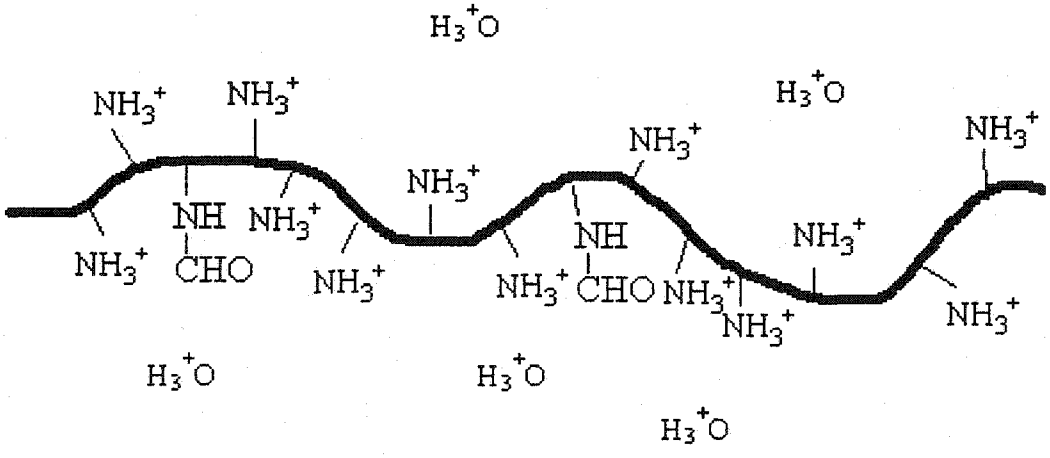

Figure 3.16 Electrostatic repulsion prevented a 100% conversion in PNVF acidic hydrolysis.

An interesting observation with the basic hydrolysis is that at base/amide ratios below 1.0, the base hydrolysis often gave an equilibrium conversion higher than the theoretical value based on the stoichiometry of the basic hydrolysis route shown in Scheme 1. These experimental data are above the equimolar lines in the graphs (Figures 3.13 ~ 15). The data reveal that one mole base (OH^-) induced the hydrolysis of more than one mole amide group. When the base/amide molar ratio was less than 1, the initial NaOH should be completely consumed before all the amide groups were hydrolyzed. However, the basic hydrolysis of an amide group produces an amine group, which is also a weak base. The hydrolysis of amine groups on the polymer chains provides additional OH^- anions (Equation 3.2) after all the NaOH is consumed. These additional OH^- anions can continue the hydrolysis of the amide groups. This can explain that basic hydrolysis usually has a higher conversion than the equimolar line in the figures. This "over shoot" phenomenon was more pronounced at the lower base/amide molar ratios (<0.5).

$$-NH_2 + H_2O \longleftrightarrow -NH_3^+ + OH^- \qquad 3.2$$

The experimental data also show that the basic hydrolysis usually proceeded to a 100% amide conversion when the base/amide ratio was over 1.0.

3.4 Conclusions

Hydrolysis kinetics and reaction equilibria of PNVF under acidic and basic conditions were examined experimentally. The hydrolysis conversions were determined by H-NMR. Basic hydrolysis usually gave higher reaction rates and higher conversions than its acidic counterpart at the same reactant concentrations, temperature and time span. The equilibrium hydrolysis data reveal that one mole base induced the hydrolysis for more than one mole amide groups, particularly at the NaOH/amide group ratio lower than 1.0. The basic hydrolysis of PNVF usually proceeded to 100% conversion when the NaOH/amide ratio was greater than 1.0. Acidic equilibrium hydrolysis did not reach 100% completion within the scope of this experimental investigation. Acidic hydrolysis also gave lower equilibrium amide conversion than basic hydrolysis at the same reaction conditions. This is probably due to the cationic repulsion established between charged polymer chains and the approaching acid (H^+).

3.5 References

Achari, A. E. Coqueret, X. Lablach-combier, A. and Louchex, C. (1993). "Preparation of Polyvinylamine from Polyacrylamide: A Reinvestigation of the Hofman Reaction". *Makromol. Chem.*, *194*, 1879.

Auhorn, W. Linhart, F. Lorencak, P. Kroener, M. Sendhoff, N. Denzinger, W. and Hartmann, H. (1992). US. Patent No. 5145559, BASF.

Badesso, R. J. Lai, T. Pinschmidt, R. K. Jr. Sagl, D. J. And Vijayendran, B. R. (1992). "High and Medium Molecular Weight Poly (vinylamine)". *Polymer Preprints*, *32*, 110.

Badesso, R. J. Nordquist, A. F. Pinschmidt, R. K. Jr. and Sagl, D. J. (1995). "Synthesis of Amine Functional Homopolymers with N-Ethenylformamide", in *Hydrophilic Polymers: Performance with Environmental Acceptance*, E. Glass ed., American Chemical Society, Washington DC, p. 489.

Badesso, R. J. Pinschmidt, R. K. Jr. and Sagl, D. J. (1993). "Synthesis of Amine Functional Homopolymers with n-Ethenylformamide". *Proc. Amer. Chem. Soc. Div. Polym. Mat. Sci. Eng.*, *69*, 251,

Burkert, H. Brunnmueller, F. Beyer, K. Kroener, M and Mueller, H. (1984). US Patent No. 4444667, BASF.

Fischer, T. and Heitz, W. (1994). "Synthesis of Polyvinylamine and Polymer Analogous Reactions". *Macromol. Chem. Phys.*, *195*, 679.

Ford, M. and Armor, J. N. (1996). US. Patent No. 5491199, Air Products and Chemicals.

Hart, R. (1959). "Synthese de la Polyvinylamine Hydrolyse du Poly-N-vinylcarbamate de tert.-Butyle". *Makromol. Chem.*, *32*, 51.

Hughes, A. R. and Pierre, T. St. *Macromolecules Synthesis*, Vol 6, J. E. Mulvaney Ed., Wiley, New York, 1977, p.6.

Monech, D. Hartmann, H. and Buechner, K. (1993). US. Patent No. 5225088 (1993), BASF.

Monech, D. Hartmann, H. Freudenberg, E. and Stange, A. (1993). US. Patent No. 5262008, BASF.

Pfohl, S. Kroener, M. Hartmann, H. and Denzinger, W. (1988). US. Patent No. 4774285, BASF.

Pfohl, S. Kroener, M. Hartmann, H. and Denzinger, W. (1989). US. Patent No. 4880497, BASF.

Pfohl, S. Kroener, M. Hartmann, H. and Denzinger, W. (1990). US. Patent No. 4978427, BASF.

Pinschimdt, R. K. Jr. and Lai, T. (1990). US. Patent No. 4931194.

Singley, E. J. (1997). "Development of Fluoroether Amphiphiles and Their Applications in Heterogeneous Polymerization in Supercritical Carbon Dioxide", Thesis (Ph.D.), University of Pittsburgh, 1997, p.221.

Stinson, S. (1993). "Quest for Commercial Polyvinylamine Advances". *Chem. & Eng. News*, 71*(36)*, 32.

Todorov, N. G. Valkov, E. N. and Stoyanova, M. G. (1996). "Chemical Modification of Poly(acrylonitrile) with Amines". *J. of Polym. Sci, Part A, Polym. Chem., 34*, 863.

Chapter 4. Synthesis and Flocculation Performance of Graft Copolymer of N-Vinylformamide and Polydimethylaminoethyl Methacrylate Methyl Chloride Macromonomer

4.1 Introduction

In previous chapters, the polymerization of N-vinylformamide (NVF) and the hydrolysis of poly (N-vinylformamide) (PNVF) were investigated. PNVF and its derivatives comprise a novel class of water-soluble polymers (Pinschmidt Jr et al, 1997). They have potential applications in such areas as wastewater treatment, sludge dewatering, and papermaking. (Auhorn et al, 1992; Burkert et al, 1984; Monech et al, 1993; Pfohl et al, 1988, 1989, 1990).

The essential roles played by PNVF class polymers in these applications are as flocculants. These polymers can flocculate colloidal particles from an aqueous phase, thereby either recovering valuable materials or removing unwanted solids. The two basic mechanisms used to explain the flocculation process are charge neutralization and chain bridging (Bolto, 1995; Rose and John, 1988). Charge neutralization accounts for the electrostatic attraction by addition of counterions into colloids. For negatively charged water born colloidal particles, low molecular weight cationic polymers (coagulants) are very useful. The chain bridging mechanism is governed by irreversible multi-point adsorption of polymer chains onto the surfaces of colloidal particles. A polymer chain subsequently brings particles together by attaching its segments to surfaces of different particles. Higher molecular weight polymers, such as PNVF and polyacrylamide (PAM), are most useful for chain bridging.

In reality, most water-soluble polymeric flocculants put both mechanisms into action. The cationic charge centres provide firm attraction to particle surfaces while long polymer chains

extend from one particle to another. To date, most commercial polymer flocculants are linear copolymers with randomly distributed cationic charge along the polymer chain. Typical examples are modified PAM or copolymers of acrylamide (AM) with cationic comonomers, usually polyquats, polyimines or polyamine (McCormick et al, 1988; McDonald and Beaver, 1979; Pelton, 1984).

It is desirable to further control the charge density distribution within the molecular structure to improve the performance of these flocculants. A proposed graft copolymer, with a long non-ionic polymer chain as a backbone and cationic polymer as grafts (comb structure, see Figure 1.2) (Ma, 1996; Subramanian et al, 1999) appears to have a better charge density distribution than traditional random linear copolymers. Instead of having randomly distributed cationic charges along the polymer chain, the graft copolymer has locally concentrated cationic charge clusters (the cationic grafts) to provide stronger polymer-surface interaction. At the same time, the high molecular backbone enables multi-point adsorption onto particle surface and inter-particle extension.

Although there were indications that grafted copolymers have better flocculation performance than their linear counterparts, this has never been verified with a graft copolymer with a well-defined comb structure. Grafting by γ-ray irradiation inevitably introduced hyperbranches into copolymers, and sometimes gelation as in Subramanian et al (1999) and Ma (1996).

In this chapter, graft copolymers of NVF and polydimethylaminoethyl methacrylate quats (cationic macromonomer) were synthesized using free radical copolymerization in an aqueous solution. Copolymerization of NVF and the macromonomer yielded a graft copolymer having a PNVF backbone and cationic grafts (side chains) with a predetermined side chain length (via anionic polymerization). Copolymerization kinetics and the cationic macromonomer incorporation rate were obtained. The copolymerization reactivity ratios were measured with two macromonomers having different molecular weights. The flocculation performance of graft copolymers were measured and compared to that of random linear cationic copolymers.

4.2 Experimental

4.2.1 Materials

NVF monomer (Aldrich) was distilled under vacuum at 70°C and stored at -15°C before polymerization. Two poly(dimethylaminoethyl methacrylate) (PDMAEMA) macromonomers bearing unsaturated diallyl end groups were synthesized by anionic polymerization method (Zeng et al, 2001). The macromonomers (for graft copolymer) were dissolved in dimethylsulfonate (DMSO, Aldrich) and quaternized to form PDMAEMA quats by benzyl chloride (Aldrich) in dimethylsulfonate (DMSO) at room temperature for 8 hours. Dimethylsulfate (Aldrich) was then added at the end and the solution was stirred for an additional hour to ensure complete quarternization. The quats were precipitated and the samples were dried in vacuum at room temperature. The two quarternized macromonomer had a number average molecular weight of 14,100 (equivalent to 50 repeating units) and a polydispersity index of 1.10, and a number average molecular weight of 28,200 (100 repeating units) and a polydispersity index of 1.11. If only dimethylsulfate was used to quarternize the macromonomer, the hydrolysis of the sulfate under the subsequent aqueous copolymerization conditions would result in strong acidity of the solution, which would hydrolyze NVF monomer and no polymer would be formed. Methyl iodine, CH_3I, (Aldrich) was also excluded as a quaternizing reagent because the I^- ion brought into the macromonomer was an inhibitor to the subsequent free radical polymerization. Dimethylaminoethyl methacrylate chloride (DMAEMA-MCQ, 70wt% aqueous solution, Dajac Lab, PA) was used for the copolymerization with NVF to produce random copolymers for comparison purpose. The molecular structures of the random and graft copolymer are presented in Figure 4. 1.

TiO_2 aqueous suspension was used as the model system for the flocculation performance evaluation. 45 mg TiO_2 powder (Aldrich, ρ=3.9g/ml) was dispersed in 1L deionized water with an ionic strength of 10^{-3} M NaCl. The stock suspension was stirred for 24 hours to ensure the

complete wetting of the particles. Prior to the flocculation tests, an ultrasonic bath for 10 minutes was used to completely disperse the TiO_2 particles.

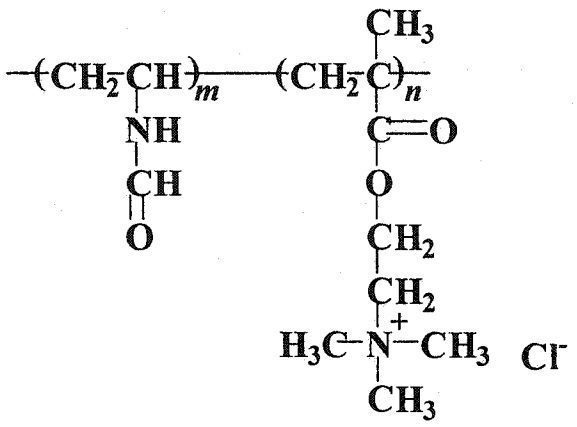

(a)

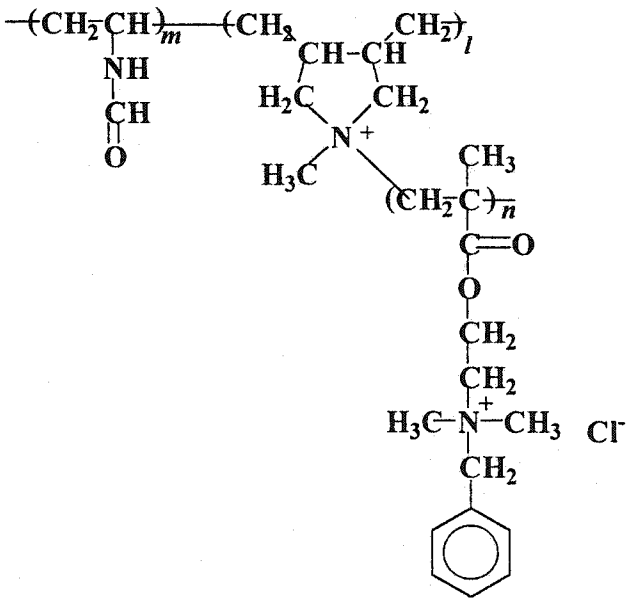

(b)

Figure 4.1 Molecular structures of random linear copolymer (a), and graft copolymer (b).

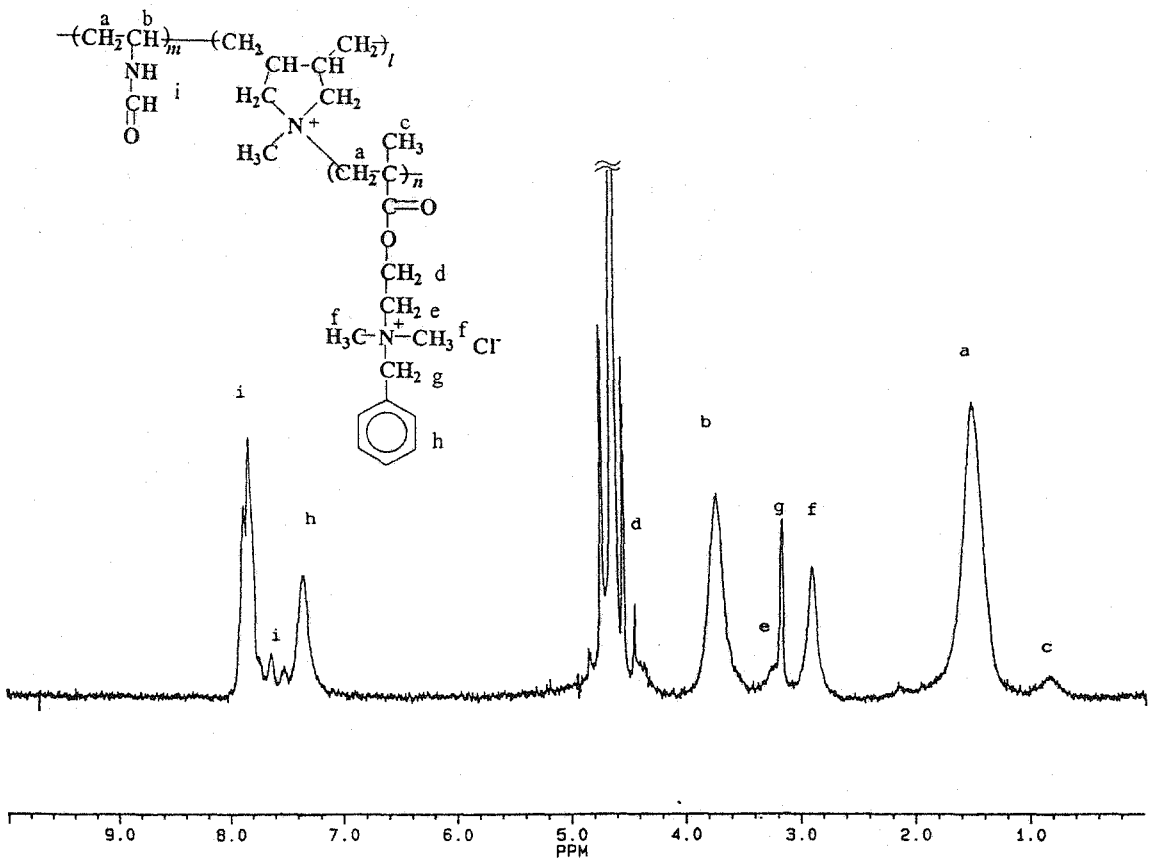

Figure 4.2 H-NMR spectrum of NVF- PDMAEMA*MCQ macromonomer copolymer

4.2.2 *Copolymerization*

The free radical copolymerization of NVF and macromonomer was carried out in aqueous solution. The initiator, 2,2'-azobis (2-methylpropionamidine) dihydrochloride (AIBA) (Aldrich), was recrystallized twice before use.

A given mixture of NVF, comonomer, AIBA and water was charged into a set of glass ampoules. After three freeze-thaw degassing cycles, the ampoules were immersed in a water bath at the polymerization temperature. The ampoules were taken out at different time intervals and quenched by freezing. The reactant mixture was dissolved in water and the polymer content was precipitated in methanol. All the samples were dried under vacuum at room temperature for 48 hours.

The polymerization conversion, x, was calculated using

$$x = \frac{W_P}{M_0} \qquad 4.1$$

where W_P is the mass of copolymer, and M_0 is the total initial charge of the monomers.

Copolymer samples with different cationic contents ranging from 0 ~ 10mol% were synthesized for flocculation performance evaluation and reactivity ratio measurement. The copolymer composition was determined by a 200MHz NMR spectrometer. An example NMR spectrum is given in Figure 4.2.

4.2.3 *Intrinsic viscosity measurement*

The intrinsic viscosity of the linear and graft copolymer samples was measured using a Cannon Ubbelohde (#50, M545) viscometer. A 0.2 M $NaNO_3$ water solution was used as solvent for all samples. Each sample solution was subject to 0.45μm filtration before injection into the viscometer. The temperature of the viscosity measurement was maintained at 25±0.1 °C.

4.2.4 Flocculation test and turbidity measurement

The pH value of the stock suspension was adjusted to a value of 8 according to a zeta potential (surface charge) measurement to ensure the negative surface charge of the TiO_2 particles (Ma, 1996). This was done by adding a small amount of 0.01 M NaOH solution. The turbidity of the TiO_2 suspension samples with and without polymers was measured using a Hach 2100P portable turbidimeter (Hach, Loveland, CO).

The flocculation experiments followed the procedure of a previously published study (Ma, 1996). A pre-set amount of polymer was added to 180ml pH-stabilized TiO_2 suspension with constant stirring. Samples were taken out at 0, 5, 10, 15, 30, 45 and 60 minutes and their turbidity was measured. The relative turbidity was the ratio of the turbidity measured at a given time to the initial turbidity ($T_r = T_t / T_0$).

4.3 Results and discussion

4.3.1 Copolymerization

Figures 4.3 and 4.4 show the kinetics of copolymerization of NVF with macromonomers at 50 °C (Figure 4.3 - macromonomer with 50 repeating units, Figure 4.4 - 100 repeating units). The total monomer concentration was 40 wt%. The initial macromonomer feed is presented as the mass percentage of macromonomer in the NVF/macromonomer mixture. The initiator (AIBA) concentration was 3.0×10^{-3} mol/L. Both figures show comparison with NVF homopolymerization (data from Chapter 2, NVF solution polymerization, 40wt% monomer concentration and [AIBA] = 3.0×10^{-3} mol/L, 50 °C). Increasing the macromonomer concentration in the reaction mixture reduced the polymerization rate as well as the final conversion level.

Figure 4.5 shows the effect of temperature on the copolymerization kinetics. The polymerization rate increased with temperature. The final conversions were almost the same at different temperatures.

All the kinetics experiment clearly showed the "gel effect", which was caused by the diffusion control of the chain radical termination. This phenomenon was also observed in NVF homopolymerization (Gu et al, 2001 and Chapter 2). Addition of macromonomers, which were essentially short chain length polymers, to the reaction mixture increases the initial viscosity and creates more resistance to the diffusion of polymer chain radicals. This should yield a more severe "gel effect" as is actually shown in the figure that the copolymerizations with higher macromonomer concentration (e.g. 20 wt% macromonomer) exhibited a higher curvature (auto acceleration) trend at the initial stage of polymerization.

Figure 4.6 shows an example of the conversion of the individual comonomers as a function of the total monomer conversion. The initial feed amount of macromonomer (50 repeating units) was 20 wt% of the total monomer mass. At every stage of the copolymerization, the conversion of NVF was always higher than that of the macromonomer. The NVF monomer was more active than the macromonomer during the copolymerization. The incorporation of the macromonomer into copolymer remained low until toward the end of the copolymerization.

4.3.2 Reactivity ratio

The reactivity ratios of copolymerization are the most important parameters in describing the relative activities of a pair of comonomers in copolymerization. In a binary copolymerization system that follows the terminal model, Equation 4.2 is used to determine the instantaneous copolymer composition,

$$\frac{d[M_1]}{d[M_2]} = \frac{[M_1]}{[M_2]} \bullet \frac{r_1[M_1]+[M_2]}{r_2[M_2]+[M_1]} \qquad 4.2$$

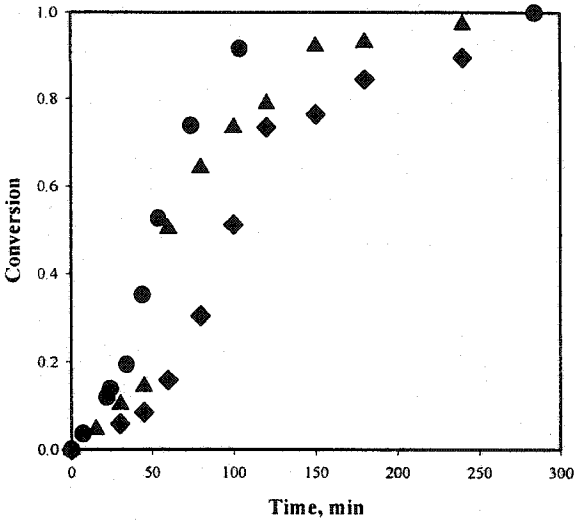

Figure 4.3 Kinetics of NVF-DMAEMA*MCQ (50 repeating units) copolymerization at 50 °C, 0.2wt% AIBA, 40wt% total monomer concentration, ● homopolymerization ▲ 10wt%, and ◆ 20wt% macromonomer.

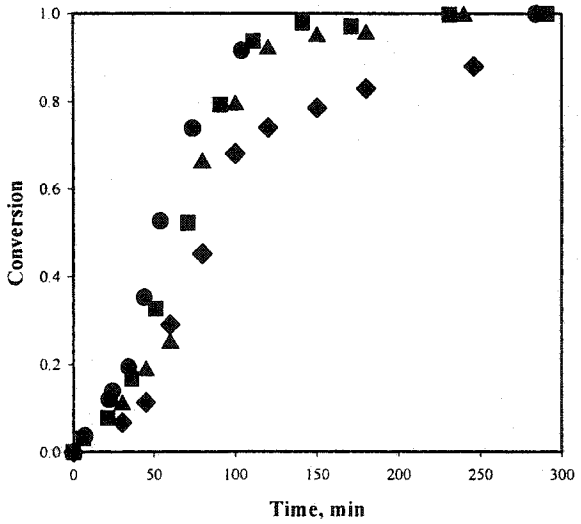

Figure 4.4 Kinetics of NVF-DMAEMA*MCQ (100 repeating units) copolymerization at 50 °C, 0.2wt% AIBA, 40wt% total monomer concentration, ● homopolymerization ■ 5wt%, ▲ 10wt%, and ◆ 20wt% macromonomer.

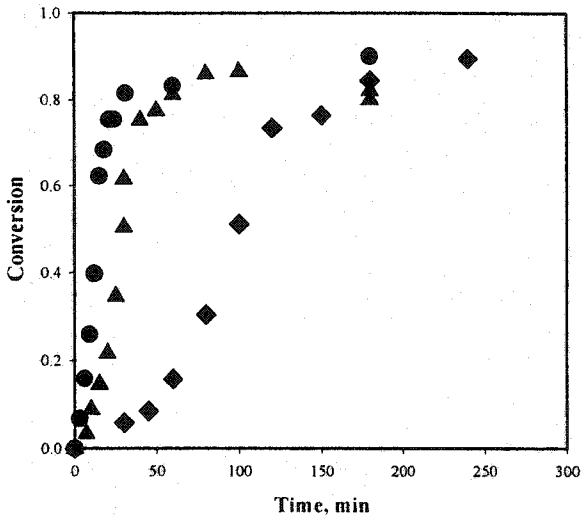

Figure 4.5 Kinetics of NVF-DMAEMA*MCQ (50 repeating units) copolymerization at different temperatures, 0.2wt% AIBA, 40wt% total monomer concentration, ● 70 ▲ 60, and ◆ 50 °C.

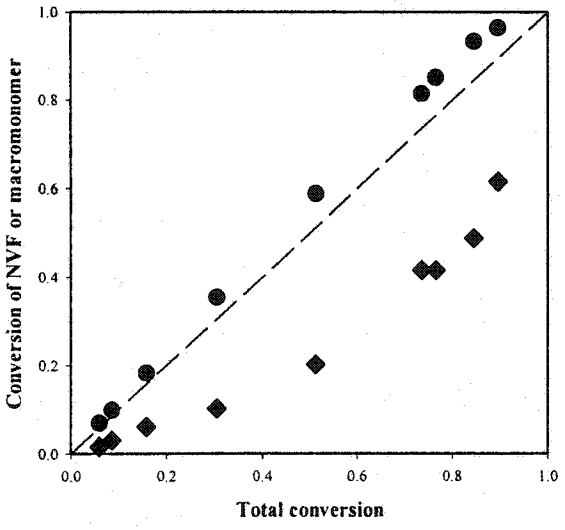

Figure 4.6 Fractional conversion of NVF and macromonomer (50 repeating units) during the copolymerization, 50 °C, 0.2wt% AIBA, 40wt% total monomer concentration, 20wt% macromonomer, ● NVF ◆ Macromonomer.

The reactivity ratios, r_1 and r_2 are defined as k_{p11}/k_{p12} and k_{p22}/k_{p21} respectively, (k_{pij} is the propagation rate constant of chain radicals ending with *i*-type monomeric unit with *j*-type monomer, *i*, *j* = 1, 2). In the case of NVF (M_1) and PDMAEMA quats macromonomer (M_2) copolymerization, the molar concentration of M_2 (macromonomer) is very low, thus

$$[M_1] >> [M_2] \tag{4.3}$$

Therefore Equation 4.2 is simplified to (Xiao et al, 1996; Meijs and Rizzardo, 1990)

$$\frac{d[M_1]}{d[M_2]} = r_1 \frac{[M_1]}{[M_2]} \tag{4.4}$$

which can be integrated to

$$r_1 = \frac{\ln(1 - x_1)}{\ln(1 - x_2)} \tag{4.5}$$

where x_1 and x_2 are the conversions of M_1 and M_2 respectively.

Equation 4.5 is often used to estimate r_1 for different macromonomers. It gives a ratio of the reactivities of NVF and macromonomer toward the NVF radical. Within the scope of this study, r_2 could not be determined owing to the very low molar concentration of macromonomer used in the copolymerization. Also in an aqueous medium, once a macromonomer is added and a macromonomer radical is thus formed at the end of a growing chain, the highly concentrated charges on the pendent graft (electrical repulsion), plus the steric barrier of macromonomer radical (Nabeshima and Tsuruta, 1989), makes it almost impossible to react with another macromonomer, i.e., $k_{p22} \approx 0$. Therefore r_2 was assumed to be negligible.

To estimate r_1, a series of NVF- macromonomer copolymer samples were first synthesized by free radical polymerization with various initial monomer ratios. The initial feed ratios of the macromonomer were 10, 20, 30, 40 and 50 wt% of the total monomer mass and the total monomer concentration was 40wt%. The initiator (AIBA) concentration was 3.0×10^{-3} mol/L. The total conversion of each copolymerization run was kept less than 15% to avoid a possible composition drift effect. These copolymer samples were recovered and their composition

measured by NMR spectrometer. The fractional conversions, x_1 and x_2, were obtained from the total polymerization conversion coupled with the copolymer composition data from H-NMR.

Figure 4.7 shows the plots of $-\ln(1-x_1)$ vs $-\ln(1-x_2)$ for copolymerization of the two macromonomers with NVF. The slopes of the regression lines through the experimental points are equal to r_1. For the macromonomer with 50 repeating units, r_1 was estimated 3.82. For macromonomer with 100 repeating units, r_1 was 6.39. This indicated a chain length effect. A macromonomer with a shorter chain length is usually more active than one with a longer chain in copolymerization. This phenomenon was also observed in other monomer-macromonomer copolymerization studies (Masuda et al, 1991; Tsukahara et al, 1990) that reported a reduction in k_p with increasing macromonomer molecular weight. The lower copolymerization reactivity is attributed to lower segmental diffusion rate of a longer macromonomer chain. It is more difficult for a macromonomer with 100 repeating units to react with a PNVF radical than for a macromonomer with 50 repeating units.

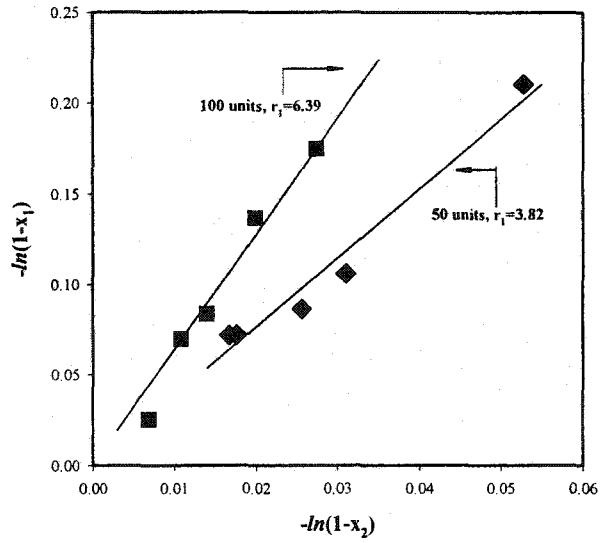

Figure 4.7 Copolymerization reactivity ratio (r_1) of NVF-macromonomer comonomer pair. r_1 is the slope of the fitted line. ◆ 50, ■ 100 repeating units.

Table 4.1 NVF cationic copolymers used for flocculation tests. Numbers in the table are the mole percentage (mol%) of the cationic charge centres

Sample No.	Random	100-unit graft	50-units graft
1	1.9	0.68	---
2	2.6	2.4	---
3	3.6	3.5	3.9
4	9.3	5.7	4.9
5	11.3	8.8	5.2
6	13.3	9.5	8.0

Table 4.2 Intrinsic viscosity (L/g) of NVF cationic copolymers used for flocculation tests corresponding to samples in Table 4.1

Sample No.	Random	100-unit graft	50-units graft
1	6.39	4.38	---
2	4.61	3.10	---
3	4.95	2.76	2.23
4	2.93	0.71	3.83
5	2.90	0.49	0.33
6	2.57	0.40	0.16

4.3.3 Flocculation tests

Several graft copolymer samples were synthesized with different cationic contents using the two macromonomers having different molecular weights. For reference and comparison purposes, several random linear copolymer samples of NVF and dimethylaminoethyl methacrylate methyl chloride quats were also prepared and tested. All these copolymer samples were synthesized by aqueous free radical polymerization with 40wt% monomer concentration and 3.0×10^{-3} mol/L initiator (AIBA) concentration.

Table 4.1 lists the copolymer samples used for flocculation tests. The molar content of the cationic charge groups as well as the total monomer conversion for each sample is included. Table 4.2 lists the intrinsic viscosities corresponding to the samples in Table 4.1. Because there is no reliable and accurate method for estimating the molecular weight of grafted cationic copolymers, only the intrinsic viscosity data are reported here as a molecular weight indicator when the samples are compared to each other. Generally, the viscosity decreased with increasing cationic content in the copolymer. This indicates a decreasing trend in the molecular weight with increasing cationic content for both the linear and the graft copolymers.

Figures 4.8 ~ 10 show the results of relative turbidity (T_r) measurements. The T_r values are plotted against the flocculation time up to 60 minutes. The polymer dosage used was 5mg/g TiO_2. The cationic charge levels of the seven random linear copolymer samples tested were 1.86, 2.61, 3.57, 9.33, 11.29, and 13.34 mol% (the mole percent is the number of the DMAEMA units over the total number of the monomeric units). The charge levels of the copolymer samples having the 50-unit grafts were 3.85, 4.93, 5.18, and 7.99 mol% (the mole percent is with respect to the DMAEMA monomeric unit and should not be confused with the macromonomer unit in the chain). The charge levels of the 100-unit graft copolymers were 0.68, 2.39, 3.54, 5.72, 8.81, and 9.48 mol%. A general trend of the $T_r \sim t$ curves was a dramatic reduction in the turbidity within 20 minutes followed by a levelling off.

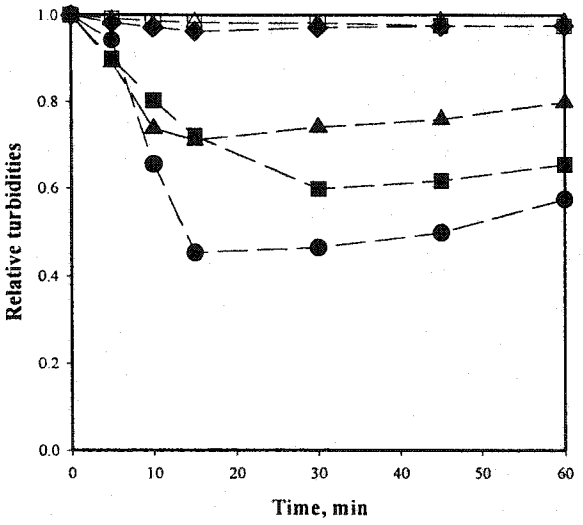

Figure 4.8 Flocculation tests of random linear copolymer samples, relative turbidity change in 60 min., 5mg copolymer /g TiO_2 dosage, △ 1.86, ❑ 2.61, ◆ 3.57, ▲ 9.33, ■ 11.29, and ● 13.34 mol% cationic content.

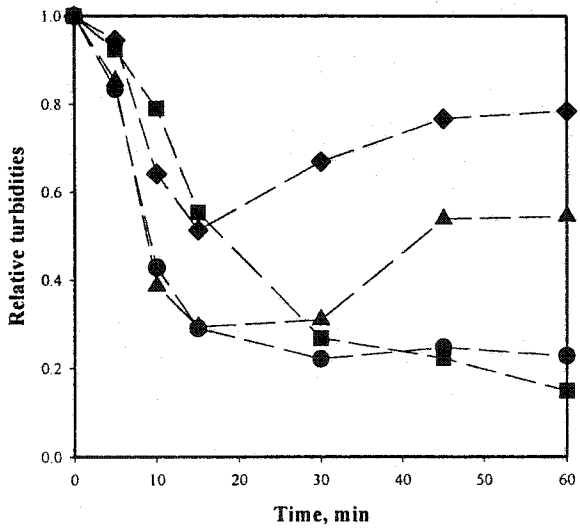

Figure 4.9 Flocculation tests of graft copolymer (50 repeating units graft) samples, relative turbidity change in 60 min., 5mg copolymer /g TiO_2 dosage. ◆ 3.85, ▲ 4.93, ■ 5.18 and ● 7.99 mol% cationic content.

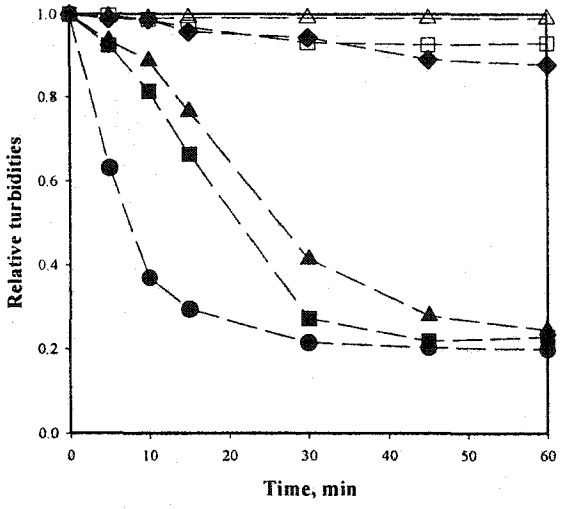

Figure 4.10 Flocculation tests of graft copolymer (100 repeating units graft) samples, relative turbidity change in 60 min., 5mg copolymer /g TiO_2 dosage. △ 0.68, ❑ 2.39, ◆ 3.54, ▲ 5.72, ■ 8.81 and ● 9.48 mol% cationic content.

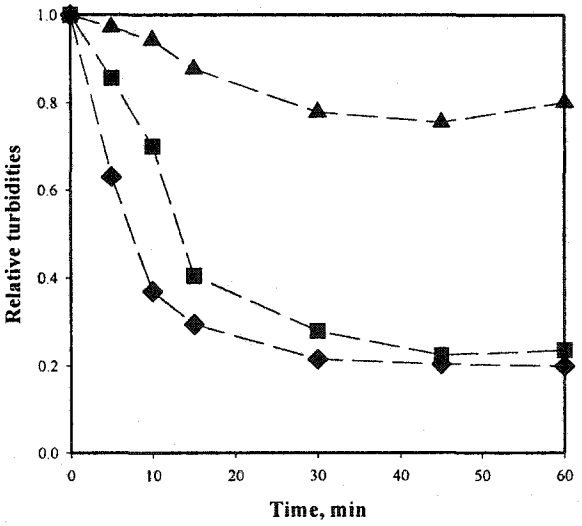

Figure 4.11 Flocculation tests of graft copolymer (100 repeating units graft) samples using different polymer dosages, relative turbidity change in 60 min. 9.48 mol% cationic content, ▲ 1, ■ 2 and ◆ 5 mg copolymer /g TiO_2.

It was also observed that, in some cases, the turbidity increased with time after the initial drop, but did not recover to the original turbidity level. This can be attributed to the break-up of the flocculated TiO_2 colloidal particles by the continuous stirring of the dispersion. Most random linear samples as well as the 3.85 and 4.93 mol% 50-unit graft samples showed the turbidity recovery effect. The flocs with the graft copolymers appeared to have greater strength than those formed by the linear samples. The copolymer samples with longer grafts (100-unit) gave stronger flocs than the samples with shorter grafts (50-unit).

The reduction in turbidity strongly depends on the charge content level. At low cationic levels, no significant impact on the turbidity was observed for all the polymer samples. Increasing the charge content improved the flocculation and thus lowered the turbidity. Compared to their random linear counterparts, the graft copolymers gave improved flocculation performance using samples with the same or lower molar cationic content. The comb-branched graft copolymers appear to be more effective than the random linear copolymers in flocculating the model TiO_2 suspension. For example, the best flocculation performance among the linear random samples was at a cationic content of 13.34 mol%. The sample reduced the relative turbidity to 40% in 15 minutes and reached a final level of about 60% of the initial turbidity. In contrast, the graft copolymer samples having as low as about 6 mol% cationic content (above 5.18 mol% for the 50-unit graft, above 5.72 mol% for the 100-unit graft) achieved a lower final relative turbidity (20~30%) than that of the previously described random sample (with 13.34 mol% cationic content). The graft copolymers having the same levels of cationic charge as their linear counterparts acted faster and achieved lower final turbidity (7.99 mol% 50-unit graft and 8.81 mol% 100-unit graft with 9.33 mol% linear copolymer).

The turbidity reduction data also show less dependence on the molecular weight than on the cationic content. For non-charged polymers, such as PAM, it is ideal to have a high molecular weight (~10^6) to be an effective flocculant (Rose and John, 1988). However, the cationic charged copolymer samples (both linear and graft) having higher cationic content usually have better turbidity reduction even with lower intrinsic viscosity, i.e. lower molecular weight. For example,

the best performance was for a 100-unit graft copolymer containing 9.5 mol% cationic content. It had the lowest intrinsic viscosity (0.4) among its own category. It is the same for linear random copolymer samples. The linear sample with the best performance contained the most, 13.34 mol%, cationic content but had the lowest intrinsic viscosity, 2.57.

The flocculation performance is also a function of the polymer dosage. Tests were also conducted at reduced polymer dosages, 1 and 2mg copolymer/g TiO_2. At a TiO_2 dosage of 1 mg/g, none of the samples tested (random or grafted copolymers) showed significant flocculation impact on the model suspension system. At a TiO_2 dosage of 2 mg/g, only the 100-unit graft copolymer with 9.48mol% cationic content significantly reduced the turbidity. Figure 4.11 shows the effect of polymer dosage on turbidity.

The reason for the flocculation performance enhancement of the graft copolymers lies in their chain structure and cationic charge distribution. For a charged polymeric flocculant to be effective, both flocculation mechanisms - chain bridging and charge neutralization must be at work simultaneously. The comb-branched graft copolymer provides highly concentrated cationic groups (clusters of DMAEMA quats), enabling strong adsorption with particle surfaces. The PNVF backbone free of charges brings particles together by anchoring its grafts to different particle surfaces. However, in a linear random copolymer, individual cationic charges are randomly distributed along the chain. The local cationic charge density may not be high enough to provide firm attraction at the adsorption sites. Meanwhile, charges situated on the bridging segments are simply wasted.

The observations in this work agree with a previous investigation using polydiallyldimethyl ammonium chloride (PDADMAC) grafted onto polyacrylamide (PAM) via a γ-ray irradiation method. However, the use of the mono-dispersed PDMAEMA quat macromonomer in preparing the NVF copolymer presented in this work ensures a comb-branched copolymer structure in the absence of gel formation. The comb-branched copolymer structure has been shown to improve flocculation performance than the random copolymer as proposed in Chapter 1.

4.4 Conclusions

Graft copolymers samples were synthesized by copolymerizing N-vinylformamide (NVF) and polydimethylaminoethyl methacrylate quats (nearly mono-dispersed molecular weight cationic macromonomer) in an aqueous solution. The polymerization kinetics and copolymer compositions were investigated at various experimental conditions. The copolymerization reactivity ratio (r_1) of the comonomer pair (NVF(M_1)-macromonomer(M_2)) was determined to be 3.82 and 6.39 for the two macromonomers with 50 and 100 repeating units. The flocculation performance of the graft copolymer was also tested on a TiO_2 aqueous dispersion model system. The graft copolymers were found to be more effective than their random linear counterparts. The comb-branched structure of the graft copolymer effectively combines the chain bridging and charge neutralization mechanisms - stronger attachment to the particle surfaces due to concentrated cationic clusters on side chains and charge-free backbones bridging different particles together.

4.5 References

Auhorn, W. Linhart, F. Lorencak, P. Kroener, M. Sendhoff, N. Denzinger, W. and Hartmann, H. (1992). US. Patent No. 5145559, BASF.

Bolto, B. (1995). "Soluble Polymers in Water Purification". *Prog. Polym. Sci.*, *20*, 987.

Burkert, H. Brunnmueller, F. Beyer, K. Kroener, M and Mueller, H. (1984). US Patent No. 4444667, BASF.

Gu, L. Zhu, S. Hrymak, A. N. and Pelton, R. H. (2001). "Kinetics and Modeling of Free Radical Polymerization of N-vinylformamide". *Polymer*, *42*, 3077.

Ma, M. (1996). "Grafting Cationic Polyelectrolytes onto Polyacrylamide for flocculation and sludge dewatering applications", Thesis (Master), McMaster University, Hamilton, Ontario, Canada.

Masuda, E. Kishiro, S. Kitarama, T. and Hatada, K. (1991). "Radical Polymerization of Highly Isotactic and Syndiotactic Poly(Methyl Methacrylate) Macromonomers". *Polym. J.*, *23*, 847.

McCormick, C. Bock, J. and Schulz, D. (1988) "Water-soluble Polymers", in H. Mark and J Kroschwitz ed. *Encyclopedia of Polymer Science and Engineering*, vol 17. Wiley, New York, p 730.

McDonald, C. and Beaver, R. (1979). "The Mannich Reaction of Poly(acrylamide)". *Macromolecules*, *12*, 203.

Meijs, G. F. and Rizzardo, E. (1990). "Reactivity of Macromonomers in Free Radical Polymerization". *J. Macromol. Sci., Rev. Macromol. Chem. Phys., C30*, 305.

Monech, D. Hartmann, H. Freudenberg, E. and Stange, A. (1993). US. Patent No. 5262008, BASF.

Nabeshima, Y. and Tsuruta, T. (1989). "Reactivity of a Polyamine Macromonomer in Radical copolymerizaiton with 2-hydroxyethyl methacrylate", *Makromol. Chimie*, *190*, 1635

Pelton, R. H. (1984). "Model Cationic Flocculants From the Mannich Reaction of Polyacrylamide". *J. Polym. Sci. Polym. Chem. Ed.*, *22*, 3955.

Pfohl, S. Kroener, M. Hartmann, H. and Denzinger, W. (1988). US. Patent No. 4774285, BASF.

Pfohl, S. Kroener, M. Hartmann, H. and Denzinger, W. (1989). US. Patent No. 4880497, BASF.

Pfohl, S. Kroener, M. Hartmann, H. and Denzinger, W. (1990). US. Patent No. 4978427, BASF.

Pinschmidt, R. Jr., Renz, W. Carroll, E. Yacoub, K. Drescher, J. Nordquist A. and Chen, N. (1997). "N-Vinylformamide – Building Block for Novel Polymer Structures". *J. Macromol. Sci.*, *A34*, 1885.

Rose, G. and John, M. R.St. (1988). "Flocculation", in H. Mark and J. Kroschwitz ed. *Encyclopedia of Polymer Science and Engineering*, vol 7. Wiley, New York, p 212.

Shen, Y. Zeng, F, Zhu, S and Pelton, R. H. (2001) "Novel Cationic Macromonomers by Living Anionic Polymerization of Dimethylaminoethyl Methacrylate". *Macromolecules*, *34*, 144.

Subramanian, R. Zhu, S. and Pelton, R. H. (1999). "Synthesis and Flocculation Performance of Graft and Random Copolymer Microgels of Acrylamide and Diallyldimethylammonium Chloride". *Colloid. Polym. Sci.*, *277*, 939.

Tsukahara, Y. Tsutsumi, K. Yamashita, Y. and Shimada, S. (1990). "Radical Polymerization Behavior of Macromonomers .2. Comparison of Styrene Macromonomers Having a Methacryloyl End Group and a Vinylbenzyl End Group". *Macromolecules*, *23*, 5201.

Xiao, H. Pelton, R. H. and Hamielec, A. (1996). "Preparation and Kinetic Characterization of Copolymers of Acrylamide and Poly(Ethylene Glycol) (Meth)Acrylate Macromonomers". *Polymer*, *37*, 1201.

Chapter 5. Synthesis of Comb Grafted Polyelectrolytes in Melts

5.1 Introduction

In Chapter 4, a macromonomer approach (grafting-through) was used to synthesize a comb-grafted polymeric flocculant. The key parameters used to describe a comb-grafted copolymer are backbone chain length (or molecular weight) and distribution, side chain length (or molecular weight) and distribution, and branching density (the distribution of grafting point along the backbone). The macromonomer (see Chapter 4) was synthesized by anionic polymerization, which provided good control over the molecular weight and gave a narrow molecular weight distribution. When such a macromonomer copolymerizes with another vinyl monomer, each incorporated macromonomer chain forms a graft (side chain) and introduces a grafting point to the backbone chain. The result is a comb-grafted copolymer with side chains having controllable molecular weight. However, the macromonomer method also has its drawbacks. There are a very limited number of techniques (e.g. anionic polymerization, ATRP (Zeng et al, 2000)) that can be chosen for the synthesis of a macromonomer with terminal double bond and good copolymerization reactivity. The processes are usually complicated and involve a variety of chemicals and large amount of solvent.

The alternative approach to the macromonomer (grafting-through) scheme to synthesize graft copolymer is the grafting-onto scheme. Two readily available pre-polymers are chosen as the initial reactants. As an example system, polydiallyldimethyl ammonium chloride (polyDADMAC) was grafted onto high molecular weight polyacrylamide (PAM) by γ-ray initiation. The cationic grafted copolymers exhibited improved flocculation and sludge dewatering performance over PAM or polyDADMAC homopolymers, their dual polymer blends,

as well as linear random copolymers of PAM and DADMAC (Ma and Zhu, 1999a). However, grafting by γ-radiation requires a very low polymer concentration (about 1%wt) in an aqueous solution (Ma and Zhu, 1999b). In addition, the generation of free radicals by γ-irradiation is less selective and less controllable compared with chemical initiation.

The polymer grafting reaction can also be carried out by reactive processing directly in polymer melts rather than in a large amount of solvent. Due to the concerns on the environmental impact of organic solvents, more and more reactions involving polymers are being carried out in solventless system(Lambla, 1993). Reactive extrusion (REX) is one of the most popular methods for reactive processing. It refers to the use of chemical reactions during extrusion processing of polymers. The extruder, which is another form of a chemical reactor (Brown and Orlando, 1990), provides an intensive degree of mixing, good temperature control and a controlled residence time distribution (RTD). Research and applications of REX have been very active in recent years. Bulk polymerization, graft reactions (Brown and Orlando, 1990), functionalization of polyolefins (Lambla and Seadan, 1993; Liu et al, 1992; Moffett and Deckers, 1992) and controlled molecular weight degradation (Triacca et al, 1993) have all been realized with reactive processing using chemical initiators.

In this chapter, two commercially available polymers, PAM and polyDADMAC were used to synthesize comb-grafted copolymers in polymer melts using free radical initiators.

5.2 Experimental

Materials: Two PAM samples were used in this work. One sample (PAM1, Aldrich), in granular form, had a nominal weight-average molecular weight of 5×10^6. The other sample (PAM2, Aldrich), dried from a 40wt% water solution, had a nominal molecular weight of 10^4. PolyDADMAC (Nalco Canada Ltd.), dried from a solution under vacuum at room temperature, had a weight-average molecular weight of 2.3×10^5. Lupersol 130 (Aldrich) and Lupersol 101

(Aldrich) were selected as peroxide initiators. Glycerol ($C_3H_8O_3$, 99.6%, Fisher Scientific) was selected as a plasticizer. All commercial materials were used without further purification.

Sample preparation for grafting: PAM and polyDADMAC polymer powders were dry blended. The polymer blend was purged with a calculated amount of initiator acetone solution. Blending continued until acetone was completely evaporated at room temperature. A pre-weighted amount of glycerol was added and blended thoroughly. The sample was allowed to swell for 24 hours at room temperature. Immediately before the reaction, the sample was put in an oven at 80 °C for 2 hours to reach ultimate swelling balance. The sample size was about 2.5 grams of swelled polymer (20~80wt%) in glycerol for each reaction run.

Devices: All grafting tests were carried out in an Atlas LMM (Laboratory Mixing Molder), or mini-mixer (Atlas, Cedar Knolls NJ). The mixer has a cylindrical mixing chamber with a sample capacity of 3~4 grams. A piston that moves vertically and rotates in the mixing chamber provides mixing. A #75 Cannon Ubbelohde semi-micro dilution viscometer was used for viscosity measurement.

Graft copolymer separation: After the reaction, all the samples were dissolved in water to form a ~30% wt solution. If no gel was found in the sample, the solution was dropped into methanol with vigorous agitation. The ungrafted polyDADMAC in solution dissolved while PAM and graft copolymer precipitated. The precipitates were collected and dried under vacuum at room temperature. If gels were found in the sample, the gel portion was collected by centrifugation and then washed with a large amount of water. The remaining gel contained only crosslinked PAM and grafted polyDADMAC.

Degree of grafting and grafting efficiency: The degree of grafting and grafting efficiency of graft copolymer were defined and experimentally determined to describe the grafting reaction.

$$\text{degree of grafting} = DG = \frac{\text{polyDADMAC}_{\text{grafted}}(wt)}{\text{PAM}_0(wt)} \qquad 5.1$$

$$\text{grafting efficiency} = GE = \frac{\text{polyDADMAC}_{\text{grafted}}(wt)}{\text{polyDADMAC}_0(wt)} \qquad 5.2$$

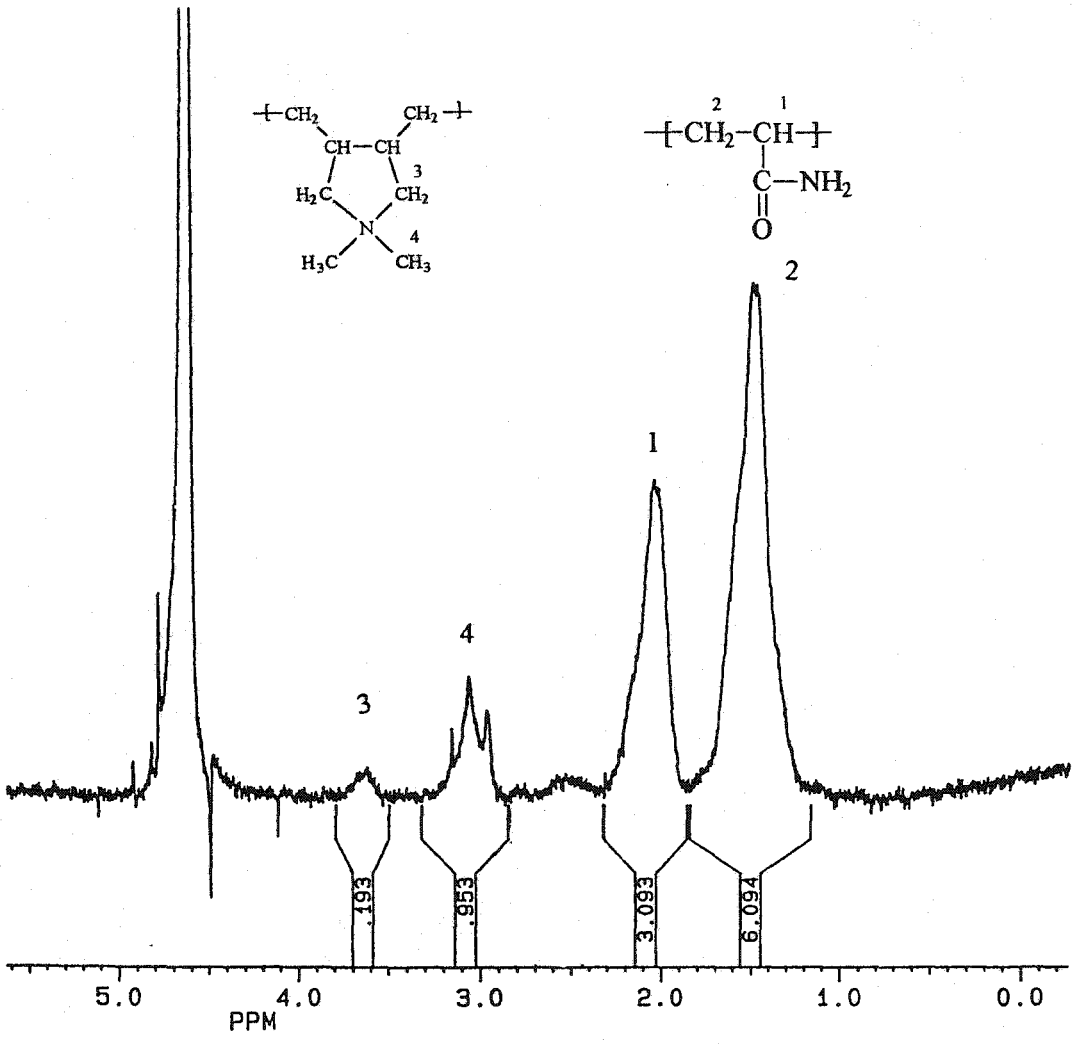

Figure 5.1 H-NMR spectrum of polyDADMAC-*graft*-PAM copolymer

The molar composition of PolyDADMAC and PAM in copolymer samples was determined by H-NMR (200MHz, D_2O solvent) and then converted to weight fractions using Equations 5.1 and 5.2 (see the sample H-NMR spectrum in Figure 5.1). $PolyDADMAC_{grafted}$ is the amount of polyDADMAC that is grafted onto PAM; $polyDADMAC_0$ and PAM_0 are the initial feed amount of polyDADMAC and PAM, respectively.

5.3 Results and discussions

The first step of the grafting-onto scheme was to find a chemical initiator that was suitable for the grafting reaction of polyDADMAC and PAM. The key factors in free radical grafting are the generation and termination of free radicals. Chain radicals of both PAM and polyDADMAC should be generated first. Then a grafted copolymer is produced by the recombination termination of PAM and polyDADMAC chain radicals. The termination between PAM-PAM and polyDADMAC-polyDADMAC chain radicals does not contribute to grafting. The half-life time data at different temperatures of the two organic peroxide initiators, Lupersol 101 and 130, calculated from ATOFINA (2001) catalog are listed in Table 2.1. Experiments were first conducted to generate PAM and polyDADMAC chain radicals separately.

5.3.1 Generation of PAM chain radicals

The generation of PAM chain radicals is a first essential step in the process. A radical is an active site on PAM that facilitates a further grafting reaction.

The reaction was carried out at 140 and 160 °C under ultra high purity (UHP) nitrogen (N_2) protection. Three different initiator levels were employed: 0.5, 1 and 2wt%. Gels were found in every sample but differed in quantity. Parallel tests with PAM1 without initiator showed no gelation under the same temperature and other reaction conditions.

Careful methods of sample preparation are necessary to quantify the gel fraction,. Formic acid (HCOOH, chemical reagent grade, Aldrich) was used as a solvent for PAM and

Table 5.1 Half life time data of initiators, min (ATOFINA, 2001)

Temperatures ,^{0}C	Lupersol 101	Lupersol 130
140	60	211
160	7.4	25
180	1.1	3.5

Table 5.2 Gel fraction (wt%, initial PAM) after reaction, 0.5%wt initiator

Conditions	Lupersol 101	Lupersol 130
160 ^{0}C, 10 min	38.3	67.2
140 ^{0}C, 60 min	33.6	66.2

initiators. The samples were dried under vacuum at room temperature. Reacted samples were put in water to wash out linear PAM. The remaining gel content was dried under vacuum at room temperature for 48 hours and weighted. The gel measurement results are listed in Table 5.2 for an initiator dosage at 0.5%wt of PAM polymer weight.

Gel formation suggests the generation and termination of PAM chain radicals. Gel fraction is proportional to the concentration of PAM chain radicals. The results show that L130 is more effective in generating PAM chain radicals.

It was reported that the hydrogen atom bound to the tertiary carbon atom could be easily abstracted compared with those bound to the primary and secondary carbon atoms (Pryor, 1966). A recent ESR study by Subramanian et al (2000) confirmed that in PAM-peroxide systems, the primary radicals from the decomposition of peroxide initiators abstracted the tertiary hydrogen on backbone of PAM and formed PAM chain radicals. These highly active chain radicals can immediately combine with each other to form crosslinkages between PAM chains.

5.3.2 Generation of polyDADMAC chain radicals

A similar procedure was followed to carry out the reaction of polyDADMAC. PolyDADMAC samples were tested at 140 and 160 °C with Lupersol 101 and 140, 160 and 180 °C with Lupersol 130. No gel was found under any or a combination of the reaction conditions. The lack of gel may be due to any of the following reasons: (1) the chain structure is stable to radical attacks, (2) chain scission is more predominant over crosslinking, (3) there is chain coupling, resulting in an increase in molecular weight, but not enough to crosslink and form gel.

Previous research by Ma (1996) showed the measurement of solution viscosity of dilute polyDADMAC water solution can be used to examine the change of molecular weight. It was found that the intrinsic viscosity decreased slightly after 5 hours of γ-irradiation at a dose of 100 krad/hour. This suggests a chain scission mechanism of polyDADMAC under the attack of a high

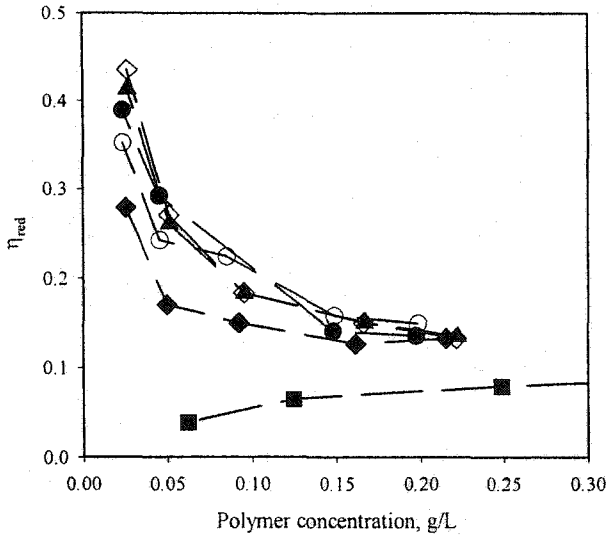

Figure 5.2 η_{red} (L/g) of polyDADMAC samples after reactions with Lupersol 101 and 130, ▲ pure PolyDADMAC, ○ with Lupersol 101, 140 °C, ◊ with Lupersol 101, 160 °C, ● with Lupersol 130, 140 °C, ◆ with Lupersol 130, 160 °C, ■ with Lupersol 130, 180 °C.

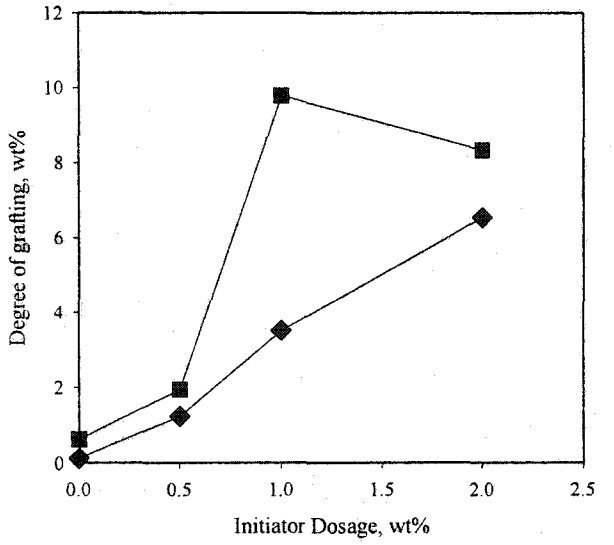

Figure 5.3 Degree of Grafting of polyDADMAC at different initiator concentrations. ■ 180 °C, ◆ 160 °C.

energy moiety. The viscosities of polyDADMAC samples after reacting with Lupersol 101 and 130 were measured to verify the chain scission mechanism in the free radical process.

The viscosities of dilute polyDADMAC solutions were measured at 25±0.1°C. Ion impurities can affect the configurations of polyelectrolyte chains in a dilute solution and influence the viscosity measurement. A 0.1M NaCl water solution was therefore used to suppress the effects of ionic impurities. PolyDADMAC samples were dissolved in the NaCl solution at about 0.2~0.3 mg/mL solution initially.

The measurement procedure in a previous study was followed (Ma, 1996). The specific viscosity η_{sp} is determined by the flow time (t) of a solution at various polymer concentrations and t_0, the solvent flow time, by Equation 5.3

$$\eta_{sp} = \frac{t}{t_0} - 1 \qquad 5.3$$

The reduced viscosity is defined as the ratio of specific viscosity and polymer concentration, C, g/L

$$\eta_{red} = \frac{\eta_{sp}}{C} \qquad 5.4$$

The results are presented in Figure 5.2. At a reaction temperature of 180 °C for 10 minutes, the sample showed a significant viscosity decrease compared with pure polyDADMAC, suggesting that the initiator induced a radical chain scission mechanism rather than crosslinking. At this reaction condition, Lupersol 130 was able to generate polyDADMAC chain radicals. Lupersol 101 was obviously unable to react with polyDADMAC at all the tested conditions. In addition, Lupersol 101 decomposes before the reaction if the temperature exceeds 160 °C (See Table 5.1).

Consider the results of both PAM and polyDADMAC tests, only Lupersol 130 was found to have the potential to generate radicals on both PAM and polyDADMAC chains. It was therefore selected for further study. The results provide an operating window from 160 °C to 180 °C. If the temperature exceeds 180 °C, then L130 decomposes before grafting. Also, both

polymers are chemically unstable at higher temperature. Below 160 °C, the initiator is not able to generate polyDADMAC chain radicals.

5.3.3 Grafting of polyDADMAC onto low-molecular-weight PAM

The reason for using low-molecular-weight PAM (PAM2) first is to minimize the diffusion effect by high molecular weight on grafting reaction so that the chemical feasibility of the grafting can be proven.

The grafting reaction was conducted in a mini-mixer using Lupersol 130 as the initiator. The total polymer content in the sample was about 80wt%. The initiator concentration was calculated based on the total weight of dry polymers. After the reaction, no gel was found in any of the samples. The graft copolymer was separated and analyzed according to the previously described procedure.

Figure 5.3 shows the degree of grafting of polyDADMAC plotted against the initiator concentration at 160 and 180°C with a reaction time of 10 minutes. The initial feed ratio of polyDADMAC/PAM was 1:1 (the degree of grafting is equal to the grafting efficiency of polyDADMAC when the ratio is 1:1). The degree of grafting increased with increasing initial concentration of initiator. If the initial ratio of polyDADMAC is increased, more grafting is expected. The degree of grafting and grafting efficiency as a function of initial polymer feeding ratio are plotted in Figures 5.4a and 5.4b. It was found that the degree of grafting could be as high as 30% with a 4:1 polyDADMAC/PAM ratio. However, the grafting efficiency was not remarkably affected by changing the PAM/polyDADMAC feed ratio, and remained less than 10%.

5.3.4 Grafting of polyDADMAC onto high-molecular-weight PAM

After the grafting of polyDADMAC onto low-molecular-weight PAM (PAM2) was confirmed, grafting tests with high-molecular-weight (M_w=5×10^6) PAM (PAM1) were conducted.

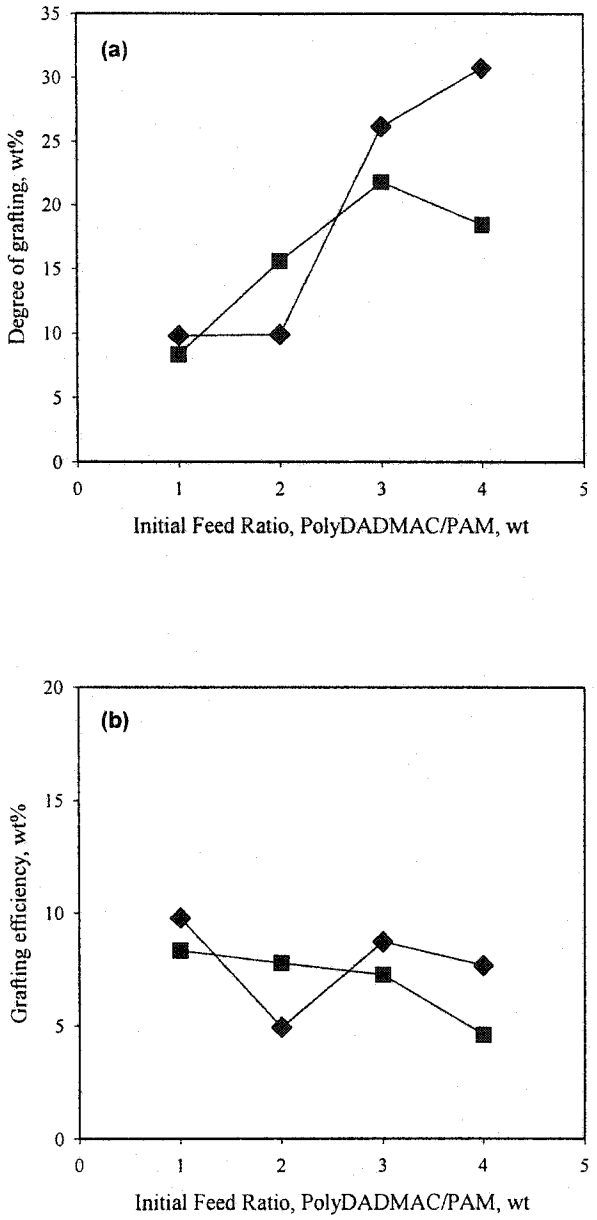

Figure 5.4 (a) Degree of grafting of polyDADMAC onto PAM at different feeding ratios after reaction at 180 °C for 10 min. ◆ 1.0 wt%, ■ 2.0 wt% initiator. (b) Grafting efficiency of polyDADMAC onto PAM at different feeding ratios after reaction at 180 °C for 10 min. ◆ 1.0 wt%, ■ 2.0 wt% initiator.

Due to the very high molecular weight of PAM1, a large amount of glycerol was used to facilitate the polymer chain mobility during the reaction. A Soft gel was found in every sample after reaction.

The results are listed in Table 5.3. During the reaction period, there are two types of chain radical recombination reactions. One is the recombination termination between PAM chain radicals, which eventually leads to gelation. The other is between PAM and polyDADMAC chain radical, which contributes to grafting. PolyDADMAC can only undergo chain scission under current conditions. When the reaction begins, these termination reactions proceed in parallel. If polyDADMAC is found grafted in gel, it must be grafted in sol as well.

After the reaction, the samples were put in water. A large portion of the sample was gel. The gels were collected and then washed with a large amount of deionized water. Glycerol, sol PAM, polyDADMAC, and their sol copolymers were removed by washing. The remaining material was a network of PAM with polyDADMAC attached to it.

As shown in Table 5.3, a maximum of 10wt% polyDADMAC was found in gel. A further increase of the initial polyDADMAC/PAM ratio beyond 2:1 prevented the mixing of the two polymers because of phase separation. The grafting of high-molecular-weight PAM is important for flocculation applications. However, a severe gelation problem always accompanies the reaction. The PAM chain radicals often favor termination with PAM radicals rather than polyDADMAC chain radicals. This in turn reduces the chance of grafting causing low yield and degree of grafting. In addition, the polymer gel is not useful for the purpose of flocculation in comparison with the grafted material in the sol. Future efforts should focus on reducing the gelation during the reactive processing.

Table 5.3 Grafting test of high molecular weight PAM (2wt% L130)

PAM / PolyDADMAC / Glycerol weight ratio	PolyDADMAC content in gel wt%
1:1:8	10.58
1:0.5:6	3.92
1:2:9	4.95

5.4 Conclusion

In this chapter, a cationic polymer polyDADMAC was grafted onto PAM by a peroxide initiator via free radical mechanism. PAM radicals were found to be in favor of crosslinking while polyDADMAC radicals experienced chain scission. The grafting reactions were performed in a mini mixer in the state of polymer melts. PolyDADMAC was grafted onto both low-molecular-weight (10^4) and high-molecular-weight (5×10^6) PAM samples. With low-molecular-weight PAM, the degree of grafting reached as high as 30wt%. However, the grafting efficiency was always less than 10wt%. With high-molecular-weight PAM, grafting was also confirmed but gelation problems occurred.

5.5 References

ATOFINA Chemicals Inc. (2001). "*Product Bulletin, Organic Peroxides, Dialkyl Peroxides*", Lupersol 101 and Lupersol 130 are now traded under the names of Luperox 101 and Luperox 130.

Brown, S. and Orlando, C. (1990). "*Reactive Extrusion*", in H. Mark et al, ed., *Encyclopedia of Polymer Science and Engineering*, vol. 14, John Wiley & Sons, New York, 2nd ed., 169.

Lambla, M. and Seadan, M. (1993). "Reactive Blending of Polymers by Interfacial Free-Radical Polymerization". *Macromol. Symp.*, *69*, 99.

Lambla, M. (1993). *Comprehensive Polymer Science* (first supplement), G. Allen and J.C. Bevingtoon eds., Pergamon Press, New York, p. 619.

Liu, N. Xie, H. and Baker, W. (1993). "Comparison of the Effectiveness of Different Basic Functional Groups for the Reactive Compatibilization of Polymer Blends". *Polymer*, *34*, 4680.

Ma, M. and Zhu, S. (1999a). "Grafting Polyelectrolyte onto Polyacrylamide for Flocculation 1. Polymer Synthesis and Characterization". *Colloid and Polym. Sci.*, *277(2-3)*, 115.

Ma, M. and Zhu, S. (1999b). "Grafting Polyelectrolyte onto Polyacrylamide for Flocculation 2. Model Suspension Flocculation and Sludge Dewatering". *Colloid and Polym. Sci.*, *277(2-3)*, 123.

Ma, M. (1996). "Grafting Cationic Polyelectrolytes onto Polyacrylamide for flocculation and sludge dewatering applications", Thesis (Master), McMaster University, Hamilton, Ontario, Canada.

Moffett, A. and Dekkers, M. (1992). "Compatibilized and Dynamically Vulcanized Thermoplastic Elastomer Blends of Poly(Butylene Terephthalate) and Ethylene Propylene Diene Rubber". *Polym. Eng. Sci.*, *32*, 1.

Pryor, A. W. (1966). *Free radicals*, McGraw-Hill: New York, 1966.

Subramanian, R., Huang, Y. Zhu, S. Hrymak, A. N. and Pelton, R. H. (2000). "Electron Spin Resonance Study and Reactive Extrusion of Polyacrylamide and Polydiallyldimethyl ammonium Chloride". *J. of App. Polym. Sci.*, *77*, 1154.

Triacca, V. Gloor, P. Zhu, S. Hrymak, A. N. and Hamielec, A. E. (1993). "Free Radical Degradation of Polypropylene: Random Chain Scission". *Polym. Eng. Sci*, *33*, 445.

Zeng, F., Shen, Y. Zhu, S. and Pelton, R. H. (2000). "Synthesis and Characterization of Comb-Branched Polyelectrolytes. 1. Preparation of Cationic Macromonomer of 2-(Dimethylamino)ethyl Methacrylate by Atom Transfer Radical Polymerization". *Macromolecules*, *33*, 1628.

Chapter 6. Modeling Molecular Weight Distribution of Comb Branched Graft Copolymers

6.1 Introduction

The previous chapters reported the experimental investigations on synthesizing graft (or comb branched) copolymers by various approaches. Branch inclusion by grafting has a significant impact on various polymer properties and thus offers many special advantages in a wide range of applications (Battaerd and Tregear, 1967; Dreyfuss and Quirk, 1988; Grest et al, 1996; Kawakami, 1988; Molau, 1971; Rempp and Franta, 1984; Small, 1975). For example, in Chapter 4, graft copolymers showed much improvement in its flocculation capability than random linear copolymers.

There are different types of branched polymers according to their molecular geometry. A dendritic polymer has branches on branches. A star polymer contains a center moiety and linear arms all chemically bonded to the center at one end. A comb branched polymer consists of one backbone chain and many side chains attached to the backbone. If the backbone chain length has only one unit, then a comb branched polymer becomes a star polymer. Synthesis and characterization of branched polymers with well-defined chain structures are of fundamental importance and practical interest. Recently (Dreyfuss and Quirk, 1988; Grest et al, 1996; Kawakami, 1988; Rempp and Franta, 1984), star and comb branched polymers received much attention.

There are various methodologies to synthesize polymers with a comb structure (Battaerd and Tregear, 1967; Dreyfuss and Quirk, 1988; Kawakami, 1988; Rempp and Franta, 1984). **Grafting-from** is the selective generation of initiation sites and growth of side chains on the pre-

formed polymer backbone. **Grafting-onto** (example, Chapter 5) is the addition of pre-formed polymers as side chains onto a polymer backbone. Another technique called **grafting-through** (example, Chapter 4) is copolymerization of pre-formed macromonomers with vinyl monomers to form comb-type graft polymers. In all these methods, the pre-formed polymers or macromonomers can be separately characterized, which facilitated structure determination for the resulting polymers.

The determination molecular parameters for a graft copolymer include the molecular weight of backbone and that of side chains, branching density, i.e. the frequency of monomeric units on backbone that have side chains attached to them. It is desirable to give a precise description of the molecular weight distribution for various types of branched polymers (random, comb, star). Numerous models have been developed in the literature over the past fifty years (Amemiya, 1967; Baltsas et al, 1996; Flory, 1941; Hamielec et al, 1987; Jackson, 1973; Saito, 1972; Soares and Hamielec, 1996; Stockmayer, 1943; Taylor and Reichert, 1985; Tobita and Hamielec, 1988; Zhu and Hamielec, 1994; Zhu et al, 1996). However, most of the previous work focused on calculating average molecular weights. A few articles dealt with analytical distribution functions, but were limited to random structure. Beasley (1953) gave an expression for branched polymers formed by chain transfer to polymer in free radical polymerization carried out in a continuous stirred tank reactor. Bamford and Tompa (1954) dealt with the same polymerization system in a batch reactor at low monomer conversion. Peebles (1971) summarized the early works in this field. Recently, Tobita (1996, 1997) proposed the random sampling technique (Monte Carlo simulation) and obtained an analytical equation for homogeneously branched polymers with randomly distributed primary chains. Previous models dealt mostly with the polymerization systems having branches generated by chain transfer to polymer and/or propagation with pendant or terminal double bonds that yielded random dendritic structures.

In this chapter, a model describing the bivariate distribution of molecular weight and branching density for the comb-branched copolymers is developed. The model is derived based on random connection of two different types of polymer chains with one type as the backbones

and the other as side chains. The model is applicable no matter whether the comb copolymers are made by grafting-from, grafting-onto, or grafting-through methods.

6.2 Polymerization mechanisms

Most polymerizations can be utilized to prepare the comb-branched polymers: condensation, free radical, ionic, and metallocene (Dreyfuss and Quirk, 1988). The grafting-onto scheme is described by the following equations:

$$B_r + S_s \xrightarrow{rK_c} C_{r,s,1} \qquad 6.1$$

$$C_{r,s,1} + S_t \xrightarrow{rK_c} C_{r,s+t,2} \qquad 6.2$$

$$C_{r,s,b} + S_t \xrightarrow{rK_c} C_{r,s+t,b+1} \qquad 6.3$$

where B_r represents the pre-formed backbone chains having r monomeric units, S_t is the pre-formed side chains having t monomeric units, $C_{r,s,b}$ is the comb-branched copolymers having r monomeric unit on backbone and a total of s monomeric units on b side chains. It should be pointed out that the symbols for molecular species such as B_r , S_t , and $C_{r,s,b}$ are also used to denote the molar concentrations of the corresponding species without the traditionally used bracket [ ]. In grafting-onto mechanism, every monomeric unit on the backbone polymer chains can facilitate the chemical reaction to become a branch point, but there is only one functionalized unit on each side chain that is able to react with any backbone units. Every unit on the backbone is assumed to have an equal opportunity to react with the side chain. The reactivities of functional groups on both pre-polymers are assumed to be independent of their chain lengths. The reaction rate constant is, therefore, rK_c. Because the number of monomeric units on the backbone r is much larger than the number of side chains b, the rate constant remains unchanged regardless of the number of side chains the comb copolymer has already had. The formation of comb polymers undergoes a random process. The branches are randomly picked up from pre-formed side chains and, thus,

Table 6.1 Elementary reactions and their rate constants in chain polymerization with comb branching — grafting-from mechanism

Slow initiation/fast propagation	
Initiation/activation	$A^* + B_r \xrightarrow{rK_i} C^*_{r,0,1}$
	$A^* + C_{r,s,b} \xrightarrow{rK_i} C^*_{r,s,b+1}$
	$T^* + M \xrightarrow{K_{i,T}} P_1^*$
Propagation	$C^*_{r,s,b} + M \xrightarrow{K_p} C^*_{r,s+1,b}$
	$P_r^* + M \xrightarrow{K_p} P^*_{r+1}$
Transfer	$C^*_{r,s,b} + T \xrightarrow{K_w} C_{r,s,b} + T^*$
	$P_r^* + T \xrightarrow{K_w} P_r + T^*$
Termination	$C^*_{r,s,b} \xrightarrow{\tau} C_{r,s,b}$
	$P_r^* \xrightarrow{\tau} P_r$
Fast initiation/slow propagation	
Activation/initiation	$bA^* + B_r \xrightarrow{K_i} C^{b*}_{r,0,b}$
	$T^* + M \xrightarrow{K_{i,T}} P_1^*$
Propagation	$C^{j*}_{r,s,b} + M \xrightarrow{jK_p} C^*_{r,s+1,b}$
	$P_r^* + M \xrightarrow{K_p} P^*_{r+1}$
Transfer	$C^{j*}_{r,s,b} + T \xrightarrow{jK_w} C^{(j-1)*}_{r,s,b} + T^*$
	$P_r^* + T \xrightarrow{K_w} P_r + T^*$
Termination	$C^{j*}_{r,s,b} \xrightarrow{j\tau} C^{(j-1)*}_{r,s,b}$
	$P_r^* \xrightarrow{\tau} P_r$

have the same molecular weight distribution as the unreacted side chains. Depending on the relative numbers of pre-formed backbone and side chains, the product is a mixture of comb copolymers with unreacted backbone and side chain pre-polymers.

The grafting-from scheme is more complicated. Table 6.1 summarizes the elementary reactions and their rate constants. It consists of initiation/activation, propagation, termination and chain transfer. In the case of slow initiation/fast propagation, once an active site is generated, it quickly goes through propagation and transfer/termination to form a side chain. The concentration of the active species in the system remains very low (for example, free radical grafting). There is little chance that one backbone has more than one active site on it simultaneously at any moment through out the grafting reaction. In the case of fast initiation/low propagation, the propagation, transfer/termination steps are rate-determining steps. The rate of generation for active species is higher than that of consumption, therefore accumulation of active sites occurs on the backbone chains (as $C^{\bullet}_{r,0,b}$ in the scheme). The active species A* can be chemical initiator/catalyst or energetic particles such as e-beam or γ-ray. The generation of an active center on the polymer backbone is a random process in most cases. Depending on the type of initiator, it can be fast or slow compared to the growth of side chains. Only termination by disproportionation is considered in this polymerization scheme. Excluded in the scheme is the termination by recombination that introduces crosslinkages and eventually leads to gel formation. In the presence of a chain transfer agent, T, the propagating centers can be transferred onto the transfer agent molecules before termination. The termination and transfer reactions determine the length of side chains. If the activated molecules, T*, reinitiate monomers, then linear polymer chains P_r are formed. The product is a mixture of comb grafted copolymer ($C_{r,s,b}$) with two types of linear homopolymers (P_r and unreacted B_r). This is often the case when the grafting-from method is employed. It is a great challenge in controlling the molecular weight of side chains in this scheme.

Table 6.2 Elementary reactions and their rate constants in chain polymerization with comb branching—grafting-through (macromonomer) mechanism

Initiation/activation	$A^* + M \xrightarrow{K_i} C^*_{1,0,0,1}$
	$T^* + M \xrightarrow{K_{i,T}} C^*_{1,0,0,1}$
Propagation	$C^*_{r,s,b,1} + M \xrightarrow{K_{p11}} C^*_{r+1,s,b,1}$
	$C^*_{r,s,b,1} + M^=_x \xrightarrow{K_{p12}} C^*_{r,s+x,b+1,2}$
	$C^*_{r,s,b,2} + M \xrightarrow{K_{p21}} C^*_{r+1,s,b,1}$
	$C^*_{r,s,b,2} + M^=_x \xrightarrow{K_{p22}} C^*_{r,s+x,b+1,2}$
Transfer	$C^*_{r,s,b,1} + T \xrightarrow{K_{tr,1}} C_{r,s,b} + T^*$
	$C^*_{r,s,b,2} + T \xrightarrow{K_{tr,2}} C_{r,s,b} + T^*$
Termination	$C^*_{r,s,b,1} \xrightarrow{\tau_1} C_{r,s,b}$
	$C^*_{r,s,b,2} \xrightarrow{\tau_2} C_{r,s,b}$

In Table 6.2, the elementary reactions involve in the formation of comb-branched copolymer through macromonomers (grafting-through) are given (Capek and Akashi, 1993; Meijs and Rizzardo, 1990; Zhu et al, 1998). In contrast to the grafting-from approach, the side chains are pre-formed, and therefore, well defined and characterized. This scheme is very similar to that of random copolymerization with subscripts 1 and 2 denoting small vinyl monomer and macromonomer. One side chain or branching point is introduced when one macromonomeris incorporated into copolymer by propagation. All the terminal double bonds are assumed to have the same copolymerization reactivity regardless of chain length. The propagating backbone chains are either terminated or transferred to form dead comb copolymers. Unlike grafting-from scheme, gelation is inherently avoided, no matter what the mode of termination is, be it disproportionation or combination. It is because there is no mechanism in this case that could yield a circuitous connection within the structure (Flory, 1953).

The comb copolymer formed in the above grafting-onto, grafting-from, and grafting-through processes can have various backbone and side-chain distributions. However, the most experimentally encountered distributions are uniform or Schulz-Zimm type, including Flory's most probable (i.e., random) functions. For example, in the grafting-from scheme, the side chain has a random distribution. In the grafting-through scheme, the backbone has a random distribution if the mode of termination is by disproportionation or transfer. The pre-formed polymers and macromonomers in all three schemes can have uniform distributions if prepared by living anionic polymerization or random distribution if by free radical mechanism. These distribution functions are, therefore, the focus in the following model derivation. It should be pointed out that deviations from the random distribution in free radical and other types of chain growth polymerization can occur due to the chain length drift during the course of batch polymerization, particularly under conditions when the chain termination becomes diffusion controlled.

Table 6.3 Molecular weight properties of various polymer species

Polymer species and symbols	Comb polymer, $C_{r,s} = \sum_{b=1}^{\infty} C_{r,s,b}$ $C_{r,0}$, free backbone chain	Backbone chain B_r	Side chain S_r
Total concentration	$C = \sum_{r=1}^{\infty}\sum_{s=1}^{\infty} C_{r,s}$	$B = \sum_{r=1}^{\infty} B_r = C + \sum_{r=1}^{\infty} C_{r,0}$	$S = \sum_{r=1}^{\infty} S_r$
Molecular weight distribution	$n_C(r,s) = C_{r,s}/B$	$n_B(r) = B_r / B$	$n_S(r) = S_r / S$
Number average molecular weight		$\bar{B}_N = \int_0^{\infty} n_B(r) r dr$	$\bar{S}_N = \int_0^{\infty} n_S(r) r dr$
Degree of grafting	$d.g. = \lambda \bar{S}_N$		

6.3 Model derivation

Consider the grafting-onto system with two types of pre-formed polymers presented in Equations 6.1~6.3. As described above, regardless of the polymerization mechanism, the formation of comb copolymers in a grafting process is a random combination of polymer chains from two different types. The molecular weight distribution of the graft copolymers $C_{r,s,b}$ is, therefore, a function of both backbone B_r and side chain S_s distributions with the branching density λ as a determining parameter. The branching density is defined as the molar ratio of branching points over monomeric units on backbone. The number average chain lengths of backbone and side chains are $\overline{B}_N$ and $\overline{S}_N$. In some cases, the linear primary chains denoted as P_r may also be generated during the reaction. Other molecular weight properties of various polymer species are defined and summarized in Table 6.3.

For a backbone chain with r units, the probability of having b branching points is

$$\binom{r}{b}\lambda^b(1-\lambda)^{r-b} \tag{6.4}$$

Because the number of branching points b is much smaller than the number of monomeric units r, the bimodal distribution can be more conveniently expressed as a Poisson distribution

$$\frac{(\lambda r)^b}{b!}\exp(-\lambda r) \tag{6.5}$$

The molar concentration of free backbone chains, without grafting of side chains, is

$$C_{r,0} = B_r(1-\lambda)^r = B_r\exp(-\lambda r) \tag{6.6}$$

The molar concentration of the comb polymers with r units on backbone and total s units on b side chains is

$$C_{r,s,b} = B_r\binom{r}{b}\lambda^b(1-\lambda)^{r-b}\xi_b(s)$$

$$= B_r\frac{(\lambda r)^b\exp(-\lambda r)}{b!}\xi_b(s) \qquad b \geq 1 \tag{6.7}$$

where $\xi_b(s)$ is a function giving the combination of b side chains

$$\xi_b(s) = \int_0^s n_S(s-u)\int_0^u n_S(u-v)\ldots\int_0^y n_S(y-z)n_S(z)dz\ldots dvdu \qquad (6.8)$$

with b-1 integrals, where $n_s(x)$ is the number fraction of side chains having x monomeric units (x = s, u, v, …, z). This combination function has the following properties

$$\int_0^\infty \xi_b(s)ds = 1 \qquad 6.9$$

$$\int_0^\infty s\xi_b(s)ds = b\bar{S}_N \qquad 6.10$$

$$\int_0^\infty s^2\xi_b(s)ds = b\bar{S}_N\left[(b-1)\bar{S}_N + \bar{S}_W\right] \qquad 6.11$$

These properties are independent of the side chain distribution $n_s(s)$; i.e., Equations 6.9~6.11 are valid with an arbitrary side-chain distribution.

Substituting a uniform side chain distribution,

$$n_S(s) = \delta(s-\bar{S}_N) \qquad 6.12$$

into Equation 6.8 yields

$$\xi_b(s) = \delta(s-b\bar{S}_N) \qquad 6.13$$

and thus,

$$C_{r,s,b} = B_r\frac{(\lambda r)^b\exp(-\lambda r)}{b!}\delta(s-b\bar{S}_N) \qquad 6.14$$

where $\delta(x-y) = 1$, if $x = y$; or else $\delta(x-y) = 0$.

If the side chain follows a Schulz-Zimm distribution,

$$n_S(s) = \frac{1}{(k-1)!}\frac{k}{\bar{S}_N}\left(\frac{ks}{\bar{S}_N}\right)^{k-1}\exp\left(-\frac{ks}{\bar{S}_N}\right) \qquad 6.15$$

where k indicates the polydispersity through $PDI_S = \bar{S}_W/\bar{S}_N = (k+1)/k$. Equation 6.15 becomes a random distribution when $k = 1$ and a uniform distribution when $k \to \infty$. Substituting Equation 6.15 into 6.8 results in

$$\xi_b(s) = \frac{1}{(kb-1)!}\frac{k}{\bar{S}_N}\left(\frac{ks}{\bar{S}_N}\right)^{kb-1}\exp\left(-\frac{ks}{\bar{S}_N}\right) \qquad 6.16$$

and subsequently, one can obtain

$$n_c(r,s,b) = \frac{C_{r,s,b}}{\int_0^\infty B_r dr} = n_B(r)\frac{(\lambda r)^b \exp(-\lambda r)}{b!(kb-1)!} \times \frac{k}{\bar{S}_N}\left(\frac{ks}{\bar{S}_N}\right)^{kb-1} \exp\left(-\frac{ks}{\bar{S}_N}\right) \qquad 6.17$$

where $n_c(r, s, b)$ and $n_B(r)$ are the number fractions of comb and backbone polymers (see their definitions in Table 6.3. The total concentration of comb polymers with r backbone units and s side chain units is the summation of Equation 6.17 in terms of b from 1 to ∞.

$$n_c(r,s) = n_B \exp(-\lambda r)\frac{k}{\bar{S}_N}\exp\left(-\frac{ks}{\bar{S}_N}\right) \times \sum_{b=1}^{\infty} \frac{(\lambda r)^b}{b!(kb-1)!}\left(\frac{ks}{\bar{S}_N}\right)^{kb-1} \qquad 6.18$$

6.4 Results and discussion

For simplicity, the following dimensionless parameters are introduced,

$$\gamma = \frac{r}{\bar{B}_N} \qquad \varsigma = \frac{s}{\bar{S}_N} \qquad \lambda_B = \lambda \bar{B}_N \qquad 6.19$$

where γ and ς are the reduced lengths of backbone and side chains. λ_B can be interpreted as the average number of branching points per backbone chain. The number-fraction molecular weight distributions of backbone chains, side chain and comb copolymers can thus be transformed to the following reduced forms accordingly.

$$n_B(\gamma) = n_B(r)dr/d\gamma = n_B(r)\bar{B}_N \qquad 6.20$$

$$n_S(\varsigma) = n_S(s)ds/d\varsigma = n_S(s)\bar{S}_N \qquad 6.21$$

and

$$n_C(\gamma,\varsigma) = n_C(r,s)(drds)/(d\gamma d\varsigma) = n_C(r,s)\bar{B}_N\bar{S}_N \qquad 6.22$$

Given the backbone chains as a Schulz-Zimm distribution,

$$n_B(\gamma) = \frac{\sigma}{(\sigma-1)!}(\sigma\gamma)^{\sigma-1}\exp(-\sigma\gamma) \qquad 6.23$$

Equation 6.18 becomes

$$n_C(\gamma,\varsigma)=\frac{k\sigma(\sigma\gamma)^{\sigma-1}}{(\sigma-1)!}\exp\left[-(\sigma+\lambda_B)\gamma-k\varsigma\right]\times\sum_{b=1}^{\infty}\frac{(\lambda_B\gamma)^b(k\varsigma)^{kb-1}}{b!(kb-1)!} \qquad 6.24$$

with the free backbone chains (with zero branching point)

$$n_C(\gamma,0)=\frac{\sigma(\sigma\gamma)^{\sigma-1}}{(\sigma-1)!}\exp\left[-(\sigma+\lambda_B)\gamma\right] \qquad 6.25$$

The number fraction of these free backbone chains is

$$\int_0^{\infty} n_C(\gamma,0)d\gamma=\left(\frac{\sigma}{\sigma+\lambda_B}\right)^{\sigma} \qquad 6.26$$

For a special case of $k = \sigma = 1$, i.e., both backbone and side chains have random distributions, Equation 6.24 has a simple form

$$n_C(\gamma,\varsigma)=\sqrt{\lambda_B\gamma/\varsigma}\times e^{-[(1+\lambda_B)\gamma+\varsigma]}\times I_1\left(2\sqrt{\lambda_B\gamma\varsigma}\right) \qquad 6.27$$

where $I_1\left(2\sqrt{\lambda_B\gamma\varsigma}\right)$ is the Bessel function of the first kind of imaginary argument of first order.

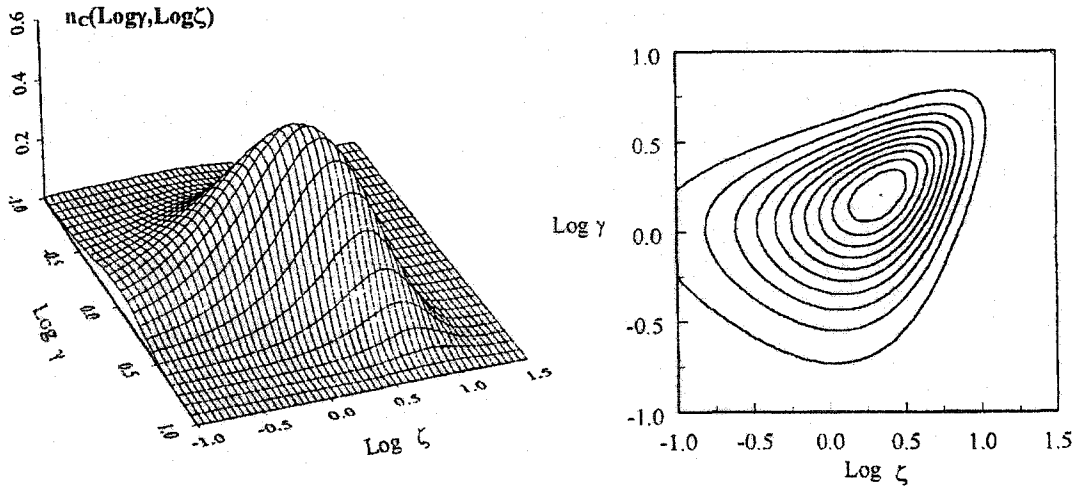

Figure 6.1 Surface and contour plots of the bivariate distribution of molecular weight and branching density of comb-grafted copolymers calculated using Equation 6.24. Both backbone and side chains assumed to be random distribution, i.e., $\sigma = k = 1$. The branching density $\lambda_B = 1$.

In general, the monomeric units of backbone and side chains have different molecular weights, $m_{w,1}$ and $m_{w,2}$. The weight fractional molecular weight distribution are then calculated by

$$w_C(r,s) = \frac{(m_{w,1}r + m_{w,2}s)n_C(r,s)}{(m_{w,1} + m_{w,2}\lambda\bar{S}_N)\bar{B}_N} \qquad 6.28$$

It can be seen in Equation 6.24 that the parameters determining the distribution function $n_C(\gamma,\varsigma)$ are λ_B, k, and σ. Figure 6.1 shows the three dimensional plot of the copolymer distribution with $k = \sigma = 1$ and $\lambda_B = 1$, and its corresponding contour plot. The distribution is normalized in terms of the log-scale axes, Log γ and Log ς (Log $\rightarrow \log_{10}$), according to

$$n_C(\mathrm{Log}_{10}\gamma, \mathrm{Log}_{10}\varsigma) = n_C(\gamma,\varsigma)(d\gamma d\varsigma)/(d\mathrm{Log}\gamma d\mathrm{Log}\varsigma) = (\ln 10)^2 \gamma\varsigma n_C(\gamma,\varsigma) \qquad 6.29$$

The distribution shown in Figure 6.1 has a smooth single-peak surface because both the backbone and side chains follow the relatively broad random distribution with a polydispersity index of 2. The molecular weights of backbone and side chains are not highly correlated in such a case. The composition of the polymer mixture includes copolymers with short backbone and long side chains and those with long backbone and short side chains.

The effect of side chain contribution on the copolymer distribution is demonstrated in Figure 6.2(A) and 6.2(B). The higher the k value in Equation 6.15, the narrower the side chain distribution. The parameter k = 10 and 100 was equivalent to the distribution polydispersity index of 1.1 and 1.01, which are close to uniform (mono-dispersed) distributions. The comb polymer distribution becomes narrower in Figure 6.2(A) comparing to Figure 6.1, exhibiting a multi-peak surface. The polymers with different branching points start to evolve. In Figure 2(A), the polymer population having one branch is clearly separated from those having two or more branches. The separation is enhanced with increasing k value. For k = 100, the copolymers has 1, 2, 3, 4 and 5 branches show distinct peaks from those having 6 or more branches, as shown in Figure 6.2(B). It can also be seen that the polymers having more side chain units are more likely to be associated with longer backbones. Figure 6.3(A) and 6.3(B) show the development of the

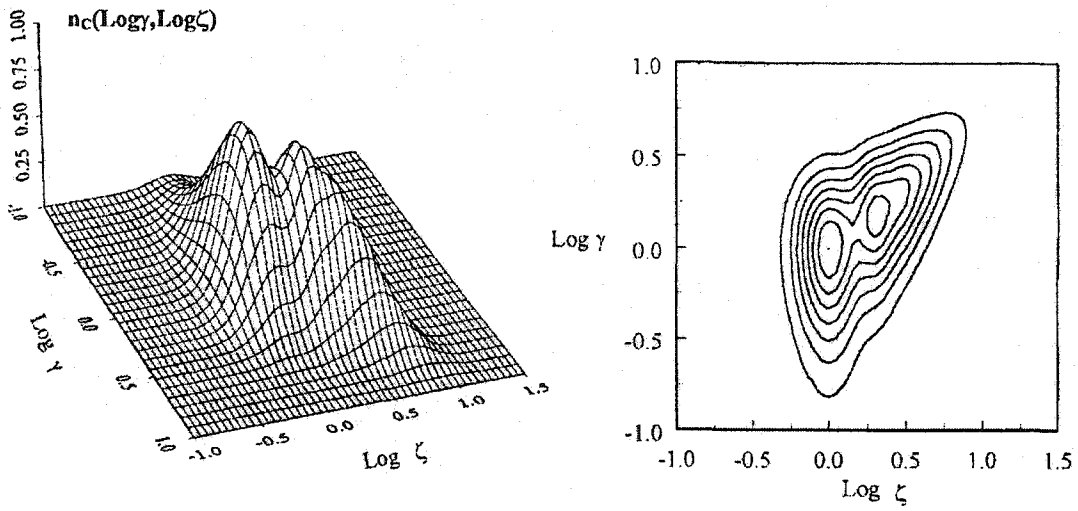

(A)

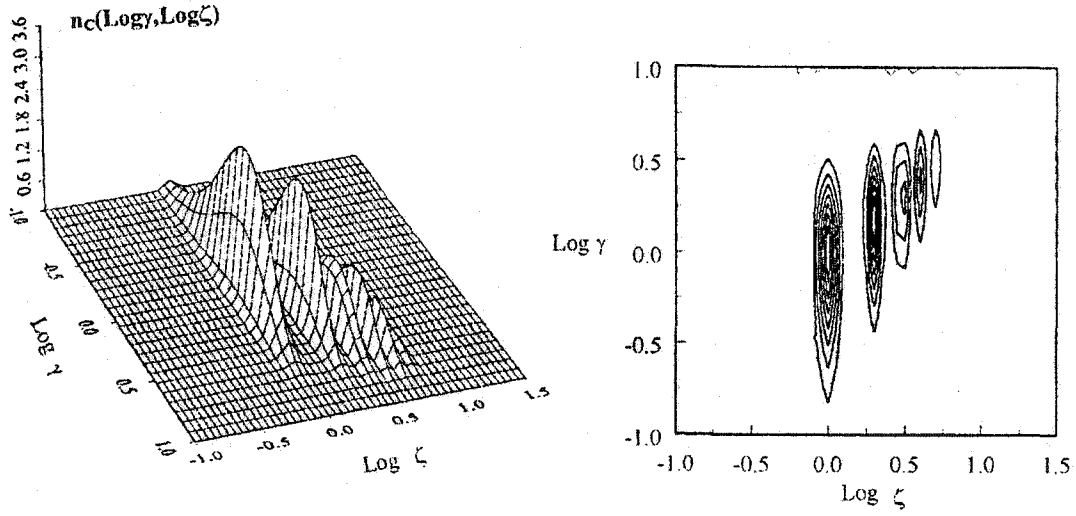

(B)

Figure 6.2 Development of the comb polymer distribution as a function of the branching density calculated using Equation 6.24: (A) k = 10 and (B) k = 100. The other parameters are $\sigma = 1$, and $\lambda_B = 1$.

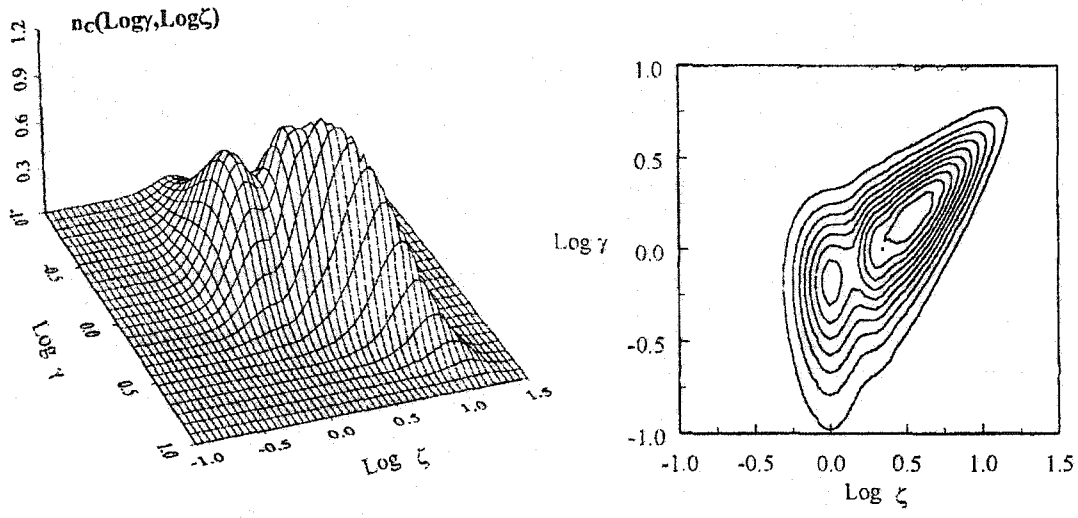

(A)

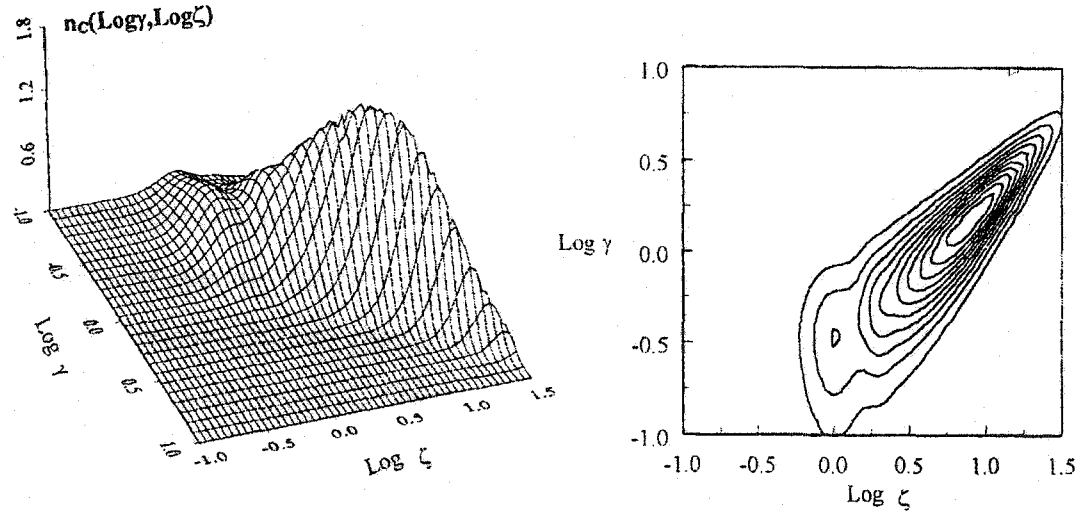

(B)

Figure 6.3 Development of the comb polymer distribution as a function of the branching density calculated using Equation 6.24: (A) $\lambda_B = 2$ and (B) $\lambda_B = 5$. The other parameters are $\sigma = 1$, and $k = 10$.

comb polymer distribution as a function of the branching density λ_B with σ = 1 and k =10. Comparing to Figure 6.2(A) with λ_B = 1, the distribution surfaces of Figure 6.3(A) and 6.3(B) become narrower and more skew toward the high molecular weight end with increasing branching density.

It should be emphasized that although the model is developed based on the grafting-onto scheme of pre-formed backbone and side chains as presented in Equation 6.1~3. It is also applicable to comb polymers obtained by grafting-from and grafting-through schemes, provided that the side chains are randomly located on the backbone. The comb polymer distribution in its reduced form, $n_C(\gamma,\varsigma)$, has the determining parameters of λ_B, σ and k. Two more parameters, the number average chain lengths of backbone $\bar{B}_N$ and side chain $\bar{S}_N$, are added to the absolute distribution from, $n_C(r,s)$. These parameters can be readily estimated. Polymer chains synthesized by radical mechanisms with disproportionation termination and transfer reactions tend to have a random distribution (σ or $k \rightarrow \infty$).

Table 6.4 summarizes the expressions for determining the parameters for the grafting-from and graft-through mechanisms. In the grafting-from scheme, the rate of branching is equal to that of initiation of active sites on backbone chains. The rate of branching can be calculated from the monomer conversion in the macromonomer approach (grafting-through). The molecular weight properties of backbone chains in the former case and those of side chains in the latter case are predetermined because these reactants are formed prior to the synthesis of comb copolymers. The number average molecular weights of side chains in the grafting-from case and of backbone in the macromonomer case are calculated by following the concentrations of the reacting species, as listed in the table. The ratio of the monomeric units on backbone to the units on side chains, defined as the degree of grafting, can be readily calculated from the product of the branching density λ and the number average chain length of side chains, $\bar{S}_N$.

Table 6.4 Determining Parameters for Molecular Weight Distribution in Chain Polymerization with Comb Branching

	Grafting-from	Grafting-through (macromonomer)
branching density, λ	$\frac{d\lambda}{dt} = K_i A^*$	$\lambda = \frac{M_0^= - M^=}{M_0 - M}$ $\frac{dM}{dt} = -K_{p11} C^* M$ $\frac{dM^=}{dt} = -K_{p12} C^* M^=$ $\frac{dC^*}{dt} = K_i A^* M - \tau_1 C^*$ $M^= = \sum_{s=1}^{\infty} M_s^= << M$ $r_2 = \frac{K_{p22}}{K_{p21}} \sim 0$
backbone chain, B and $\bar{B}_N$	Pre-polymer B_r	$\frac{dB}{dt} = K_i A^* M$ $\bar{B}_N = \frac{M_0 - M}{B}$
side chain, S and $\bar{S}_N$	$S = \lambda W_B$, $W_B = B\bar{B}_N$ $\bar{S}_N = \frac{W_S}{S}$, $\frac{dW_S}{dt} = K_p C^* M$ $\frac{dM}{dt} = -K_p (C^* + P^*) M$ $\frac{dC^*}{dt} = K_i W_B A^* - (K_{tr} T + \tau) C^*$ $\frac{dP^*}{dt} = K_{tr} T C^* - \tau P^*$ $\frac{dT}{dt} = -K_{tr} T (C^* + P^*)$	Reacted macromonomer
primary chain, P and $\bar{P}_N$	$P = T_0 - T$	unreacted macromonomer, $M_s^=$

6.5 Conclusion

In this chapter, analytical expressions are derived to describe the bivariate distribution of molecular weight and branching density for comb-branched copolymers, $n_C(r,s,b)$. The side chains are assumed to have either uniform or Schulz-Zimm distributions. This model is based on the random grafting of pre-formed side chains onto backbones (grafting-onto). However, it is also applicable to the comb polymers synthesized by grafting-from and grafting-through mechanisms shown in Tables 6.1 and 6.2. The major parameters determining the comb copolymer bivariate distribution are the molecular weight distributions of both backbone ($n_B(r)$, or σ, $\overline{B}_N$) and side chains ($n_S(s)$, or k, $\overline{S}_N$) and the branching density (λ_B). These parameters can be estimated by solving the population equations of reactants involved in the mechanism as summarized in Table 6.4. The effects of the side-chain distribution and branching density on the copolymer distribution are illustrated in Figure 6.2(A) and (B). The copolymer distribution with a broad side-chain distribution gives a smooth single-peak surface. Multi-peak surface copolymer distributions are observed with increasing values of k.

6.6 References

Amemiya, A. and Saito, O. (1967). "Mathematical Theory of Polymer Gelation". *J. Phys. Soc. Jpn.*, *23*, 1394.

Baltsas, A., Achilias, D. S. and Kiparissides C. (1996). "A Theoretical Investigation of the Production of Branched Copolymers in Continuous Stirred Tank Reactors". *Macromol. Theory Simul.*, *5*, 477.

Bamford, C. H., and Tompa, H. (1954). "The Calculation of Molecular Weight Distribution from Kinetic Schemes". *Trans. Faraday Soc.*, *50*, 1097.

Battaerd, H. A. J. and Tregear, G. W. (1967). *Graft Copolymers*, Wiley–Interscience, New York.

Beasley, J. K. (1953). "The Molecular Structure of Polyethylene. IV. Kinetic Calculation of the Effect of Branching on Molecular Weight Distribution". *J. Am. Chem. Soc.*, *75*, 6123.

Capek, I. and Akashi, M. (1993). "On the Kinetics of Free-Radical Polymerization of Macromonomers". *J. Macromol. Sci., Rev. Macromol. Chem. Phys.*, *C33*, 369.

Dreyfuss, P. and Quirk, R. P. (1988). "Graft Copolymers", in H. Mark and J. Kroschwitz ed. *Encyclopedia of Polymer Science and Engineering*, 2nd ed., vol. 7, Wiley Interscience, New York, p. 551.

Flory, P. J. (1941). "Molecular Size Distribution in Three Dimensional Polymers. II. Trifunctional Branching Units". *J. Am. Chem. Soc.*, *63*, 3091.

Flory, P. J. (1953). *Principles of Polymer Chemistry*, Cornell University Press, Ithaca, NY.

Grest, G. S., Fetters, L. J., Huang, J. S and Richter, D. (1996). "Star Polymers - Experiment, Theory, and Simulation". *Adv. Chem. Phys.*, *94*, 67.

Hamielec, A. E., MacGregor, J. F. and Penlidis, A. (1987). "Multicomponent Free-Radical Polymerization in Batch, Semi-Batch and Continuous Reactors". *Makromol. Chem., Macromol. Symp., 10/ 11*, 521.

Jackson, R. A., Small, P. A. and Whiteley, K. S. (1973). "Prediction of Molecular Weight Distributions in Branched Polymers". *J. Polym. Sci., Polym. Chem., 11*, 1781.

Kawakami, Y. (1988). "Macromers", in H. Mark and J. Kroschwitz ed. *Encyclopedia of Polymer Science and Engineering*, 2nd ed., vol. 9, Wiley Interscience, New York, p. 195.

Meijs, G. F. and Rizzardo, E. (1990). "Reactivity of Macromonomers in Free Radical Polymerization". *J. Macromol. Sci., Rev. Macromol. Chem. Phys., C30*, 305.

Molau, G. E. (1971). *Colloidal and Morphological Behaviour of Block and Graft Copolymers*, Plenum Press, New York.

Peebles, L. H. Jr. (1971). *Molecular Weight Distributions in Polymers*, John Wiley & Sons, Inc., New York, p. 233.

Rempp, P. F. and Franta, E. (1984). "Macromonomers - Synthesis, Characterization and Applications". *Adv. Polym. Sci., 58*, 1.

Saito, O. (1972). *The Radiation Chemistry of Macromolecules*, M. Dole, ed., Academic Press, New York, p. 223.

Small, P. A. (1975). "Long-Chain Branching in Polymers". *Adv. Polym. Sci., 18*, 1.

Soares, J. B. P. and Hamielec, A. E. (1996). "Bivariate Chain Length and Long Chain Branching Distribution for Copolymerization of Olefins and Polyolefin Chains Containing Terminal Double-bonds". *Macromol. Theory Simul., 5*, 547.

Stockmayer, W. H. (1943). "Theory of Molecular Size Distribution and Gel Formation in Branched-Chain Polymers". *J. Chem. Phys., 11*, 45.

Taylor, T. W. and Reichert, K. H. (1985). "The Influence of Reactor Type and Operating Conditions on the Molecular Weight Distribution in Vinyl Acetate Polymerization". *J. Appl. Polym. Sci., 30*, 227.

Tobita, H. and Hamielec, A. E. (1988). "A Kinetic Model for Network Formation in Free Radical Polymerization". *Makromol. Chem., Macromol. Symp.*, *20/ 21*, 501.

Tobita, H. (1996). "Random Sampling Technique to Predict the Molecular Weight Distribution in Nonlinear Polymerization". *Macromol. Theory Simul.*, *5*, 1167.

Tobita, H., (1997). "Formation of Homogeneously Branched Polymers Using Terminal Double-Bond Polymerization". *Polymer*, *38*, 1705.

Zhu, S. and Hamielec, A. E. (1994). "Gel Formation in Free Radical Polymerization via Chain Transfer and Terminal Branching". *J. Polym. Sci., Polym. Phys.*, *32*, 929.

Zhu, S., Li, D. Zhou, W. and Crowe, C. M. (1998). "Molecular Weight Distribution of Comb Polymers by Chain Polymerization with Macromonomer". *Polymer*, *39*, 5203.

Zhu, S., Ma, M. and Zhou, W. (1996). "Theory of Nonrandom Cross-Linking: Free-Radical Polymer Grafting". *Macromolecules*, *29*, 5688.

Chapter 7. Conclusions and recommendations

The overall contributions of this thesis to the field of polymer reaction engineering and flocculation are summarized in the following.

7.1 Free radical polymerization of N-vinylformamide

The free radical polymerizations of N-vinylformamide (NVF) in bulk and aqueous solution were examined in a great detail. The molar heat of reaction for NVF polymerization was measured to be 79.4 kJ/mol. A comprehensive set of kinetic data, molecular weights and molecular weight distributions were obtained. The bulk polymerization showed a severe "gel effect" from the start of polymerization. For the solution polymerization, the "gel effect" was still pronounced at monomer concentrations equal to or greater than 40wt% (2.31 mol/L). A semi-empirical model based on the free volume theory was developed to describe both bulk and solution polymerizations. Gelation was found in certain polymerization runs. Hydrolysis experiments conducted on the gel samples confirmed that the amide group provided crosslinking points in forming PNVF gels.

7.2 PNVF acidic and basic hydrolysis

The hydrolysis kinetics and equilibrium hydrolysis of PNVF under acidic and basic conditions were examined. Basic hydrolysis usually gave higher reaction rates and higher conversions than acidic hydrolysis at the same reactant concentrations, temperature and time span. The equilibrium hydrolysis data revealed that one mole base was capable of inducing the hydrolysis for more than one mole of amide groups, particularly at a NaOH/amide group ratio lower than 1.0. The basic hydrolysis of PNVF usually proceeded to 100% conversion when the

NaOH/amide ratio was greater than 1.0. The acidic equilibrium hydrolysis did not reach 100% completion. It also gave lower equilibrium amide conversion than basic hydrolysis at the same reaction conditions. This was probably due to the charge repulsion established between cationic charged polymer chains and the approaching acid (H^+) during the hydrolysis.

7.3 Synthesis of cationic grafted polymeric flocculants

Two methods were used to synthesize cationic grafted copolymers for flocculation purposes.

In the first method, NVF monomer was copolymerized with two cationic poly dimethylaminoethyl methacrylate (polyDMAEMA) methyl chloride macromonomers to produce a series of comb-grafted copolymers with different cationic contents. The copolymerization kinetics was examined. The copolymerization reactivity ratio (r_1) of the comonomer pair (NVF(M_1)-macromonomer(M_2)) was determined to be 3.82 and 6.39 for the two macromonomers with 50 and 100 repeating units. Graft copolymers containing up to 10mol% cationic contents were obtained.

In the second method, polydiallyldimethyl ammonium chloride (polyDADMAC) was grafted onto polyacrylamide (PAM) in a mini-mixer in melts with an organic peroxide initiator. The radical mechanisms in grafting were confirmed. The degree of grafting was found to be a strong function of initial polymer feed ratios. Higher polyDADMAC/PAM ratio gave higher degree of grafting. However, the grafting efficiency was always less than 10wt%. Severe gelation problem with high molecular weight PAM that occurred during the process also hampered the grafting efforts.

7.4 Flocculation performance

The grafting samples synthesized by the polyDMAEMA MCQ macromonomer and NVF copolymerization were tested for their flocculation performance and compared to that of random

copolymers of NVF and DMAEMA MCQ. These grafted samples had a well-defined comb molecule structure with a non-ionic backbone chain and many cationic side chains. The flocculation tests on a TiO_2 model suspension confirmed that cationic grafted copolymers having a similar cationic content as the random copolymers gave faster flocculation and stronger flocs. The results also confirmed for the first time the hypothesis presented in Chapter 1 that by rearranging the charge distribution within the polymer chain through grafting, flocculation performance should be improved.

7.5 Grafting modeling

A theoretical model was derived to describe the bivariate distribution of molecular weight and branching density for comb-grafted copolymers. The side chains were assumed to have either uniform or Schulz-Zimm distributions. The effects of the side-chain distribution and branching density on the copolymer distribution were illustrated. This model was based on the random grafting of pre-formed side chains onto a polymer backbone (grafting-onto) mechanism. However, it is also applicable to the comb polymers synthesized by grafting-from and grafting-through mechanisms as long as the inclusion of the branching point is a random process.

7.6 Recommendations for future research

7.6.1 N-vinylformamide polymerization

This research utilized homogeneous polymerization method (bulk and solution) to obtain fundamental knowledge about NVF free radical polymerization and copolymerization. In reality, heterogeneous polymerization methods (suspension and inverse emulsion) have more industrial significance for their better heat removal, mixing, simplicity of product recovery, and monomer recycling. There has been no report on the detailed research in this field, especially the inverse

emulsion polymerization of NVF. The inverse emulsion polymerization is a major method used to produce high molecular weight polyacrylamide and copolymers for commercial flocculants. It is of fundamental importance and practical significance to look into the inverse emulsion polymerization of N-vinylformamide in detail.

7.6.2 Synthesis of graft copolymer by reactive extrusion

This thesis presented an example of grafting polyDADMAC onto PAM in mini-mixer. This process resembled reactive processing usually carried out at a larger scale in extruders to handle highly viscous polymer reactions. However, the gelation problem encountered during the free radical grafting process both in the mini-mixer and an extruder prevented the practical application of this process. Future research should be focusing on reducing or eliminating gelation, either by changing the processing procedure and recipe or choosing different pre-polymers. Polyacrylamide is easy to obtain with high molecular weights. However, it is also easy to gel in free radical process. A suitable candidate with high molecular weight and less gelation tendency in free radical process has yet to be found.

7.6.3 Graft modeling

The model developed in Chapter 6 assumed the molecular weight distributions in both backbones and side chains to be relatively simple distributions, Schultz-Zimm and uniform distributions. It is desirable to expand the model to grafting system with more general arbitrary molecular weight distribution. The expansion to arbitrary distributions may not result in analytical equations as derived in this research. Numerical approaches may be the solution to handle the complexities involving arbitrary molecular weight distributions.

Nomenclature

Letters

α: volume expansion coefficient

ε: volume contraction factor

ϕ: volume fraction

γ: reduced backbone chain length

λ: density of grafting

λ_B: average branching point per backbone chain

λ_i: the *i*th moment of living polymer chains

μ_i: the *i*th moment of dead polymer chains

σ: parameter of Schulz-Zimm distribution

τ: overall apparent termination reaction rate constant

ς: reduced side chain length

A: initiator

B: volume ratio of solvent and initial monomer, $B=V_s/V_0$ (Chapter 2), or backbone polymer (Chapter 6)

$\overline{B}_N$: number average chain length of backbone

C: comb polymer

C_{fp}: chain transfer rate constant to polymer

C_m: chain transfer rate constant to monomer

d_m: monomer density, g/cm^3

d_p: polymer density, g/cm^3

f: initiation efficiency

k: parameter of Schulz-Zimm distribution

K_c: chain recombination reaction rate constant

K_i: initiation reaction rate constant

k_{pij}: propagation rate constant of chain radicals ending with i-type monomeric unit with j-type monomer during copolymerization, i, j = 1, 2, L/(mol*S)

k_p or K_p: propagation rate constant, L/(mol*S)

k_t: termination rate constant, L/(mol*S)

K_{tr}: chain transfer reaction rate constant

[I]: initiator concentration, mol/L

M: monomer

[M]: monomer concentration, mol/L

M_0: initial mass of monomer, g

$\overline{M}_n$: number average molecular weight

$\overline{M}_w$: weight average molecular weight

$M_x^=$: macromonomer or macromonomer concentration, mol/L

n(): number chain length distribution

P: primary polymer

[P]: total dead polymer chain concentration, mol/L

$[P_n]$: concentration of dead polymer chains with n repeat units, mol/L

r_1 reactivity ratio of monomer 1 during copolymerization, $r_1 = \frac{k_{p11}}{k_{p12}}$

r_2 reactivity ratio of monomer 2 during copolymerization, $r_1 = \frac{k_{p22}}{k_{p21}}$

$[R^\bullet]$: total free radical concentration, mol/L

$[R_n^\bullet]$: concentration of free radical chains with n repeat units, mol/L

R_p: rate of polymerization, mol/(L*S)

S: side chain polymer

$\bar{S}_N$: number average chain length of side chain

T: chain transfer agent or chain transfer agent concentration, mol/L

V_0: initial monomer volume, L

V_f: free volume fraction of polymerization system

V_s: solvent volume, L

w(): weight chain length distribution

W_p: mass of polymer, g

x: polymerization conversion

Superscript:

*: active center

b and j: number of active center

Subscripts:

0: initial condition or at zero conversion

b: branch point

B: backbone

c: with chemical control

d: with diffusion control

g: glass temperature

m: monomer

N: number average

p: polymer or propagation

r: monomeric units of backbone

s: solvent (Chapter 2) or total monomeric units of side chains (Chapter 6)

S: side chain (Chapter 6)

t: termination

1: monomer 1 or species ended with monomer 1

2: monomer 2 or species ended with monomer 2

Publications related to the thesis

1. **Synthesis and Flocculation Performance of Graft Copolymer of N-vinylformamide and Polydimethylaminoethyl Methacrylate Methyl Chloride Macromonomer,** L.Gu, S. Zhu and A. N. Hrymak, *J. Colloid & Polym. Sci.*, to appear, 2001.
2. **The Nature of Crosslinking in N-vinylformamide Free Radical Polymerization,** L. Gu, A. N. Hrymak, S. Zhu and R. H. Pelton, *Macromol. Rapid Commun.*, **22**, 212 (2001)
3. **Kinetics and Modeling of Free Radical Polymerization of N-vinylformamide,** L. Gu, A. N. Hrymak, S. Zhu and R. H. Pelton, *Polymer*, **42**, 3077, (2001)
4. **Grafting Cationic Polyelectrolyte onto PAM in Near Solid State,** L. Gu, A. Hrymak and S. Zhu, *J. Appl. Polym. Sci.*, **74**, 1412 (1999)
5. **Modeling Molecular Weight Distribution of Comb Branched Graft Copolymers,** L. Gu, S. Zhu and A. Hrymak, *J. Polymer Sci., Part B: Polymer Physics.* **36**, 705 (1998)
6. **Radical Polymerization kinetics of N-vinylformamide,** L. Gu, S. Zhu and A. Hrymak, *49th CSChE Conf.,* Saskatoon, Saskatchewan, October, 1999
7. **Grafting of PolyDADMAC onto PAM by Reactive Processing,** L. Gu, S. Zhu and A. Hrymak, *PPS North American Meeting,* Toronto, Ontario, August, 1998
8. **Molecular Weight Distribution of Branched Polymers with Random, Comb and Star Structures,** S. Zhu, D. Li, L. Gu, J. McLachlan, *47th, CSChE Conf.,* Edmonton, Alberta, October, 1997
9. **Bivariate Distribution of Molecular weight and Branching Density: Comparison of Dendritic, Comb and Star Polymers,** S. Zhu, D. Li, J. McLachlan, L. Gu, *AICHE 1997 Annual Meeting*, Los Angeles, California, November, 1997